THE IMPACT OF LONG TERM TESTOSTERONE WITHDRAWAL ON CARDIAC EXCITATION-CONTRACTION COUPLING IN THE MOUSE

by

Omar Ayaz

Submitted in partial fulfilment of the requirements
for the degree of Doctor of Philosophy

at

Dalhousie University
Halifax, Nova Scotia
August 2017

TABLE OF CONTENTS

List of Figures

List of Tables

Abstract

The impact of chronic testosterone withdrawal on the structure and function of the heart was investigated in male C57BL/6 mice following bilateral gonadectomy (GDX) or a sham-operation at 4 weeks of age. *In vivo* echocardiography showed few changes, although hearts were smaller and relaxation was slowed in GDX compared to sham controls. Peak contractions and Ca^{2+} transients were similar in sham and GDX field-stimulated ventricular myocytes, although both were prolonged in GDX cells. However, when the duration of depolarization was controlled by voltage clamp, GDX suppressed peak contractions and Ca^{2+} transients. Underlying cellular mechanisms were investigated by examining cardiac excitation-contraction coupling mechanisms. Peak Ca^{2+} current was smaller and Ca^{2+} current decay was prolonged in GDX myocytes, but there was no effect on net Ca^{2+} flux across the sarcolemma. This change in L-channel function was not due to effects of GDX on the underlying protein (*e.g.* Cav1.2) expression. Both the sarcoplasmic reticulum (SR) Ca^{2+} content and fractional Ca^{2+} release from the SR were reduced by GDX. GDX had no effect on the expression of the major cardiac SR Ca^{2+} release channel isoform (*e.g.* RyR2). However, spontaneous Ca^{2+} sparks, which represent fundamental Ca^{2+} release units from the SR, were smaller, less frequent and decayed more slowly in GDX myocytes. There was no change in expression of the cardiac sarco/endoplasmic reticulum Ca^{2+}-ATPase (*e.g.* SERCA2), however, the expression of its endogenous inhibitor, phospholamban, was increased by GDX. Microelectrode studies showed that action potential duration (APD) was prolonged in GDX cells compared to sham controls. This was not due to effects on K^{+} channel expression (*e.g.* Kv1.5), but possibly due to the prolonged Ca^{2+} current decay, which would be expected to prolong repolarization. These longer action potentials disrupted electrical activity in the myocytes by increasing the number of early afterdepolarizations and spontaneous contractions. These findings suggest that GDX disrupts Ca^{2+} handling and may promote diastolic dysfunction and fatal arrhythmias, such as “torsade de pointes”, in older men with low testosterone.

List of Abbreviations Used

+dP/dT	Left ventricular pressure rise
-dP/dT	Left ventricular pressure decay
APD	Action potential duration
CaMKII	Ca^{2+}/calmodulin-dependent kinase II
cAMP	Cyclic adenosine monophosphate
Cav1.2	Pore-forming subunit of the L-type Ca^{2+} channel
CYP	Cytochrome P450
CVD	Cardiovascular disease
DHEA	Dehydroepiandrosterone
DHT	Dihydrotestosterone
EC	Excitation-contraction
EDV	End-diastolic volume
EF	Ejection fraction
FS	Fractional shortening
HFpEF	Heart failure with preserved ejection fraction
HFrEF	Heart failure with reduced ejection fraction
HSD3β	3β-hydroxysteroid dehydrogenase
ICa-L	L-type Ca^{2+} current
IK1	Inward rectifier K^+ current
IKs	Slow delayed rectifier K^+ current
IKur	Ultra-rapid delayed rectifier K^+ current
ISS	Steady-state K^+ current
ITO	Transient outward current
IVS	Interventricular septal thickness
Kv1.5	Potassium voltage-gated channel
LH	Luteinizing hormone
LV	Left ventricle

LVDA	Left ventricle diastolic area
LVDP	Left ventricular developed pressure
LVID	Left ventricle internal dimensions
LVM	Left ventricle mass
LVPW	Left ventricle posterior wall
LVSA	Left ventricle systolic area
MHC	Myosin heavy chain
NCX	Na^{+}/Ca^{2+} exchanger
PKA	Protein kinase A
PLB	Phospholamban
RMP	Resting membrane potential
RWT	Relative wall thickness
RyR	Ryanodine receptor
S.E.M.	Standard error of the mean
SERCA	Sarco/endoplasmic reticulum Ca^{2+}-ATPase
SR	Sarcoplasmic reticulum
SV	Stroke volume

Acknowledgements

I would like to express my sincere gratitude to Dr. Susan Howlett for her unrelenting mentorship and tremendous patience and support. Her guidance and, more importantly, honesty have been instrumental in my research planning and in the preparation of this thesis.

I would also like to thank Dr. Robert Rose and his research team for providing me with access to their laboratory and equipment and for accommodating me like another member of their wonderful team.

My sincere thanks to my thesis committee, Dr. Eileen Denovan-Wright and Dr. Kishore Pasumarthi, for their constructive criticisms and encouragements. Coming in to a meeting was undoubtedly intimidating, but this committee always left me inspired and motivated to take on more challenges.

A special thank you to Peter Nicholl and Dr. Jie-Quan Zhu for their technical support and instructions. Also, thank you to the many members and friends that have been a part of Dr. Howlett's research team over the years. It has been a great pleasure working with and learning from you all.

I extend thanks to Luisa, Cheryl, and Sandi for your administrative assistance and gentle reminders of important dates.

Last but not the least, my warmest expression of thanks to my parents for their many years of unconditional love and support. Thank you for believing in me every step of the way.

CHAPTER 1 Introduction

1.0 Overview

Cardiovascular diseases (CVD) are a leading cause of hospitalization and death for both men and women (Roger et al., 2012). As advanced age is a major risk factor for the development of CVD in both sexes, the incidence and prevalence of these diseases is expected to escalate as our population ages (Go et al., 2013). The knowledge that the incidence of CVD in women rises as estrogen levels fall after menopause has fueled interest in its potential cardioprotective effects (Vitale et al., 2009). What is less well appreciated is that testosterone levels also decline with advancing age, both in men and women (Oskui et al., 2013; Araujo et al., 2004; Pluchino et al., 2013). This suggests that low-testosterone levels may contribute to the pathogenesis of CVD. Indeed, a number of clinical studies have shown that low endogenous levels of testosterone are associated with CVDs such as coronary artery disease, hypertension, and congestive heart failure (Oskui et al., 2013). Furthermore, testosterone-replacement therapy, which is used to treat testosterone deficiency secondary to aging (Tsujimura A., 2013), may have beneficial effects in the setting of heart failure and ischemic heart disease (Oskui et al., 2013; Edelman et al., 2014; Mirdamadi et al., 2014). However, controversy remains about the safety of testosterone supplementation in patients with an underlying CVD due to incomplete knowledge of its cellular mechanisms and the potential adverse effects of the therapy not being clearly defined. The clinical literature suggests there are conflicting views of the use of testosterone supplementation in patients with an underlying CVD. Some studies report that it increases the risk of developing major adverse cardiovascular events, while others suggest the opposite and report that

testosterone supplementation actually may have beneficial effects in reducing the risk of major adverse cardiovascular events (Cassimatis et al., 2016).

Despite the popularity of testosterone supplementation in potentially vulnerable older adults, how testosterone affects the heart is not fully understood. The discovery of androgen receptors in individual heart cells (myocytes) (Marsh et. al., 1998; Lizotte et. al., 2009) suggests that testosterone might modulate heart function, at least in part, by effects on the ventricular myocytes themselves. Testosterone has also been implicated as a critical mediator of adverse myocardial remodelling and there is some evidence that it may promote contractile dysfunction at the cellular level (Saccà, 2009). Evidence indicates that the levels of testosterone in rodent models may modulate the expression of proteins involved in myocyte Ca^{2+} handling (Golden et al., 2003; Golden et al., 2004), although some of the literature contains conflicting data on testosterone's effects. However, on balance these studies suggest that low levels of testosterone may modify Ca^{2+} handling, which could possibly lead to deterioration of cardiomyocyte contractile capacity. If low levels of testosterone disrupt cardiac contractile function, this may contribute to the progression of diseases such as heart failure in older men (Saccà, 2009).

This thesis aims to determine how low levels of testosterone influence myocardial contractile function *in vivo* as well as at the cellular and molecular levels. The overall hypothesis is that low testosterone adversely affects cardiac contractile function by modifying key processes involved in excitation-contraction (EC) coupling, the process that links cardiac excitation to Ca^{2+} release and contraction. As disruption of Ca^{2+} handling plays a key role in many CVDs (Bers, 2014; Canty and Suzuki, 2012), understanding the mechanisms underlying the effects of low testosterone on myocardial

Ca^{2+} homeostasis may help explain its influence on cardiovascular health and disease expression.

1.1 Cardiac EC Coupling

The cardiac action potential is the electrical signal that initiates myocardial contraction. The heart uses an intrinsic conduction system to distribute these electrical impulses from the atria to the ventricles, and coordinate the movement of blood to the blood vessels (Fukuta and Little, 2008). The electrical signal originates from the spontaneous firing of the sinoatrial node in the right atrium, and spreads over the heart as a wave of excitation (Fearnley et al., 2011). The wave of excitation spreads from the atria to the ventricles, along the sarcolemma from cell-to-cell via electrically conducting gap junctions, and reaches the interior of the cell via the T-tubules, which are invaginations of the sarcolemma (Pluciennik et al., 1996). The action potential propagates along the cell membrane (sarcolemma) and stimulates the opening of fast Na^+ channels, causing the transmembrane potential to become more positive (Williams et al., 2010). The process that pairs myocyte depolarization with mechanical contraction is known as EC coupling (Winslow et al., 2005).

EC coupling begins when an action potential causes the transmembrane potential of the sarcolemma to rise and opens voltage-sensitive L-type Ca^{2+} channels (Greenstein et al., 2006). This results in extracellular Ca^{2+} flowing down its electrochemical gradient into a restricted subspace between the plasma membrane and the closely associated sarcoplasmic reticulum (SR) (Fearnley et al., 2011). This small influx of Ca^{2+} triggers

channels on the SR, known as ryanodine receptors (RyRs), to open and release their Ca^{2+} stores (Niggli et al., 2013). This raises the intracellular Ca^{2+} concentration from about 10^{-7} to 10^{-5} M (Wang et al., 2001). The phenomenon of the small influx of Ca^{2+} triggering a larger release of Ca^{2+} stores is known as Ca^{2+}-induced Ca^{2+} release (Williams et al., 2010). SR Ca^{2+} stores are released in the form of discrete subcellular units called Ca^{2+} sparks, which reflect the opening of a cluster of RyRs complexed with nearby L-type Ca^{2+} channels (Williams et al., 2010). Ca^{2+} sparks fuse together to form what is called a Ca^{2+} transient (Fearnley et al., 2011). The frequency and amplitude of spontaneous Ca^{2+} sparks are proportional to the SR Ca^{2+} load, and determine the size of the Ca^{2+} transient (Launikonis et al., 2006). If, for example, SR Ca^{2+} load is high, the SR will spontaneously release Ca^{2+} in the form of sparks (Cheng and Lederer, 2008). This serves as a mechanism to limit SR Ca^{2+} overload and attenuate spontaneous SR Ca^{2+} release in the heart (Satoh et al., 1997). A higher SR Ca^{2+} load also elevates the magnitude of the Ca^{2+} sparks, which produces enhanced contractions (Fearnley et al., 2011). Several mechanisms are involved in modulating the release and uptake of Ca^{2+} from SR stores, which ultimately determines the size of the Ca^{2+} transient, and the rate of relaxation. Phosphorylation of RyRs by protein kinase A (PKA) at Ser2808 and Ser2030, as well as at Ser2814 by Ca^{2+}/calmodulin-dependent kinase II (CaMKII), sensitizes RyRs to the Ca^{2+} trigger and increases the channel's open probability (Niggli et al., 2013). Phosphorylation of the L-type Ca^{2+} channel by PKA and CaMKII may also modulate Ca^{2+} influx, and thus alter Ca^{2+}-induced Ca^{2+} release process (Fearnley et al., 2011).

The Ca^{2+} released from the SR interacts with thin and thick myofilaments to cause contraction. The main contractile elements of the myofilaments are actin and

myosin (De Tombe, 2003). Myosin has globular heads containing myosin ATPase and it forms the thick filaments. Thin filaments are woven between the thick filaments. Thin filaments consist of two chains of actin protein arranged in an alpha-helix, rod-shaped proteins termed tropomyosin which are interdigitated along actin, and the troponin complex is attached to tropomyosin at regular intervals (Fearnley et al., 2011). The troponin complex is a heteromeric protein made up of 3 subunits: troponin-T attaches to the tropomyosin, troponin-C serves as a Ca^{2+} binding protein, and troponin-I inhibits the myosin binding site on actin (Gunning et al., 2015). Ca^{2+} binding to troponin-C causes a conformational change that displaces troponin-I from the ATPase on myosin heads. ATP hydrolysis supplies energy for the formation of cross-bridges between a myosin head and the active site on actin. A "power stroke" moves actin filaments toward the centre of the sarcomere, resulting in sarcomere shortening and myocyte contraction (Sen-Chowdhry et al., 2016).

A number of cellular processes are involved in the decline of the intracellular Ca^{2+} transient that leads to relaxation. L-type Ca^{2+} channels inactivate toward the end of phase 2 of the action potential, which arrests the Ca^{2+} influx, and abolishes the Ca^{2+} induced Ca^{2+} release trigger (Fearnley et al., 2011). Ca^{2+} is sequestered within the SR by a Ca^{2+} pump called the sarco/endoplasmic reticulum Ca^{2+}-ATPase (SERCA) (Braunwald, 2013). The activity of SERCA is regulated by the endogenous inhibitor, phospholamban (PLB). Phosphorylation of PLB at sites Ser16 by PKA, and at Thr17 by CaMKII, increases the Ca^{2+} uptake activity of SERCA (Currie and Smith, 1999). A small quantity of Ca^{2+} is also removed from the cell by the bidirectional Na^{+}/Ca^{2+} exchanger (NCX), which removes one Ca^{2+} from the cell in exchange for 3 Na^{+} (Fearnley et al., 2011). As

the concentration of intracellular Ca^{2+} falls, Ca^{2+} ions dissociate from troponin-C, tropomyosin-dependant inhibition of the actin-myosin interaction is restored and the sarcomere returns to its basal length (Gordan et al., 2015). The membrane potential returns to rest, which is maintained by the Na^{+}/K^{+}-ATPase until the depolarization by the next action potential (Fearnley et al., 2011).

As is evident from the preceding discussion, intracellular Ca^{2+} concentrations are tightly regulated by many different cellular process; disruption of one or more of these process can promote CVD (Wehrens et al., 2005). Thus, the adverse effects of low testosterone on cardiac contractile function may arise through effects on one or more components of this EC coupling pathway. The next section will review how testosterone is synthesized, and discuss what is known about its effects on the hearts of men and women.

1.2 Biosynthesis of testosterone

Testosterone biosynthesis in men is controlled by the hypothalamic-pituitary-gonadal axis (Borst and Mulligan, 2007), as shown in the overview of major gonadal pathways for testosterone biosynthesis in Figure 1.1. The first step is the release of gonadotropin-releasing hormone (GnRH), which is synthesized and secreted from hypothalamic neurons (Herbison et al., 2008). GnRH binds to receptors on the anterior pituitary gland and stimulates the synthesis and secretion of luteinizing hormone (LH) into circulation (Borst and Mulligan, 2007; Levine, 1997). LH binds to LH receptors on Leydig cells in the testes and stimulates a G-protein, Gs, to activate the cyclic adenosine

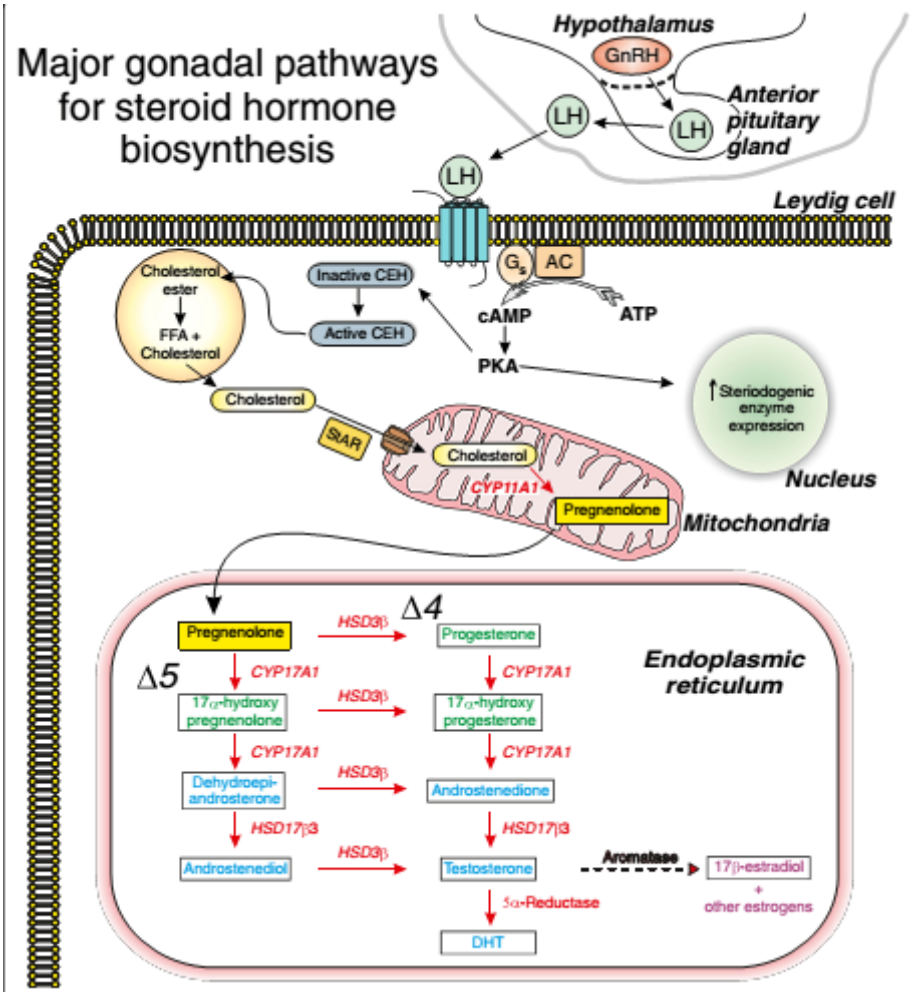

Figure 1.1 Major gonadal pathways for testosterone biosynthesis. Gonadotropin-releasing hormone (GnRH) secreted from the hypothalamus releases luteinizing hormone (LH) from the pituitary. LH binds to LH receptors on Leydig cells, stimulates Gs, and activates the cAMP/protein kinase A (PKA) pathway. PKA promotes the transport of cholesterol into mitochondria and increases transcription of genes involved in testosterone biosynthesis. Cholesterol is converted to pregnenolone, which diffuses into the endoplasmic reticulum for testosterone biosynthesis via Δ4 and Δ5 pathways. Testosterone is formed by 17 β-hydroxysteroid dehydrogenase 3 (HSD17 β3) in the Δ4 pathway and by 3 β-hydroxysteroid dehydrogenase (HSD3 β) in the Δ5 pathway. Testosterone is converted to dihydrotestosterone (DHT) by 5 α-reductase, and some are aromatized to 17ß-estradiol. Reproduced from Ayaz & Howlett, 2015, with permission.

monophosphate (cAMP)/PKA pathway. This promotes the transport of cholesterol into the mitochondria and increases transcriptional activation of gene-encoding enzymes involved in testosterone biosynthesis (Chen et al., 2007).

The levels of testosterone in circulation are under tight hormonal regulation via a negative feedback mechanism that prevents the release of GnRH and LH when testosterone levels are high (Borst and Mulligan, 2007). When serum testosterone levels are low, cholesterol in Leydig cells is transported to the inner mitochondrial membrane via a multi-protein complex in conjunction with the steroidogenic acute regulatory protein (Miller, 2013). The rate-limiting reaction in the production of steroid hormones is the conversion of cholesterol to pregnenolone by the cholesterol side chain cleavage enzyme, a cytochrome P450 (CYP) enzyme known as CYP11A1 (Miller, 2013). When pregnenolone is formed, it diffuses into the endoplasmic reticulum where testosterone biosynthesis proceeds via Δ4 and Δ5 pathways.

In the Δ4 pathway, pregnenolone is converted to progesterone by 3β-hydroxysteroid dehydrogenase (HSD3β) (Miller and Auchus, 2011; Ye et al., 2011; Hanukoglu I., 1992). CYP17A1 converts progesterone to 17α-hydroxyprogesterone by a hydroxylation reaction and then to androstenedione by a lysis reaction. Testosterone is formed by 17β-hydroxysteroid dehydrogenase 3 (HSD17β3). In the Δ5 pathway, CYP17A1 converts pregnenolone (via a hydroxylation reaction) to 17α-hydroxypregnenolone followed by a lysis reaction to yield dehydroepiandrosterone (DHEA) (Miller and Auchus, 2011; Ye et al., 2011; Hanukoglu I., 1992). DHEA is then converted to androstenedione by HSD3β. In the final step, HSD17β3 converts androstenedione to testosterone. DHEA can also be converted to androstenediol by

HSD17β3 and then converted to testosterone by HSD3β (Miller and Auchus, 2011; Ye et al., 2011). Some testosterone is converted to the more potent androgen, dihydrotestosterone (DHT), by 5α- reductase (Ye et al., 2011).

In the Leydig cells, the major androgens (testosterone and DHT) leave by passive transport into circulation, where most bind to proteins including sex-hormone-binding globulin and/or albumin, although some circulate as free androgens (Borst and Mulligan, 2007). The total amount of testosterone in human serum exists as the sum of protein-bound and unbound testosterone. Testosterone, which is tightly bound to sex-hormone-binding globulin (68%), is unable to bind androgen receptors and is therefore considered to be biologically inactive (Morris and Channer, 2012). Testosterone's affinity for albumin is about 1,000-fold less than its affinity to sex-hormone-binding globulin (Pardridge et al., 1985), which makes albumin-bound testosterone readily dissociable. Circulating albumin-bound testosterone (30%) (Morris and Channer, 2012), and unbound free testosterone (0.5–3%) (Dent et al., 2012), are considered to be "bioavailable" (Manni et al., 1985). Bioavailable testosterone stimulates multiple genomic effects on target tissues through androgen receptor stimulation, and also completes a feedback loop to inhibit GnRH and LH secretion (Borst and Mulligan, 2007).

1.3 Androgen receptors in the heart

Androgen receptors are present in tissues such as the liver, kidney, brain, skeletal muscle, and heart (Marsh et al., 1998; Ahtiainen et al., 2011; Dart et al., 2013). This has

promoted interest in the role of androgens in regulation of physiological processes including myocardial function. Classic receptor-binding studies provided the first evidence for androgen receptors in the atria and ventricles of the heart (McGill et al., 1980; Lin et al., 1981). Other studies showed that mRNA for the androgen receptor is present in cardiomyocytes isolated from men and women, as well as in cardiomyocytes from rats and dogs (Marsh et al., 1998). More recent work has shown that androgen receptor protein is expressed in both the atria and ventricles of male and female mice (Lizotte et al., 2009). This latter study also shows that androgen receptors are predominantly expressed in the cytosol and nucleus of heart tissue from adult mice (Lizotte et al., 2009). Together, these studies demonstrate that androgen receptors are present in the heart and raise questions about the role of testosterone in the regulation of myocardial function.

Most of the biological actions of endogenous and exogenous androgens are genomic effects mediated by androgen receptors that are members of the nuclear receptor gene superfamily. In the absence of androgens, the androgen receptor forms a complex with heat-shock proteins in the cytosol (Matsumoto et al., 2013). The binding of androgens causes receptor dissociation from heat-shock proteins and translocation to the nucleus, where the ligand-activated receptor homodimerizes and associates with chromatin by DNA-binding or through binding to other chromosomal proteins (Matsumoto et al., 2013). This causes transcriptional activation or repression of androgen-responsive genes, which are cell-specific according to transcription factors and *cis*-acting DNA elements in the particular tissue (Jiang et al., 2009; Jin et al., 2013). Transcriptional activation of androgen-responsive genes results in slow, long-lasting

effects that can persist for hours after androgen receptor stimulation (Walker, 2011). This androgen-mediated transcriptional regulation is considered the canonical/genomic pathway for testosterone signaling and is thought to be responsible for most of the effects of androgens on the heart.

While the classic genomic pathway mediates many of the biological effects of androgens, it is unlikely to be responsible for the rapid and reversible responses to androgens observed in some tissues, including those in the cardiovascular system. Evidence of non-genomic pathways producing rapid cellular responses have been described in the literature, although the underlying mechanisms are not well understood. For example, there is strong evidence that testosterone induces rapid vasorelaxation in both large arteries and smaller resistance vessels (Perusquia and Stallone, 2010). Acute application of androgens also increases intracellular Ca^{2+} levels in osteoblasts, platelets, skeletal muscle cells, neurons, and, importantly, in cardiac myocytes (Vicencio et al., 2011). Indeed, testosterone rapidly elicits voltage-dependent Ca^{2+} oscillations and IP3-receptor-mediated Ca^{2+} release from internal stores in neonatal rat cardiomyocytes (Vicencio et al., 2006). These pathways may involve androgen receptor signalling activating the mitogen-activated protein kinase signaling cascades, and extracellular signal-regulated kinase (McCubrey et al., 2007; Roberts et al., 2007). Other non-genomic pathways of rapid androgen action have been described by activation of plasma membrane receptors. Androgens have been shown to modulate intracellular Ca^{2+} concentration by activating G protein coupled receptors (Mellström and Naranjo, 2001), and activation of the sex-hormone-binding globulin-receptor has been shown to modulate cAMP levels (Heinlein and Chang, 2002). A cell-membrane-associated

androgen receptor may also be responsible, although at present its identity is unknown and other mechanisms, such as direct activation of ion channels and signaling pathways, may be involved (Matsumoto et al., 2013; Perusquia and Stallone, 2010; Vicencio et al., 2011). Some recent data has suggested that non-genomic androgen receptor signaling may regulate classical genomic signaling to serve as an integrated mechanism for cellular processes such as cardiomyocyte hypertrophy (Wilson et al., 2011; Rahman and Christian, 2007). These data also suggests that non-genomic and genomic androgen receptor signaling may regulate gene expression by working together (Wilson et al., 2011). Thus, although the canonical/genomic pathway is primarily responsible for the effects of androgens on the heart, the nongenomic pathway also may contribute.

Testosterone plays important roles in men and women by regulating libido, muscle strength, fat distribution, bone density, and production of red blood cells (Kloner et al., 2016). Low testosterone levels have been shown to have adverse impacts in men and women, such as an increased incidence of CVD and associated mortality (Khaw et al., 2007; Hyde et al., 2012). This has motivated considerable interest in the study of the mechanism of testosterone actions in the hearts of men and women. This has highlighted the need to investigate the mechanisms responsible for the actions of testosterone in the heart.

1.4 Testosterone in men and women

There is evidence that circulating testosterone rises to peak levels in men and women during puberty (Giusti et al., 1975), and then decreases with age in both sexes

(Pluchino et al., 2013; Krause, 2006; Feldman et al., 2002; Davison and Davis, 2003). Men and women have different levels of circulating testosterone, with men having approximately 20-fold higher compared with women (Longcope et al., 1981). Normal total testosterone levels in men are variable, and can range anywhere from 300–1000 ng/dL (Schwarz et al., 2011). Men experience a gradual decline of testosterone at a constant rate of 1-1.5% annually after approximately age 35 (Schwarz et al., 2011). The rate of testosterone's decline with advancing age varies between men (Morris and Channer, 2012). Results from the Baltimore Longitudinal Study of Aging suggest that levels decline at an average rate of 0.11 nmol L^{-1} $year^{-1}$ (Harman et al., 2001). By the age of 70, 35% of men have significantly lower testosterone levels than younger men (Vermeulen and Kaufman, 1995).

In aging men, the fall in serum testosterone is largely due to a decrease in the ability of Leydig cells to produce testosterone in response to LH (Midzak et al., 2008). This arises as a result of age-associated attenuation of the cAMP/PKA pathway, leading to less transfer of cholesterol into the mitochondria and a reduction in the production of steroidogenic enzymes (Midzak et al., 2008). Interestingly, a similar mechanism has been proposed to lead to the age-dependent decrease in testosterone levels in male rats (Zirkin and Tenover, 2012). Thus, the aging process reduces the amount of testosterone available to interact with androgen receptors.

Men who experience a faster rate of testosterone decline may reach clinically low levels (300 to 400 ng/dL) (Elsherbiny et al., 2017) at an earlier age than what is considered normal. Some men experience symptoms in middle-age similar to those of elderly men. These men may experience low energy levels, decline in libido, increase in

body fat, and a decrease in muscle mass at an earlier age then expected, and are considered candidates for testosterone replacement therapy (Morgentaler et al., 2014).

Testosterone levels also vary with age in women. Several studies (Sternfeld et al., 2008; Spencer et al., 2007; Kushnir et al., 2006), but not all (Labrie et al., 1997; Salameh et al., 2010), report that testosterone levels reach their peak in women during puberty (1.04–2.43 nmol/L) and then decline with advancing age, with a faster rate of decline occurring during the early childbearing ages. Women experience a well characterized sudden, and rapid decline, in the levels of some sex hormones during menopause (Morris and Channer, 2012). Whether testosterone levels decline even further after menopause is difficult to accurately determine due to the very low testosterone levels in women. Clinical studies have also noted that older women with lower than normal testosterone levels experience symptoms similar to those seen in men such as low energy levels, decreased libido and muscle weakness (Glaser and Dimitrakakis, 2013). While it is difficult to assess the contribution of declining testosterone levels to these symptoms in women due to low levels of the androgen, clinical studies have demonstrated improvements in physical strength and libido with the use of testosterone therapy in women (Wierman et al., 2014).

Low testosterone levels in older men and women have been associated with poor cardiovascular health, an increased incidence of certain CVDs and mortality. This has led physicians to prescribe testosterone replacement therapy for older adults of both sexes. However, it is unclear whether the drug is beneficial and safety of this treatment has not been established.

1.5 Testosterone and CVD

Older men and women with low testosterone levels are more likely to have symptoms of poor cardiovascular health, and higher incidences of CVD. In recent decades, men and women have been prescribed testosterone replacement therapy to improve their symptoms. Clinical studies have tried to determine if testosterone supplementation not only improves cardiovascular health, but reduces the risk of CVD. Most of the clinical literature described in this section has studied the effects of testosterone and CVD in men, and comparatively little is known about its effect in women. Prescriptions of testosterone replacement therapy for older men with low testosterone levels have increased dramatically over the past two decades (Bassil et al., 2009). Testosterone replacement in older women is also on the rise (Glaser and Dimitrakakis, 2013). Physicians have described improvement in symptoms such as low libido, depression, sexual dysfunction, and weak muscle strength in older men (Bhasin et al., 2010; Zitzmann et al., 2006) and post-menopausal women (Wierman et al., 2014) taking testosterone. Clinical trials have investigated links between low endogenous levels of testosterone and CVD to determine the value of testosterone-replacement therapy in the setting of heart failure and ischemic heart disease (Oskui et al., 2013; Edelman et al., 2014; Mirdamadi et al., 2014). However, the benefit and safety of prescribing testosterone in these patients has not been well established. Reviews of clinical studies have described mixed results regarding testosterone's effect on mortality, and CVD, as described in more detail below.

Several, but not all, reviews of the literature have described an association between low endogenous testosterone levels and a higher cardiovascular risk profile

(Barrett-Connor, 1995; Khaw and Barrett-Connor, 1988), as well as an increased risk of overall and cardiovascular mortality (Araujo et al., 2011). A review of the literature found that low testosterone levels in men 70 years of age and older was associated with an increased risk of overall mortality (Ruige et al., 2011). Two longitudinal epidemiological studies also supported the association of low serum testosterone with high mortality in older men (Haring et al., 2010; Malkin et al., 2010). However, these studies were conducted in populations of normal men, without evidence of overt CVD. Epidemiological and observational studies have demonstrated an association between low testosterone levels and increased CVD risk in men (Araujo et al., 2004; Corona et al., 2011; Ruige et al., 2011). Additionally, low testosterone levels are linked to an increased risk of mortality due to CVD compared to men with normal testosterone levels (Gencer and Mach, 2015). A review of male patients diagnosed with CVD found significantly low testosterone levels, and this relationship remains significant even after investigators adjusted for age and body mass index (Corona et al., 2011), which suggests that low testosterone contributes to the overall risk of CVD. Several studies have found that men with low testosterone levels and certain CVD have higher rates of mortality compared to men with normal levels. For example, mortality is twice as high in men with coronary artery disease, confirmed using angiography, plus low levels of bioavailable testosterone (Malkin et al., 2010). Together these studies suggest that low testosterone levels are involved in the pathogenesis of at least some CVDs.

Hormones such as testosterone are heavily involved in maintaining the health of artery wall (Liu et al., 2003). Low testosterone levels in men may promote the progression of atherosclerosis and coronary artery disease (English et al., 2000; Hak et

al., 2002). Atherosclerosis is the accumulation of plaque, which is made of several substances including cholesterol, inside the walls of the arteries. Plaque buildup inside the walls of arteries causes them to become narrower, and slows down the flow of blood (Kelly and Jones, 2013). In a clinical study of middle-aged men with type 2 diabetes, patients with low testosterone levels generally exhibited atherosclerotic plaques, endothelial dysfunction, and higher levels of high-sensitivity C-reactive protein, a biomarker predictive of future cardiovascular problems, such as myocardial infarction and stroke (Farias et al., 2014). Low endogenous testosterone levels in men and women may promote plaque buildup and inflammation in the coronary arteries. The inflammation and narrowing of the coronary arteries results in myocardial ischemia (Crossman, 2004), and can damage the arterial wall over time leading to the development coronary artery disease (Ashley and Niebauer, 2004). In support of this, some studies have found a negative correlation between the degree of coronary artery disease and bioavailable testosterone (Rosano et al., 2007; Hu et al., 2011; Li et al., 2012). Low serum testosterone levels are even predictive for premature coronary artery disease in men 45 years of age and younger (Alkamel et al., 2014). Together, these observations support testosterone's role in maintaining a healthy arterial wall, and suggest that low endogenous testosterone levels may promote the progression of atherosclerosis, and ischemic heart disease.

The mechanism(s) by which low testosterone promotes ischemic heart disease are not fully understood. Testosterone interacts with androgen receptors on vascular smooth muscle cells and endothelial cells (Negro-Vilar, 1999). Most studies describe testosterone as a vasoactive hormone that predominantly has vasodilatory actions on

several vascular beds (Kelly and Jones, 2013). Acute and chronic testosterone administration has been shown to increase coronary artery diameter and flow in clinical studies (Webb et al., 1999). The mechanism of the action of testosterone on the vasculature is unclear although studies have shown that testosterone acts as an L-type calcium channel blocker, and induces potassium channel activation in vascular smooth muscle cells (Jones et al., 2003). Both these actions act to dilate vascular smooth muscle. Dilation of the vasculature may also occur by testosterone supplementation increasing nitric oxide production in vascular endothelial cells (Miller and Mulvagh, 2007). Together these observations suggest that testosterone may be beneficial for patients with ischemic heart disease by improving coronary blood flow. In support of this, testosterone supplementation in men with chronic stable angina has been shown to improve symptoms of cardiac ischemia (Mathur et al., 2009; English et al., 2000). Testosterone replacement therapy also reduces peripheral vascular resistance in chronic heart failure (Caminiti et al., 2009).

Vascular function plays a central role in the development and progression of heart failure. Endothelial function and nitric oxide availability affect myocardial function, systemic and pulmonary hemodynamics, and coronary and renal circulation. Arterial stiffness modulates ventricular loading conditions and diastolic function, which are key components of heart failure with preserved ejection (HFpEF). Endothelial dysfunction is characterized by reduction of the bioavailability of vasodilators, particularly nitric oxide (NO), and/or an increase in endothelium-derived contracting factors. The resulting imbalance leads to an impairment of endothelium-dependent vasodilation (Hadi et al., 2005). The severity of heart failure is associated with nitric

oxide imbalance and endothelial dysfunction (Davignon and Ganz, 2004; Bauersachs and Widder, 2008). Endothelial dysfunction increases afterload due to systemic (Varin et al., 2000) and pulmonary vascular constriction (Ben Driss et al., 2000; Moraes et al., 2000). Endothelial dysfunction results in regional vasomotor dysregulation and decreases coronary circulation (Treasure et al., 1990). The impaired myocardial perfusion worsens ventricular function (Bauersachs and Widder, 2008). Endothelial dysfunction contributes to impaired arterial distensibility and increased vascular stiffness, enhancing myocardial damage (Buus et al., 2001; Scherrer-Crosbie et al., 2001; Massion et al., 2003).

One of the consequences of low testosterone levels that contributes to the development and progression of heart failure is endothelial dysfunction (Lopes et al., 2012). Endothelial dysfunction is prevalent in heart failure patients, and is a predictor of adverse events in these patients (Marti et al., 2012). As diseases of the arteries in men and women progress with advancing age, there is gradual stiffening of the aorta and central elastic arteries in addition to vessel obstruction and ischemia (Quinn et al., 2012). Arterial stiffness is associated with adverse cardiovascular events independent of atherosclerosis (Fleenor and Berrones, 2015). Low endogenous testosterone levels in older men are also associated with increased arterial stiffness (Dockery et al., 2003).

Arterial stiffness is also implicated in the pathogenesis of heart failure (Marti et al., 2012). The stiffening of the arteries is associated with adverse cardiovascular events in heart failure patients (Quinn et al., 2012). The underlying process responsible for arterial stiffness is manifest as systolic hypertension (high blood pressure) (Fleenor and Berrones, 2015). The stiffening of the arteries by arterial remodeling and intimal

calcification increases the risk of fatal and non-fatal cardiovascular events (Quinn et al., 2012). Arterial stiffness may exacerbate heart failure, especially HFpEF (Marti et al., 2012). In an *in vitro* study, testosterone supplementation was shown to inhibit vascular smooth muscle calcification via an androgen receptor pathway (Lopes et al., 2012). Pulse wave velocity was ameliorated by testosterone supplementation in hypogonadal men with coronary artery disease (Yaron et al., 2009).

Stiffening of the aorta occurs with advancing age, and is a primary cause of the major form of hypertension, isolated systolic hypertension, in older men and women (Franklin et al., 2001; Amery et al., 1991). Testosterone acting on androgen receptors is thought to stimulate the adrenergic system and effect blood pressure (Ely et al., 1997). The levels of endogenous testosterone are inversely related to systolic blood pressure (Khaw and Barrett-Connor, 1988; Fogari et al., 2005). Testosterone is also an activator of the renin-angiotensin-aldosterone system (Rocha et al., 2007). However, clinical studies have reported that testosterone supplementation to treat patients with hypogonadism had no effect on systolic or diastolic blood pressure (Hak et al., 2002), thus the cause–effect relationship of testosterone on blood pressure is not established. Some evidence suggests that hypertension may hasten the age-related fall in testosterone levels (Gray et al., 1991; Fogari et al., 2002). Studies in 18-week-old rodents have demonstrated that testosterone supplementation can produce hypertension, and this can be prevented by a gonadectomy (Dubey et al., 2002). Studies in rodent models also demonstrate that a gonadectomy inhibits excess of the renin-angiotensin system (Lim et al., 2002) and cellular angiotensin-converting enzyme mRNA production (Freshour et al., 2002). Blood pressure differences between male and female mice are likely

mediated through androgen receptor stimulation, as evident from the fact that flutamide, an androgen receptor inhibitor, removes any difference (Reckelhoff et al., 1999). However, as described before, contrary to the effect of testosterone enhancing hypertension, its direct effect on the vasculature is vasodilatation rather than vasoconstriction (Kelly and Jones, 2013). The association between systolic blood pressure and testosterone levels is not well established, although testosterone may influence pathways that generate hypertension (Wilson et al., 2011). There is evidence that low endogenous testosterone levels contribute to endothelial dysfunction, arterial stiffness, and hypertension, all of which have been implicated in the pathogenesis of heart failure. In summary, low testosterone levels cause endothelial dysfunction and arterial stiffening. Low testosterone disrupts vascular function in men and women, which may contribute to the pathogenesis of heart failure.

1.6 Congestive heart failure

With advancing age, several hormones and metabolic signals are altered in a way that instigates progression of heart disease. Testosterone deficiency may contribute to the pathophysiology of heart failure by impairing the anabolic/catabolic balance (Saccà, 2009). Congestive heart failure is among the most common reasons for hospitalization, and has a 1-year mortality that may be as high as 30% (Kaushik et al., 2010). Congestive heart failure is caused by a progressive impairment of the ability of the ventricles to contract and pump blood (Raymond et al., 2003). In systolic heart failure, also referred as heart failure with reduced ejection fraction (HFrEF), systolic function is impaired, which is followed by a state of low cardiac output (Fontes-Carvalho and Leite-

Moreira, 2011). If systolic function is preserved, left ventricular filling in diastole can be impeded and result in elevation of filling pressure and symptoms of heart failure. This kind of heart failure is called diastolic heart failure. Diastolic heart failure is referred to as HFpEF (Fontes-Carvalho and Leite-Moreira, 2011). Even though diastolic heart failure is a common condition worldwide, its pathophysiology is unclear. This is thought to be the reason for a lack of established treatment methods for diastolic heart failure (Komamura, 2013). The main differences between diastolic and systolic heart failure are the presence of contractile dysfunction and left ventricular remodeling. In systolic heart failure, progressive ventricular dilatation, or eccentric cardiac hypertrophy, can be seen. By contrast, diastolic heart failure exhibits concentric ventricular remodeling without dilatation or concentric cardiac hypertrophy (Komamura, 2013).

Observational studies in humans reveal that the levels of testosterone are lower in patients with severe heart failure. An interventional pilot study that randomized 20 men with chronic heart failure to receive weekly injections of testosterone enanthate (100 mg) or placebo for 12 weeks found that testosterone treatment significantly improved left ventricular ejection fraction and exercise capacity compared with placebo (Pugh et al., 2002). In contrast, Chung et al. found no improvement in left ventricular ejection fraction and cardiac contractility in congestive heart failure patients treated with 4 weeks of testosterone or nandrolone (Chung et al., 2007). The limited follow-up period of 4 weeks was probably too short to notice any change in echocardiographic parameters in this study. A more recent double-blind randomized control trial by Malkins et al. addressed some of the deficiencies in the previous trials and showed significant clinical benefit in exercise tolerance in patients with moderately severe heart failure following testosterone supplementation for twelve months (Malkin et al., 2006).

There is also emerging evidence that low levels of circulating testosterone may predispose towards the development of congestive heart failure, although, the physiological pathways have not been fully delineated. The effects of bioavailable testosterone have mostly been investigated in patients suffering from HFrEF (Toma et al., 2012). In one study, low testosterone levels occurred in 26 – 37% of men with heart failure of any etiology (Kontoleon et al., 2003; Malkin et al., 2006). Patients with HFrEF frequently have an impaired exercise tolerance (Wilson et al., 1993; Esposito et al., 2010). By contrast, very little is known about the links between testosterone and HFpEF, even though the incidence of HFpEF increases dramatically with age (Tribouilloy et al., 2008; Fonarow et al., 2007; Moutinho et al., 2008). Testosterone therapy may not be appropriate in older patients with HFpEF because testosterone supplementation may increase left ventricular mass, and some of these patients already have enlarged ventricles (Upadhya et al., 2015).

Based on evidence that low testosterone contributes to the pathogenesis of HFrEF, testosterone replacement therapy has been investigated in HFrEF patients with low testosterone levels. Intravenously administered testosterone acutely increases cardiac output and reduces peripheral vascular resistance in these patients (Toma et al., 2012; Pugh et al., 2003). Higher testosterone levels in HFrEF patients treated with testosterone replacement therapy is a significant predictor for an increase in peak oxygen consumption during exercise testing (Caminiti et al., 2009). The effectiveness of testosterone replacement therapy on the exercise capacity of heart failure patients (mean age 67 years of age) was assessed in a meta-analysis of randomized controlled trials. Results showed that 35% of patients treated with testosterone replacement therapy saw an improvement in the New York Heart Association functional class by ≥ one grade

compared to 9.8% of patients in the placebo groups (Toma et al., 2012). The New York Heart Association (NYHA) Functional Classification places patients in one of four categories based on their level of physical activity, breathing, and degree of angina (Miller-Davis et al., 2006). Although some studies of the effects of testosterone replacement therapy on the heart have shown improved left ventricular function in HFrEF patients (Toma et al., 2012), most report no significant changes in left ventricular ejection fraction (Malkin et al., 2006; Iellamo et al., 2010; Pugh et al., 2004; Caminiti et al., 2009). In addition, testosterone therapy has no effect on the higher levels of B-type natriuretic peptide associated with the progression of heart failure (Malkin et al., 2004; Malkin et al., 2006). However, the improvement in exercise capacity and oxygen consumption in HFrEF patients has increased the use of testosterone replacement therapy, even though relatively little is known about the effects of testosterone on the myocardium.

1.7 Effects of testosterone on cardiac structure and function

The mechanism of testosterone effects on left ventricular (LV) structure, and how it affects function is not well understood. Peripheral vasodilation by testosterone reduces cardiac afterload and increases cardiac output (Pugh et al., 2004; Čulić and Bušić, 2013). Testosterone also causes coronary vasodilation causing improved myocardial oxygenation. Testosterone also has other effects such as increased skeletal muscle strength and peak oxygen consumption, increased baroreflex sensitivity and higher hemoglobin levels. These actions of testosterone may help to improve quality of life and functional capacity of patients with heart failure (Toma et al., 2012; Jankowska et al.,

2009). Testosterone possibly directly improves muscle strength by stimulating change of skeletal muscle composition from type II fibers to type I muscle fibers which are associated with greater physical strength (Czesla et al., 1997). There is also evidence that exercise may increase in endogenous testosterone levels (Vingren et al., 2010; Hawkins et al., 2008). For example, higher testosterone levels in heart failure patients are associated with interval training exercise (Caminiti et al., 2014; Hackney et al., 2012).

Low testosterone levels are associated with diastolic dysfunction in men (Jin et al., 2014), and testosterone supplementation may prevent diastolic dysfunction (Jin et al., 2014; Čulić and Bušić, 2015). Half of patients with HFpEF have underlying diastolic dysfunction (Alagiakrishnan et al., 2013; Borlaug and Redfield, 2011). Interestingly, higher serum total and free testosterone in men is associated with decreasing prevalence of diastolic dysfunction. The diameters of the left ventricle and left atrium increase with decreasing total and free serum testosterone. In addition, N-terminal pro-brain natriuretic peptide levels increases and New York Heart Association functional class increases with decreasing total and free serum testosterone (Čulić et al., 2016). N-terminal pro-brain natriuretic peptide is a prohormone that is cleaved to release brain natriuretic peptide. High levels of brain natriuretic peptide in the blood is associated with high pressures inside the heart (Braunwald, 2013).

Clinical studies have explained testosterone's role in preventing diastolic dysfunction in men (Jin et al., 2014; Čulić and Bušić, 2015). The authors noted that a clinical study excluded patients with previous myocardial infarction because testosterone may have adverse effects in hearts where pathological myocardial remodeling has

occurred (Čulić, 2015). In male and female rodent models, testosterone had detrimental effects on post infarction myocardial healing, and worsened cardiac dysfunction. In animal models, testosterone was demonstrated to have anti-proliferative, anti-collagen, and anti-fibrotic effects (Chung et al., 2014). These actions lead to attenuation of cardiac fibrosis in models of heart failure (Kang et al., 2012). In one of the few clinical studies on the subject, an inverse relation was observed between circulating total testosterone and the severity of diastolic dysfunction in patients without a previous incidence of myocardial infarction (Čulić et al., 2016).

Clinical studies have shown that there are male-female differences in the ability of the heart to contract, even in the absence of CVD. For example, women have a higher ejection fraction at rest than men (Buonanno et al., 1982), but men respond to exercise with a greater increase in ejection fraction than women (Hanley et al., 1989; Merz et al., 1996). There is growing experimental evidence that estrogen plays a role in these male-female differences in myocardial contractility (Parks and Howlett, 2013), although testosterone also may contribute.

The influence of androgens on myocardial contractility in humans has been investigated by examining the effects of anabolic-androgenic steroids on heart function. These steroids are synthetic derivatives of testosterone that are used therapeutically, in particular, to stimulate muscle growth (Woerdeman and de Ronde, 2011). They also are used as performance-enhancing drugs in sports, where their use is banned due to potential unfair advantage as well as adverse effects of high doses of these drugs (Kanayama et al., 2010). While some echocardiography studies report that left ventricular mass is increased by anabolic steroid use (Angell et al., 2012; Nottin et al.,

2006; De Piccoli et al., 1991; Urhausen et al., 1989), others report no effect (Hajimoradi and Kazerani, 2013; Thompson et al., 1992; Palatini et al., 1996; Salke et al., 1985), and the apparent increase in mass is abolished when it is indexed to fat-free body mass (Angell et al., 2014). Echocardiography studies also have shown that anabolic steroid use adversely affects myocardial function, although again the data are not consistent. While some report that ejection fraction is attenuated by chronic anabolic steroid use (Angell et al., 2012; Angell et al., 2014), others have found no change in ejection fraction in steroid users (Nottin et al., 2006; Urhausen et al., 1989; Hajimoradi and Kazerani, 2013; Thompson et al., 1992; Palatini et al., 1996). Similarly, although some studies report that anabolic steroid use slows cardiac relaxation (Angell et al., 2012; Nottin et al., 2006; De Piccoli et al., 1991; Urhausen et al., 1989; Angell et al., 2014), others report no effect (Hajimoradi and Kazerani, 2013; Thompson et al., 1992; Palatini et al., 1996). These divergent results likely reflect the difficulties inherent in studies of anabolic steroid use. These include differences in drugs between and within studies, variations in the doses used and the difficulty in obtaining a precise history of drug use in participants. Nonetheless, these clinical studies provide evidence that testosterone may influence cardiac contractile function.

Consistent with these clinical studies describing the impact of androgen abuse in athletes are animal studies which demonstrate the importance of testosterone in the pathogenesis of heart failure at the cellular level. Cardiac remodeling is characterized by compensatory myocyte hypertrophy, and enlargement of the affected cardiac chamber. Cardiac remodeling also involves the formation of scar tissue, and the removal of

destroyed necrotic tissue (Čulić, 2015). Hormones, such as testosterone, are important in maintaining the structure and function of the left ventricle.

Animal studies have demonstrated that supraphysiological levels of testosterone produce a larger myocyte size, an increased left ventricular dimension, and a reduced ejection fraction (Cavasin et al., 2003). Testosterone is thought to affect metabolic parameters at the cellular level, which significantly influence the evolution of myocardial dysfunction and establishment of heart failure. Animal studies have demonstrated that supraphysiological levels of testosterone contribute to cardiac pathologies by stimulating myocyte hypertrophy (Papamitsou et al., 2011). Myocyte hypertrophy was proven to be androgen receptor-mediated (Marsh et al. 1998). Testosterone may also have cytoprotective effects mediated through non-genomic actions (Er et al., 2004).

Testosterone may have a role in modulating cardiac fibrosis. Some animal studies have demonstrated that testosterone may attenuate cardiac fibrosis and the progression of heart failure. Experiments demonstrate that testosterone may attenuate cardiac fibrosis in rodent hearts by inhibiting cardiac fibroblast migration and proliferation (Chung et al., 2014). Testosterone was also shown to inhibit myofibroblast differentiation induced by transforming growth factor-β1. In normal mouse hearts, testosterone also modulated cell signaling and the response of cardiac fibroblasts by decreasing production of collagen via transforming growth factor-β1 and angiotensin II stimulation (Chung et al., 2014). These studies demonstrate that testosterone has androgen receptor-mediated antiproliferative, anti-collagen, and anti-fibrotic effects in the heart.

A study investigated the impact of sex hormones on cardiac remodeling post-myocardial infarction. This study demonstrated that testosterone has detrimental chronic effects on post infarction healing and aggravates cardiac dysfunction in rodent hearts. It also showed that testosterone worsened cardiac remodelling and promoted cardiac dysfunction in both male and female animals (Cavasin et al., 2003). Testosterone supplementation in animals also lead to myocyte rupture, and possibly lethal outcomes. Interestingly, some studies showed that castration of rodents reversed the occurrence of some of these adverse effects of testosterone (Cavasin et al., 2003).

Taken together, these animal studies suggest that testosterone levels within the physiological range have beneficial cardiovascular effects in healthy men and women. However, in pathological conditions, the effects of testosterone can be quite the opposite. Thus, if the pathological cascade of myocardial remodeling has occurred in diseased hearts such as in myocardial infarction or in obesity, then testosterone may have detrimental effects.

Androgens may affect cardiac remodeling in disease conditions, although the effects of androgens on mammalian cardiac myocytes are no fully understood. Testosterone has been shown to activate the cardiac renin angiotensin aldosterone system in rats, and this is associated with increased maladaptive remodeling (Rocha et al., 2007). Testosterone supplementation in men with low testosterone has been shown to reduce remodeling and improve left ventricular ejection fraction (Zhang et al., 2007). Testosterone is also thought to mediate its effects by modulating the balance between interleukin-10 and tumor necrosis factor-α (Zhang et al., 2007). Testosterone may have beneficial effects at the cellular level promoting myocyte survival. It may promote

myocyte survival by inducing the expression of heat shock protein 70 in myocytes (Liu et al., 2006).

Testosterone may prevent or reverse pathological myocardial remodelling (Nahrendorf et al., 2003; Kuhar et al., 2007), however, not all animal studies have supported these findings (Cavasin et al., 2006; Wang et al., 2005). The beneficial effect of testosterone on the myocardium may be due to its anti-inflammatory (Credit et al., 2002) and antioxidant (Barp et al., 2002) properties. Testosterone supplementation in healthy male rats decreases interleukin-6 levels in the myocardium (Credit et al., 2002). Castration activates matrix metalloproteases (Siwik et al., 2001) and reduces myocardial activity of superoxide dismutase, an important element of cellular antioxidative system (Barp et al., 2002).

Testosterone induces protein synthesis and promotes hypertrophy in cardiomyocytes by increasing amino acid incorporation into proteins (Altamirano et al., 2009). Testosterone supplementation in a post-infarction model of heart failure lead to myocardial hypertrophy with significant increase in left ventricular mass, without collagen accumulation or an increase in hypertrophy markers (Nahrendorf et al., 2003). The two isoforms that constitute the functional myosin motor molecule in the heart are the α-myosin heavy chain (α-MHC) and the β-myosin heavy chain (β-MHC). The α-MHC is able to generate a larger force per cross-bridge cycle compared to the β-MHC, and thus is associated with a greater force of contraction (Miyata et al., 2000). Testosterone supplementation stimulates the expression of α-MHC as opposed to β-MHC as is seen in pathological cardiac hypertrophy. This may act as a compensatory

mechanism where testosterone induces a type of cardiac hypertrophy with potentially long term improvement in cardiac function (Marsh et al., 1998).

Studies in rodents have demonstrated several changes that accompany the loss of physiological testosterone levels after castration. These include a smaller heart mass (Schaible et al., 1984), and systolic and diastolic dysfunction (Schaible et al., 1984; Scheuer et al., 1987). Additionally, castration results in an increases β-MHC and a decrease in α-MHCs in cardiomyocytes (Golden et al., 2004). These changes are part of maladaptive remodelling in the pathogenesis of heart failure. Castration is also associated with a decrease in the amount of mRNA for androgen receptors, NCX, L-type calcium channel, and β1-adrenergic receptors in cardiomyocytes (Golden et al., 2002; Golden et al., 2003). The expression of some of these genes return to normal levels following testosterone supplementation in rodent models (Scheuer et al., 1987; Golden et al., 2002; Golden et al., 2003; Golden et al., 2004). These changes in gene expression and translation are associated with a reduced cardiomyocyte contractile capacity (Golden et al., 2003; Golden et al., 2004).

In summary, testosterone may improve the functional capacity of patients with heart failure by modifying the heart at a cellular level. Some, but not all, studies have shown that testosterone has beneficial effects at the cellular level which may allow the heart to compensate for heart failure. The loss of testosterone in animal studies has been shown to have detrimental effects on the heart by modifying the expression of structural and Ca^{2+} handling proteins in the myocyte.

1.8 Testosterone and Arrhythmias

Testosterone also has effects on cardiac electrophysiology and arrhythmogenesis. Experiments have shown that testosterone can modulate the electrophysiological properties of the myocardium by influencing Ca^{2+} and K^{+} channels in the cardiac membrane (Bidoggia et al., 2000; Brouillette et al., 2005; Fulop et al., 2006; James et al., 2007).

Animal studies have shown that testosterone supplementation is associated with higher occurrence of atrial fibrillation (Tsai et al., 2014). The QT interval represents electrical depolarization and repolarization of the ventricles on an electrocardiogram, which can correct the QT interval (QTc) to account for the effect of the heart rate. An abnormally long QT interval is associated with an increased risk of ventricular arrhythmias such as "torsade de pointes" (James and Hancox, 2003; Tisdale, 2016). Higher levels of testosterone in men are associated with shorter QT and QTc intervals. This consequently leads to a reduced incidence of arrhythmogenesis (van Noord et al., 2010). Supraphysiologic doses of testosterone promote ventricular arrhythmias by increasing QTc interval and dispersion (Maior et al., 2010). This was demonstrated by treating congestive heart failure patients with testosterone supplementation, which lead to reduced QT dispersion (Malkin et al., 2003). Supraphysiologic doses of testosterone promote ventricular arrhythmias by predisposing the heart to reentry mechanisms (Sculthorpe et al., 2010). This may be why athletes who abuse anabolic steroids are prone to episodes of atrial fibrillation (Lau et al., 2007; Sullivan et al., 1999).

Low testosterone levels also have been shown to prolong QT interval in castrated animal models. This is restored when testosterone returns to physiological levels (Bai et

al., 2005; Herring et al., 2013; Liu et al., 2003; Scheuer et al., 1987). There is conflicting evidence that questions if testosterone is protective against atrial fibrillation (Magnani et al., 2014; Tsuneda et al., 2009). There is a question of the data's clinical significance as the results from pre-clinical models are not well established. The association of testosterone supplementation with atrial fibrillation is contradicted by a meta-analysis of clinical studies which included middle-aged and older men (Calof et al., 2005).

In summary, low testosterone levels affect cellular changes in the myocardium which affect the electrophysiology of the cell and promotes arrhythmogenesis. Testosterone may have protective effects against electrical disturbances in the myocyte such as atrial fibrillation.

1.9 The impact of testosterone on cardiac contractile function in animal models

Various animal models have been used to investigate the influence of testosterone on myocardial function *in vivo* and in intact hearts. Some investigators have examined the influence of long-term supplementation with testosterone, or other androgens, on cardiac contractile function. However, most have inferred information about chronic testosterone effects from gonadectomy (GDX) experiments, where animals were subjected to bilateral removal of the testes (± testosterone replacement) for varying periods of time. As discussed in detail below, results of these investigations demonstrate that male sex hormones modulate cardiac contractile function in animal models. Relatively little is known about the influence of testosterone on cardiac contractile function in animal models *in vivo*, although one study has investigated the effect of GDX

on myocardial structure and function with M-mode echocardiography (Sebag et al., 2011). These authors report that 10 weeks of hormone deprivation attenuates contractile function, as demonstrated by a decrease in both fractional shortening and ejection fraction compared to hormone-replete control mice (Sebag et al., 2011). GDX also causes concentric remodeling of the heart, characterized by increased left ventricular posterior wall thickness and reduced left ventricular internal diameter in diastole, as well as increased relative wall thickness when compared to intact males (Sebag et al., 2011). These echocardiographic data suggest that prolonged absence of male sex hormones modifies the structure and function of the heart. Still, whether this affects cardiac relaxation and promotes diastolic dysfunction has not yet been investigated with techniques such as tissue Doppler. Such studies would be of considerable interest, as there is evidence that GDX slows relaxation in intact hearts and in isolated myocytes, as discussed below.

A number of studies have explored the effects of testosterone supplementation on myocardial contractility in intact hearts isolated from various animal models. These studies typically used various anabolic-androgenic steroids at high doses to mimic anabolic steroid abuse in exercise training. Most found that chronic administration (8–12 weeks) of 5–50 mg/kg/week of anabolic steroid (e.g., nandrolone decanoate, stanozolol, or 17α-methyl testosterone) suppresses peak left ventricular contractile performance in young adult rats (LeGros et al., 2000; Rocha et al., 2007; Bocalini et al., 2014) but *cf.* (Liang et al., 1993). By contrast, high doses of anabolic steroids have no effect on the rates of left ventricular pressure rise (+dP/dT) or the rates of left ventricular pressure decay (−dP/dT), which indicates that these agents do not affect the time course

of contraction or relaxation (LeGros et al., 2000; Rocha et al., 2007; Liang et al., 1993) but *cf.* (Bocalini et al., 2014). The impact of more physiological steroid concentrations also has been examined. Eleawa et al. (Eleawa et al., 2013) treated young intact rats with concentrations of testosterone propionate (1.5 mg/kg/week; 12 weeks) designed to produce plasma testosterone levels between 3–11 ng/ml, to mimic more physiological concentrations. They found that these lower levels of testosterone had no effect on left ventricular developed pressure (LVDP), +dP/dT, or −dP/dT in Langendorff-perfused hearts (Eleawa et al., 2013). These observations indicate that while high levels of anabolic-androgenic steroids can negatively affect peak cardiac contractile performance, lower concentrations have few effects in animal models. Other investigators have examined the influence of chronic testosterone withdrawal on cardiac contractility in GDX rodents. Studies in Langendorff-perfused hearts show that LVDP is not affected by short-term (2–9 weeks) GDX (Callies et al., 2003; Tsang et al., 2009), but declines after longer-term GDX (e.g., 16 weeks) (Eleawa et al., 2013).

There is evidence that these deficits in contractile function in low-testosterone states may be more prominent at high physiological loads. For example, LVDP is attenuated 3–10 weeks after GDX in working hearts models, but only when hearts are exposed to high left atrial pressures (Schaible et al., 1984; Scheuer et al., 1987). Furthermore, although left ventricular end-diastolic pressure is unaffected by GDX in Langendorff-perfused (Callies et al., 2003) and catheterized hearts (Sebag et al., 2011), it declines when GDX hearts are subjected to high left atrial pressures (Schaible et al., 1984; Scheuer et al., 1987). The time course of contraction is also modified by withdrawal of male hormones. While most studies report that +dP/dT is not affected by

GDX (Sebag et al., 2011; Tsang et al., 2009) but *cf.* (Eleawa et al., 2013), there is evidence that -dP/dT is slowed following GDX (Eleawa et al., 2013; Schaible et al., 1984; Scheuer et al., 1987) but *cf.* (Sebag et al., 2011; Tsang et al., 2009). Consistent with these results, recent work has shown that +dP/dT is also slower in young adult male mice that overexpress aromatase and have much lower testosterone levels (and higher estrogen levels) compared to wild type controls (Bell et al., 2014). Interestingly, these changes in the amplitude and time course of cardiac contraction in hearts from GDX animals are reversed by testosterone replacement (Eleawa et al., 2013). Together, these observations suggest that chronic testosterone withdrawal attenuates peak contraction and slows relaxation, especially when hearts are working under high loads. As cardiac contraction is initiated by a transient rise in cytosolic Ca^{2+} in individual cardiomyocytes, effects of testosterone on contractile function may arise from effects on mechanisms involved in intracellular Ca^{2+} handling.

1.10 Long-term influence of testosterone on the EC-coupling pathway

The effects of testosterone on cardiac contractile function may arise through effects on components of the EC coupling pathway at the level of the myocyte. As SR Ca^{2+} release and contraction are initiated by the cardiac action potential, some investigators have explored the influence of testosterone on action potential properties. Chronic exposure to testosterone itself has no effect on resting membrane potential (RMP), action potential amplitude, or action potential duration at 50% repolarization (APD_{50}) but actually prolongs APD_{95} in rat papillary muscle (D'Antona et al., 2001). By contrast, more recent work in isolated mouse ventricular myocytes has shown that, while

chronic DHT treatment has no effect on RMP, it does cause a marked abbreviation of both APD_{50} and APD_{90} (Brouillette et al., 2005). One factor that might account for discrepancies between these two studies is the difference between chronic exposures to testosterone versus DHT. As reviewed in the 'Biosynthesis of testosterone' section, testosterone can be converted to estrogen by the enzyme aromatase whereas DHT cannot (Stocco, 2012; Cheatham et al., 2008). Therefore, estrogen may contribute to observed effects in studies where testosterone is used as the androgen receptor ligand (D'Antona et al., 2001). Consistent with this idea, chronic exposure to estrogen has been shown to prolong APD in some models (Parks and Howlett, 2014), in particular, when animals are in the estrus stage where estrogen levels peak (MacDonald et al., 2014; Saito et al., 2009; James et al., 2004). Thus, apparent prolongation of APD by testosterone may be due to estradiol produced by aromatization. Certainly the DHT data (Brouillette et al., 2005) suggest that chronic exposure to androgens actually abbreviates APD.

Information about the effects of testosterone on the cardiac action potential also has been inferred from studies where animals were subjected to bilateral GDX through removal of the testes. It seems clear that GDX has no effect on either RMP or action potential amplitude (Brouillette et al., 2005; D'Antona et al., 2001). By contrast, there is general agreement that GDX prolongs APD_{50} (Brouillette et al., 2005; D'Antona et al., 2001) and $APD_{90/95}$ (Brouillette et al., 2005) but *cf.* (D'Antona et al., 2001) in both intact ventricular muscle and in isolated ventricular myocytes. Taken together with the DHT work reviewed above, these observations suggest that chronic exposure to testosterone abbreviates the cardiac action potential, and in its absence, APD is prolonged. Whether this increase in APD leads to abnormal electrical activity that could promote arrhythmias has not been established.

GDX may act to prolong the cardiac action potential by modifying ionic currents to either attenuate repolarization or prolong depolarization. Therefore, a number of investigators have examined the influence of GDX on sarcolemmal proteins and currents. Most studies have examined repolarizing K^+ currents in rodent models 13 to 16 weeks after GDX. There is general agreement that GDX has no effect on transient outward current (ITO), steady state K^+ current (ISS) and inward rectifier K^+ current (IK1), or on the expression of proteins or mRNA levels linked to these currents (Brouillette et al., 2003; Eleawa et al., 2013). By contrast, GDX reduces the magnitude of the ultra-rapid delayed rectifier K^+ current (IKur) and decreases the expression of the corresponding Kv1.5 protein (Brouillette et al., 2003) although this has not been consistently reported (Eleawa et al., 2013). This reduction in peak IKur could contribute to the prolongation of the APD in rodent models. In the rabbit model, where the slow delayed rectifier K^+ current (IKs) is the major repolarizing current (Nerbonne and Kass, 2005), peak IKs also is slightly reduced by GDX (Zhu et al., 2013). These observations suggest that long-term testosterone withdrawal attenuates repolarizing currents, which may help explain the longer action potentials seen in cardiac muscle and myocytes from GDX animals.

Prolongation of the action potential by GDX also could arise through changes in ionic currents that prolong depolarization. Whether Na^+ currents are influenced by GDX has not yet been investigated. However, a few studies have investigated the effect of GDX on L-type Ca^{2+} current (ICa-L). Voltage-clamp studies show that GDX has no effect on peak ICa-L, at least in the rabbit model (Pham et al., 2002). By contrast, the density of 1,4-dihydropyridine (DHP) receptors (L-type Ca^{2+} channels) is markedly reduced by GDX in hearts from male rodents, and this effect is reversed by testosterone

replacement (Golden et al., 2002; Golden et al., 2003). This suggests that GDX may actually reduce Ca^{2+} influx in the heart. In support of this, peak L- and T-type Ca^{2+} currents are enhanced in neonatal rat cardiomyocytes chronically exposed to testosterone (24–30 h in culture), an effect blocked by the nuclear androgen receptor antagonist, flutamide (Er et al., 2007; Michels et al., 2006). Chronic exposure to DHT also increases peak ICa-L and increases the expression of Cav1.2 (the pore-forming subunit of the L-channel) in cultured human ventricular myocytes (Er et al., 2009). These findings suggest that testosterone may increase inward Ca^{2+} currents and that this effect is attenuated by GDX. Thus, Ca^{2+} influx may actually be inhibited by GDX, so enhanced Ca^{2+} influx does not account for the increase in APD observed in the GDX heart. On the other hand, Ca^{2+} influx via ICa-L is the primary trigger for SR Ca^{2+} release. Thus, effects of testosterone on ICa-L could have important effects on cardiac contractility.

Another important sarcolemmal protein that regulates intracellular Ca^{2+} levels is NCX. This exchanger primarily operates to remove one Ca^{2+} from the cell in exchange for three Na^{+} (Fink and Noble, 2010). This generates an inward current that helps maintain the action potential plateau (Fink and Noble, 2010) and could, in theory, help prolong APD in GDX. Whether NCX is modified by testosterone has been investigated in GDX rodents with biochemical and molecular approaches. While several studies have shown that NCX activity and protein expression are unchanged 2 to 10 weeks after GDX (Callies et al., 2003; Tsang et al., 2009; Witayavanitkul et al., 2013), others report that NCX protein levels are reduced (Witayavanitkul et al., 2013) but *cf.* (Sebag et al., 2011). There is also evidence that mRNA levels decline after both short-term (2 weeks) and long-term (16 weeks) GDX, and this effect is abolished by testosterone supplementation (Golden et al., 2002; Golden et al., 2003). As NCX helps remove Ca^{2+} from the cell, a

reduction in NCX in GDX hearts could slow relaxation, as observed in perfused hearts from GDX animals. Still, at present, there is no consensus on the effect of GDX on NCX, and it is uncertain whether NCX helps prolong the APD.

As testosterone modifies electrical activity in the heart, this would be expected to modify Ca^{2+} release and contraction. Indeed, several investigators have directly investigated the impact of GDX on contractions and Ca^{2+} transients in individual ventricular myocytes (reviewed by Ayaz & Howlett, 2015). There is evidence that GDX may slow the rates of relaxation and Ca^{2+} transient decay (Golden et al., 2003; Curl et al., 2009), although whether GDX affects peak responses is unclear (Golden et al., 2003; Tsang et al., 2009). Furthermore, for the most parts the underlying mechanisms responsible for these effects have not been investigated.

1.11 Hypothesis and Objectives

The current clinical and basic science literature strongly suggests that testosterone has an impact on normal cardiac physiology and may contribute to the pathogenesis of various CVDs. The loss of testosterone may facilitate Ca^{2+} dysregulation at the level of the cardiomyocyte. The overall hypothesis to be tested in this thesis is: **Testosterone withdrawal adversely affects the function of the heart via effects on key components of the EC coupling pathway.**

Specific Objectives

The specific objectives that will be addressed in this thesis are:

1. To determine whether GDX modifies myocardial structure and contractile function *in vivo*.

2. To evaluate the impact of GDX on cardiac structure and contractile function *in vitro* at the cellular level.

3. To investigate the impact of GDX on cellular Ca^{2+} handling mechanisms.

4. To determine GDX affects expression of key Ca^{2+} handling proteins.

5. To determine whether changes in cellular electrophysiology accompany changes in Ca^{2+} handling in GDX myocytes.

CHAPTER 2 Materials and Methods

2.0 Animals

Male C57BL/6J mice were purchased from Charles River Laboratories (St. Constant, QC, Canada). These mice were subjected to either a bilateral gonadectomy (GDX), which is a surgical removal of the testis, or a sham surgery at ~ 1 month of age, at the breeding facility. Sham and GDX mice were housed separately in groups of 1-5 at the Dalhousie University Carlton Animal Care Facility. Mice were maintained on a 12-hour light/dark cycle, with free access to food and water.

Mice were aged before experimentation. The hearts of sham and GDX mice were evaluated with echocardiography at ~8-months age. Ventricular myocytes were isolated from both groups of mice at ages 9-12 months. Ventricles were isolated from a subset of mice from both groups for Western blotting experiments. Physical measurements including body weight, heart weight, and tibia bone length were made to determine if GDX resulted in cardiac hypertrophy. The bone mineral density of tibia bones was also measured in a subset of mice.

All animal protocols were approved by the Dalhousie University Committee on Laboratory Animals and conformed to the "Guide to the Care and Use of Experimental Animals" (Canadian Council on Animal Care, Ottawa, ON: Vol. 1, 2nd ed., 1993; Vol. 2, 1984).

2.1 Body composition/Morphometric Assessment

Standard morphometric measures of sham and GDX mice were obtained including body weight, heart weight, and tibia length. In some cases, the tibia bone density was determined with dual energy x-ray absorptiometry (Lunar PIXImus2; GE Medical Systems). Cardiac mass was calculated from the ratio between heart weight and body weight. Cardiac mass was also calculated from the ratio between heart weight and tibia length or tibia bone density.

2.2 Echocardiography

Two-dimensional M-mode and pulse wave Doppler echocardiography were performed to determine the effect of GDX on heart structure and function. Sham and GDX mice were anesthetized with 1-2% isoflurane delivered in 100% oxygen. The chest area was shaved, and electrocardiographic electrodes were placed subcutaneously. Mice were assessed with a high-resolution linear transducer connected to a Vivid 7 imaging system. Images were acquired from the parasternal short-axis view at the mid-ventricular level with a 14-mHz, i13L linear-array transducer (Vivid 7; GE Medical Systems).

Measurements of heart rate were gathered from three consecutive beats. The LV internal dimensions (LVID), interventricular septal thickness (IVS), and posterior wall (LVPW) thicknesses were measured using M-mode acquisition. The stroke volume (SV) was calculated as the difference between the end diastolic volume at systole (EDVs) and the end diastolic volume at diastole (EDVd). Ejection fraction (EF) was calculated as

[(LVDA - LVSA)/LVDA] X 100, where LVDA is LV diastolic area and LVSA is LV systolic area. Fractional shortening (% FS) was calculated as [(LVIDd - LVIDs)/LVIDd] X 100. The LV mass (LVM) was calculated as 1.055 [(IVSd + LVPWd + LVIDd)^3 - (LVIDd^3)]. Relative wall thickness (RWT) was calculated as [(LVPWd + IVSd)/LVIDd].

LV diastolic function was assessed by measuring mitral inflow with pulsed wave Doppler. Passive LV filling peak velocity [E (cm/s)] and atrial contraction flow peak velocity [A (cm/s)] plus deceleration time of E (DT-E), were acquired from the images of mitral valve Doppler flow. The ratio of the E to A waves was calculated to assess LV diastolic filling. The time between LV outflow and mitral inflow was measured to determine isovolumic relaxation time (IVRT). The E-A velocity time index (E-A VTI) was the computed velocity time integral of both E and A wave forms.

2.3 Ventricular myocyte isolation

Sham and GDX mice were alternately chosen during experimentation. Mice were removed from the Carlton Animal Care Facility and then transferred to the laboratory in clean cages. Animals were allowed to acclimate for 30-60 min prior to the start of the myocyte isolation protocol, and then anesthetized via intraperitoneal injection with 120 mg/kg of sodium pentobarbital, co-administered with 3300 IU/kg of heparin. The mice were returned to their cage until they were fully anesthetized (typically 5-10 minutes). The depth of anesthesia was confirmed by observing the absence of the blinking reflex, as well as the absence of the pain reflex in response to a pinched hind

paw. The mice were gently laid in a supine position with each forearm restrained, and their chest was generously soaked with 70% ethanol.

The isolation procedure started by surgically exposing the mouse's ventral thorax by cutting the tissue where the diaphragm attaches below the rib cage. Next, the lateral ribs on both sides were cut rostrally, and the ventral rib cage was folded back to expose the heart. The aorta was then cut, and a cannula was gently inserted into the aorta. The cannula was then secured by a silk suture (A-55, Ethicon Inc., Somerville, NJ). The cannulated heart was then connected to a perfusion apparatus, and a Cole Parmer pump (Cole Parmer Instruments, Chicago, IL) was activated to perfuse the coronary circulation at a rate of 2 mL/min. All perfusion solutions were initially warmed to 37°C by a Haake D1 circulating water heater (Fisher Scientific, Ottawa, ON), and then delivered through a water-jacketed heating coil (Radnoti Glass Technology Inc., Monrovia CA, USA) to ensure that solutions maintained a temperature of 37°C. A "bubble trap" was created in the perfusion system by a partial bifurcation in the heating coil, so that any bubble was trapped and removed before reaching the heart. The success of the bilateral GDX, or sham surgery, was confirmed by visual inspection of the presence, or absence, of testis.

Hearts were first perfused (2 mL/min) with oxygenated (100% O_2, Praxair, Halifax NS) isolation buffer solution containing (in mM): 105 NaCl, 5 KCl, 25 HEPES, 0.33 NaH_2PO_4, 1.0 $MgCl_2$, 20 glucose, 3.0 Na^+-pyruvate, and 1.0 lactic acid, 100 μM Ca^{2+} for 5 min, then with nominally Ca^{2+} free buffer for 10 min (pH 7.4, with NaOH). After about 10 minutes the blood was washed out of the heart, and any spontaneous contractions stopped. The heart was then perfused with an enzyme solution composed of the isolation buffer supplemented with 50 μM Ca^{2+}, collagenase (8 mg/30 ml,

Worthington Type I, 250 U/mg), dispase II (3.5 mg/30 ml, Roche) and trypsin (0.5 mg/30 ml, Sigma). Hearts were digested by the enzyme solution for 5-7 min, at which point the tissue colour changed from opaque to translucent. Digestion was confirmed by measuring a drop in perfusion pressure to between 0.5 and 1 psi, as read on a low pressure gauge (5 psi, Ashcroft, Stratford CT, USA).

The heart was then placed in a petri dish containing a high K^+ buffer solution of the following composition (in mM): 50 L-glutamic acid, 30 KCl, 30 KH_2PO_4, 20 taurine, 10 HEPES, 10 glucose, 3 $MgSO_4$, and 0.5 EGTA (pH 7.4, with KOH). The ventricles were excised, minced, and then stored at room temperature in this solution. Individual ventricular myocytes were released by gentle, circular, agitation of the beaker storing the minced ventricles in the high K^+ buffer solution. Ventricular myocytes were isolated for three different cellular experiments. All cells selected for experiments were quiescent, rod shaped myocytes, with clear striations, and no observable membrane damage.

2.4 Ventricular myocyte experiments

Ventricular myocytes were isolated and then loaded with a Ca^{2+} sensitive dye (fura-2 AM) to measure intracellular Ca^{2+} handling and contraction simultaneously in field stimulation experiments. Myocytes were also voltage clamped using discontinuous-single electrode voltage-clamp techniques. In some experiments, cells were current clamped to record action potentials. Experiments were also conducted where myocytes were loaded with another Ca^{2+} sensitive dye (fluo-4 AM) to measure spontaneous Ca^{2+} sparks.

2.4.1 Field Stimulation

In field stimulation experiments, ventricular myocytes were loaded with the Ca^{2+} sensitive dye fura-2 AM and field stimulated with platinum electrodes to record contractions and Ca^{2+} transients. An aliquot of the stored myocyte suspension was filtered, through a 225 μm polyethylene mesh filter (Spectra/Mesh) to exclude large cell aggregates, and then incubated with 2.5 μM fura-2 AM (fura-2 AM stock solution in anhydrous DMSO, 0.2% DMSO in cell suspension). Fura-2 AM (Invitrogen, Burlington ON) has an acetoxymethyl ester (AM) derivative group which increases its lipophilicity, and therefore cell permeability (Tsien, 1981). The ester derivative of fura-2 AM is cleaved by non-specific esterases in the cytosol, which results in the loss of its lipophilic derivative and retains fura-2 AM in the cytosol (Tsien, 1981). The esterified derivative form of fura-2 AM is not active, and therefore has little potential for background fluorescence. The fura-2 AM loaded cells were then placed in an experimental chamber attached to the stage of an inverted microscope (Nikon Eclipse TE200, Nikon Canada, Mississauga, ON), and protected from light for 20 minutes at room temperature.

The experimental chamber was a custom-made plexiglass bath chamber with an optical grade glass coverslip (no. 1, 22 x 40 mm VWR International, Montreal, QC) at the bottom of the chamber. The bath was fitted with an inflow channel connected to tubing which delivered solutions to the chamber at a rate of 3 mL/min with a Gilson Minipulse 3 peristaltic pump (Mandel Scientific, Guelph ON). All solutions were warmed to 37°C by a custom designed heat exchanger before entering the bath chamber. On the opposite end of the chamber was an outflow channel connected to tubing for

solution disposal. Cells were superfused with physiological buffers for at least 10 minutes to wash out any fura-2 AM not taken up by the cells.

A Leica micromanipulator (Fine Science Tools Inc., North Vancouver BC) was then used to lower platinum electrodes to the bottom of the chamber on either side of a chosen cell. The threshold to stimulate contraction was then determined and myocytes were paced at 150% of that threshold value, to a maximum of 100 mA with a stimulator (Model # SIU-102; Warner Instruments, Hamden, CT). Myocytes were paced with 3 msec pulses at stimulation frequencies of 2 and 4 Hz. Contractions were recorded simultaneously with $[Ca^{2+}]$ (fura-2 fluorescence). A custom made dichroic mirror (Chroma Tech. Corp. Rockingham, VT) and a red filter (Nikon Canada), exclusive to the long wavelengths of red (>600 nm) light, were installed in the light path of microscope illumination system. The custom made dichroic mirror separated the long wavelength of red light from the fluorescence emission light (discussed later). The cells red light image was directed towards a closed circuit television camera (model TM-640, Pulnix, America), and was used to orient the cells along their long axis when viewed on a closed-circuit television monitor (Electrohome Ltd., Kitchener ON). Raster lines were synced with the edges of the cell to track its movement during contraction with a video edge detector (Crescent Electronics, Sandy UT) at 120 Hz. The difference between cell length at rest to peak contraction was calculated as cell shortening, (normalized to diastolic cell length). Cell length and width were measured for all cells, and used to calculate cell area.

Recordings of fura-2 Ca^{2+} fluorescence were obtained from cells with a Photon Technologies International (PTI, Brunswick, NJ, USA) system. A photomultiplier tube

located above the microscope captured the cell's Ca^{2+} fluorescence. Ca^{2+} bound fura-2 is excited by 340 nm excitation light, while unbound fura-2 is excited by the 380 nm wavelength of excitation light (Grynkiewicz et al., 1985). Excitation light at both wavelengths was generated using a DeltaRAM high speed multiwavelength illuminator (PTI), which cycled between transmitting 340 nm and 380 nm wavelengths of light every 2 msec. Both wavelengths of excitation light were collected at a sampling rate of 200 Hz and then transmitted with a fiber optic coupler (PTI) towards the objective. A computer driven shutter device (SC-500 shutter controller, PTI) was used to remotely control excitation events. At both excitation wavelengths, cells emitted fluorescent light at a wavelength of 510 nm wavelength from the Ca^{2+} bound, and Ca^{2+} unbound fura-2. The emitted light was collected by the photomultiplier tube and recorded by Felix software (version 1.4, PTI, Brunswick NJ, USA). The background was subtracted from recordings at each wavelength, the ratio of emissions was then calculated and the ratios were converted to intracellular Ca^{2+} concentrations using a fura-2 calibration curve. The difference between the peak systolic Ca^{2+} and diastolic Ca^{2+} were calculated as the Ca^{2+} transient amplitude. pClamp software (version 8.2; Molecular Devices, Sunnyvale, CA) was used to record and analyze contraction data. The buffer used for field stimulation experiments is shown in Table 2.1 and the buffer used in voltage clamp experiments is shown in Table 2.2.

2.4.2 Voltage clamp experiments

High resistance microelectrodes (16–24 M Ω) were pulled with a Model P-97 Flaming/Brown Micropipette Puller (Sutter Instruments CO., Novato, California, USA). The tip of the electrode was then filled with filtered 2.7 M KCl up to one-third of the way up the shaft. The electrode was then affixed to an Axon Instruments HL-U microelectrode holder, and a silver wire was inserted into the KCl solution in the electrode. The electrode holder was then inserted into the jack at the front of the headstage (Axon HS-2A Headstage, Gain x 0.1 LU) amplifier, and mounted on a micromanipulator for precision movement of the electrode. A salt bridge was created, made up of 1% agar in 2.7 M KCl in a "C" shaped glass tube, to ground the experimental chamber after the electrode tip was inserted into the bath solution. One end of the agar bridge was placed in the bath chamber, with the other end placed in a well of 2.7 M KCl, which also contained a chloride coated silver ground wire. The other end of the ground wire extended to back of the headstage, where it was soldered to a brass pin inserted into the grounding jack.

An Axoclamp 2B amplifier (Molecular Devices, Sunnyvale, CA) was used for discontinuous single electrode voltage clamp. The electrode resistance (18-28 MΩ) was determined by passing 1 nA of current through the electrode. The resistance was neutralized by balancing the bridge control. The voltage waveform created by the microelectrode capacitance charging and decay was visualized on an oscilloscope (Model COR5541U, Kikusui Electronic Corp., Japan). The rate of charging to decay was then maximized using the amplifier in discontinuous current-clamp mode.

The microelectrode headstage was then used to lower the electrode to a myocyte. The electrode was in position when it was moved close enough to dimple the cell membrane. A brief, high frequency oscillatory current then facilitated the electrode through the cell membrane. Myocytes were then superfused with the solution described above, with the addition of lidocaine (0.3 mM) to inhibit Na^+ current, and 4-aminopyridine (4 mM) to inhibit transient outward K^+ current. A pre-pulse to -40 mV prior to test pulses also inactivated the Na^+ current. Discontinuous single-electrode voltage clamp mode was then used to measure transmembrane currents. This mode enabled the separate measurement of membrane voltage, and injection of current, through a single electrode. Briefly, the Axoclamp amplifier sampled the membrane voltage, and compared it to the user-set command voltage. The amplifier cycled rapidly (5-6 KHz) between sampling the membrane voltage and injecting current to achieve the command voltage.

Voltage clamp protocols were designed using pClamp software (version 8.2; Molecular Devices, Sunnyvale, CA). Myocytes were paced with a series of five, 50-ms conditioning pulses from -80 mV to 0 mV (2 Hz) to generate common activation histories, followed by repolarization to -40 mV for 450 ms to facilitate inhibition of Na^+ currents. Myocyte shortening, Ca^{2+} transients, and ICa-L currents were recorded simultaneously during 250 ms test pulses to varying potentials. Ca^{2+} transient amplitudes were calculated as the difference between peak systolic and the Ca^{2+} concentration prior to the test pulse (at -40 mV). The diastolic Ca^{2+} of voltage clamped cells was measured at -80 mV. The difference in cell length from diastolic length to peak contraction was calculated as cell shortening, which was then normalized to resting

cell length. Peak Ca^{2+} currents were measured and normalized to cell capacitance as described previously (Parks et al., 2014). The Ca^{2+} current was integrated to measure total Ca^{2+} flux, and the decay of the Ca^{2+} current (tau) was measured by fitting the recordings with an exponential function (Clampfit 8.2, Molecular devices). The gain of EC coupling, which represents the amount of SR Ca^{2+} released per unit Ca^{2+} current, was calculated as the absolute ratio of the Ca^{2+} transient (nM) per unit of normalized Ca^{2+} current (pA/pF). The rendered cell volume was calculated by dividing cell capacitance by 8.44 pF/pl, which is the calculated capacitance-volume ratio of ventricular myocytes isolated from rats (Satoh et al., 1997)

The SR Ca^{2+} content in voltage clamped cells was assessed by first giving a series of conditioning pulses, then holding at -60 mV before applying caffeine using a rapid solution switcher (control valves: LFAA1201710H; The Lee Company, Westbrook, CT) controlled with pClamp software. Caffeine is a strong activator of the RyR and thus causes the release of Ca^{2+} from the SR (Bers, 2001). The SR Ca^{2+} content of each cell was determined by the rapid application (1s) of 10 mM caffeine solution containing (in mM): 10 caffeine, 140 LiCl, 4 KCl, 10 glucose, 5 HEPES, 4 $MgCl_2$, 4-aminopyridine, and 0.3 lidocaine. The difference between peak caffeine-induced Ca^{2+} transient and the Ca^{2+} concentration prior to test pulse was calculated as SR Ca^{2+} content. Fractional release of SR Ca^{2+} was calculated as the ratio of the Ca^{2+} transient amplitude to the total SR Ca^{2+} released.

2.4.3 Confocal microscopy: Measurement of spontaneous Ca^{2+} Sparks

Ca^{2+} sparks were recorded and measured as described previously (Fares et al., 2012). Myocytes were loaded with Fluo-4 AM (20 μM, 30 min at room temperature; Invitrogen, Burlington, ON) in a laminin-coated chamber (1 mg mouse laminin/100 ml M199 medium) on the stage of a laser scanning confocal microscope (Zeiss LSM 510-Meta, Carl Zeiss Canada Ltd, Toronto, ON). The myocytes were superfused at 4 ml/min with buffer (pH 7.4; 37°C) containing (in mM): 135.5 NaCl, 4 KCl, 10 HEPES, 1 $MgCl_2$, 10 glucose, 2 $CaCl_2$, and 2 probenecid. LSM software (version 3.2, Carl Zeiss Canada Ltd) was used to control the argon laser (488 nm) and collect line scan images (525 nm, 98 μm pinhole size, scan speed=649.35 lines/s, 512 pixels/line, 20% laser intensity). Myocytes were first visualized with an x-y scan, and then line scanned for 4 seconds per cell.

Spontaneous Ca^{2+} sparks were analyzed with the SparkMaster plug-in (Picht et al., 2007) for ImageJ software (v1.34, NIH). Ca^{2+} sparks were identified as areas of fluorescence intensity (F) greater than 3.8 times the standard deviation above background (F_0). Each image was then inspected to exclude clusters of multiple sparks that were calculated as a single spark and extended bright lines that were also erroneously detected as sparks. The spark amplitude ($\Delta F/F_0$) was calculated as the change in fluorescence intensity from the background fluorescence intensity. The full width at half maximum (FWHM), the time-to-peak (TTP), full duration at half maximum (FDHM), and decay (tau) of the spontaneous Ca^{2+} sparks were measured. Ca^{2+} spark frequencies (sparks/100 μm/sec) of sham and GDX myocytes were also examined.

2.5 Western blotting

Western blotting was performed to determine protein levels of Cav1.2, NCX, RyR2, SERCA, PLB, and Kv1.5. Sham and GDX mice were first anesthetized and prepared for surgery (as described in section 2.4). The ventricles were then cut away from the atria, flash frozen in liquid nitrogen, and stored at -80ºC until use. The ventricles were homogenized (1 min) with a glass Dounce homogenizer (Sigma) in cold Radioimmunoprecipitation assay buffer containing: 1% Triton X-100, 1% sodium deoxycholate, 0.1% SDS, 150 mM NaCl, 50 mM TRIS-HCl pH 7.8, 1 mM EDTA, 1 mM EGTA plus a protease inhibitor cocktail (Halt protease inhibitor cocktail, Thermo) and phosphatase inhibitor cocktail (Halt™ Phosphatase Inhibitor Cocktail, Thermo). The homogenates were then centrifuged (12000 RPM, 4ºC, Beckman Coulter) for 10 min to remove cellular debris. The supernatant was aliquoted, flash frozen in liquid nitrogen, and then stored at -80ºC. One aliquot from each sample was used for quantifying the sample's protein concentration (DC Protein assay, BioRad, CA, USA).

Homogenates were reconstituted in 4X Laemelli sample buffer, and then heated (70ºC, 5 mins). In all Western blot experiments, equal amounts of sham and GDX sample protein (25 μg per well) were resolved on 7% polyacrylamide gels. Primary antibodies used were Na^+/Ca^{2+} exchanger (NCX; SWANT, R3F1, Marly, Switzerland), L-type Ca^{2+} Channel ($Ca_v1.2$; Alomone, ACC-003-AG, Jerusalem, Israel), SERCA (SERCA2; Thermo Fisher Scientific, MA3-919, Illinois, USA), Ryanodine receptor (RyR2; Sigma, R129, Missouri, USA), potassium voltage-gated channel (Kv1.5; Alomone labs, APC-004, Jerusalem, Israel), phospholamban (PLB; Badrilla, A010-12, Leeds, UK), and β-actin (β-actin, Sigma, A5441, Missouri, USA). Secondary antibodies

used were anti-mouse (Abcam, ab97046) and anti-rabbit (Abcam, ab6721) HRP-conjugated polyclonal antibodies.

The membrane (5 min) was incubated with Clarity™ Western ECL substrate (Biorad, CA, USA), and the chemiluminescent signals of the proteins was imaged using a ChemiDoc MP System (Bio-Rad, CA, USA). Image J software (v1.34, National Institutes of Health) was used for quantification of protein band intensities, and the data obtained was analysed for differences between sham and GDX groups using Sigmaplot software (v12.0, Systat Software Inc.). Some target proteins were normalized by staining the PVDF membrane using either amido black (Naphthol blue, Sigma) or Coomassie blue (Sigma) staining solution to verify equal loading of protein samples.

2.6 Statistical Analyses

Sigmaplot (v12.0, Systat Software Inc.) was used to perform all statistical analyses and construct figures. Data for sham and GDX groups were expressed as the means ± S.E.M. Differences between groups were assessed with a Students t-test for normally distributed data. A Mann-Whitney rank sum test was used for data that were not normally distributed. A Chi-square test was used to evaluate differences between the incidence of spontaneous activity in sham and GDX groups.

2.7 Chemicals

Most chemicals were dissolved in purified deionized water (Elix 3 and Milli-Q plus, Millipore Corporation, Cambridge ON), unless otherwise indicated, and prepared as stock solutions for use in superfusion buffers. Lidocaine, choline chloride, HEPES buffer, EGTA, $MgCl_2$, anhydrous DMSO, and caffeine were purchased from Sigma-Aldrich Canada Ltd. (Oakville, ON, Canada). Fura-2 acetoxymethyl (AM) and fluo-4 AM were obtained from Invitrogen Inc. (Burlington, ON, Canada), prepared as stock solutions, and then stored at -20°C until use. Fura-2 AM was prepared in anhydrous dimethyl sulfoxide (DMSO), and fluo-4 AM was prepared in fetal bovine serum supplemented with Pluronic® F-127 in anhydrous DMSO. Fura-2 AM stock solution was prepared by dissolving 50 µg of fura-2 AM in 20 µL anhydrous DMSO. The solutions for experiments with sham and GDX cells contained the same concentration of DMSO. There was no effect of DMSO (0.02 to 0.1 %) on any of the measured parameters including Ca^{2+} transients, contractions, Ca^{2+} currents, and Ca^{2+} sparks.

Radioimmunoprecipitation assay (RIPA) buffer was prepared for Western blotting experiments, containing: 1% Triton X-100 (Biorad, CA, USA), 0.5% sodium deoxycholate (Sigma), 0.1% SDS (Fisher), 150 mM NaCl (Fisher), 50 mM Tris-HCl pH 8.0, 1 mM EDTA (Sigma), 0.5 mM EGTA (Sigma), protease inhibitor cocktail (100X; Thermo Scientific) and phosphatase Inhibitor Cocktail (100X; Thermo Scientific). The sample protein concentration was determined by dissolving BSA (Sigma) in RIPA buffer.

Table 2.1: Physiological buffer (pH 7.4) superfusing ventricular myocytes during field stimulation experiments.

Chemical[1]	Concentration (mM)
NaCl	135.5
HEPES	10
Glucose	10
KCl	4
$MgCl_2$	1
$CaCl_2$	2

[1]pH with NaOH to 7.4

Table 2.2: Buffer (pH 7.4) superfusing ventricular myocytes during voltage clamp experiments.

Chemical	Concentration (mM)
NaCl	135.5
HEPES	10
Glucose	10
KCl	4
$MgCl_2$	1
$CaCl_2$	2
4-aminopyridine	4
Lidocaine	0.3

CHAPTER 3 Results

3.1 Influence of GDX on cardiac morphology

3.1.1 GDX does not affect heart weight, regardless of the normalization method used

Initial experiments investigated the impact of GDX on physical characteristics of the mice, in particular cardiac morphology, as shown in Table 3.1. Table 3.1 shows that the ages and total body weights of the mice were similar in sham and GDX groups. The mean heart weight was smaller in GDX animals, but this was not statistically significant (Figure 3.1A). Mean heart weight was also not different when normalized to either body weight or tibia length, although GDX mice had longer tibia bones compared to sham controls (Figure 3.1B,C,D). As tibia bones were longer in the GDX group, tibia bone mineral density was also measured with densitometry in the two groups to determine if this was a better index for normalization. Interestingly, tibia bone mineral density was similar in the two groups and heart weight to tibia density ratios showed no evidence of hypertrophy in the GDX group (Figure 3.1E,F). The mean morphological data are summarized in Table 3.1.

3.1.2 Ventricular myocyte length decreases following GDX

Morphological characteristics of isolated ventricular myocytes were also compared between sham and GDX groups, as shown in Table 3.2. Ventricular myocytes from sham and GDX mice were similar in length and width (Figure 3.2A,B), however, GDX myocytes had a smaller cell surface area compared to sham controls (Figure 3.2C).

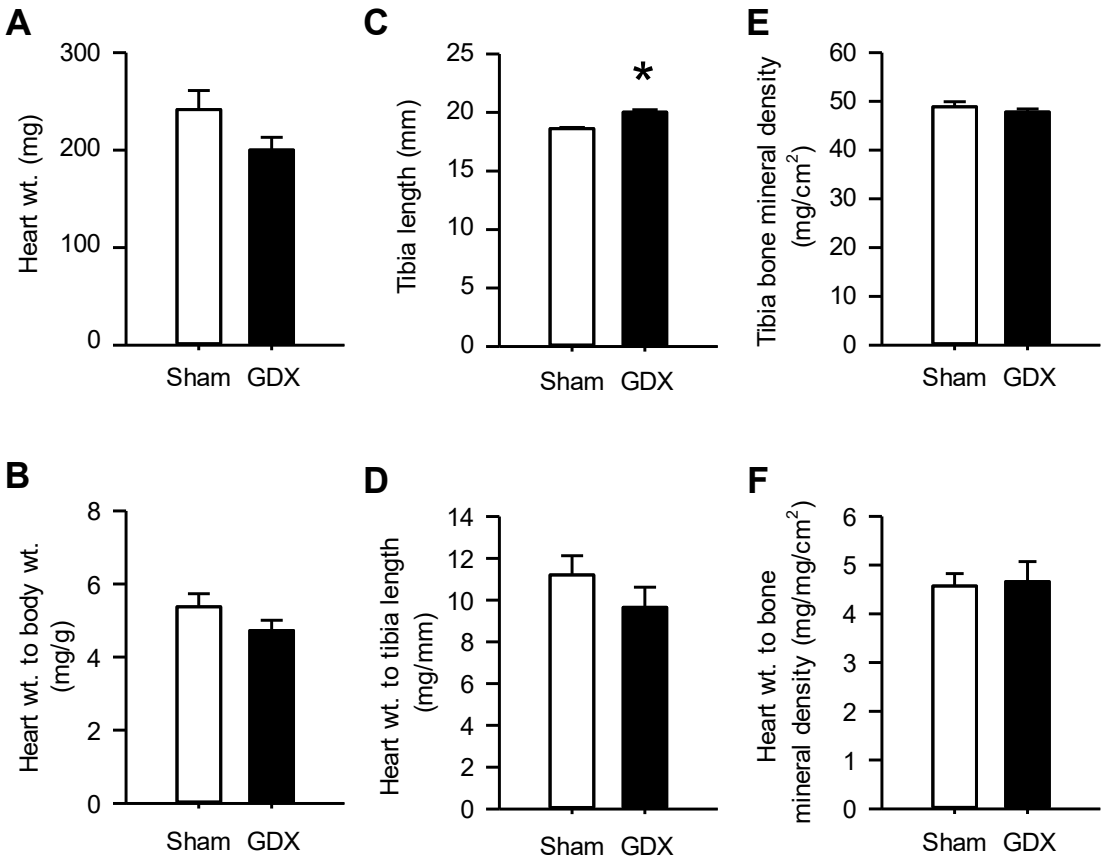

Figure 3.1. Gonadectomy did not result in cardiac hypertrophy in male C57Bl/6 mice when heart weight was normalized to physical parameters. A. The loss of testosterone had no effect on total heart weights or (B) heart weight to body weight ratios in age-matched C57Bl/6 mice. C. Chronic testosterone withdrawal increased tibia bone length in the GDX group of mice compared to sham controls, however, (D) heart sizes were still similar when normalized to respective tibia bone lengths. E. Bone mineral density of tibias were similar in both groups of mice. F. Heart sizes normalized to tibia bone mineral density were also not different. (N=9 sham and 9 GDX animals; * denotes $P<0.05$).

Table 3.1: Physical characteristics of sham and GDX male C57BL/6 mice.

Parameter	sham	GDX	P-value
Age (mos)	15.7 ± 1.7	17.6 ± 0.8	P=0.69
N	9	9	
Body weight (g)	45.5 ± 3.4	43.3 ± 3.0	P=0.63
N	9	9	
Heart weight (mg)	241.4 ± 19.6	200.2 ± 12.9	P=0.10
N	9	9	
Tibia length (mm)	18.6 ± 0.1	20.0 ± 0.2	P=0.01 *
N	5	5	
Tibia bone mineral density (mg/cm^2)	48.8 ± 0.6	47.8 ± 0.7	P=0.31
N	4	4	
Heart to body weight (mg/g)	5.4 ± 0.4	4.7 ± 0.3	P=0.17
N	9	9	
Heart weight to tibia length (mg/mm)	11.2 ± 0.9	9.6 ± 1.0	P=0.28
N	5	5	
Heart weight to bone mineral density ($mg/mg/cm^2$)	4.7 ± 0.4	4.6 ± 0.2	P=0.86
N	4	4	

These are values for mice used in biochemical experiments.
N=number of sham and GDX mice; values represent mean ± SEM.
* denotes significant for $P<0.05$.

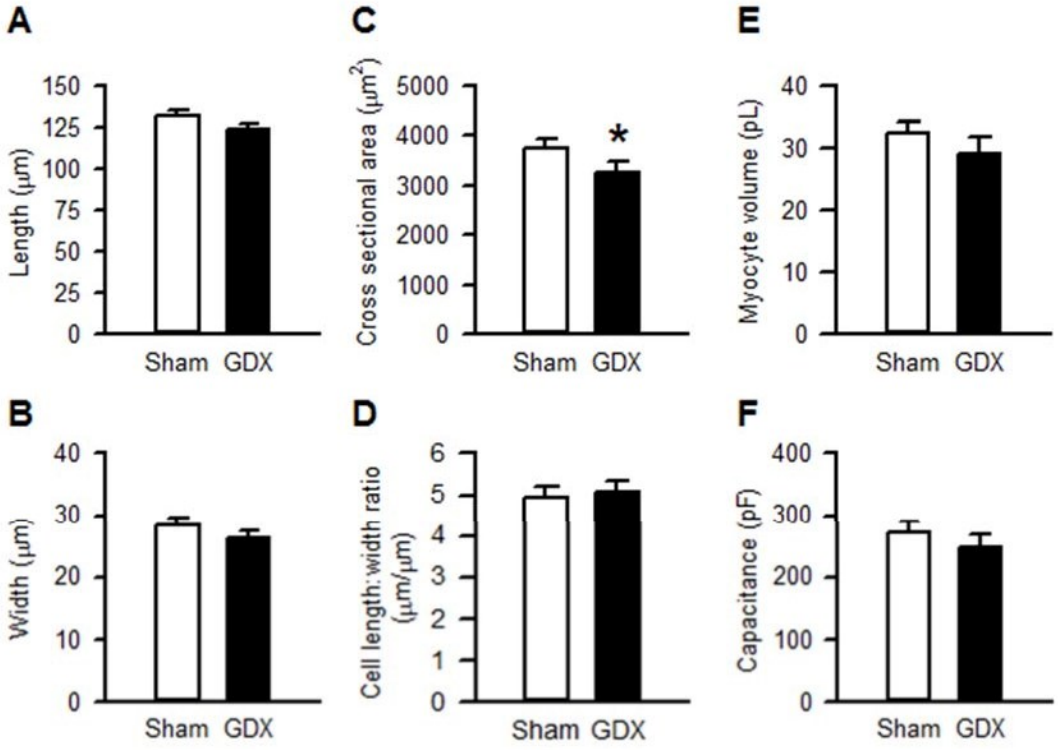

Figure 3.2. Gonadectomy reduced the size of isolated ventricular cardiomyocytes in adult C57Bl/6 mice. A. The resting cell lengths and (B) widths of isolated ventricular cardiomyocytes were slightly smaller in cells from sham compared to GDX, although this difference was not statistically significant. C. However, the cross-sectional areas of cells isolated from GDX mice were significantly smaller compared to sham controls. D. There was no difference in the cell length to width ratios and (E) myocyte volume between the two groups of mice. F. There was no difference in myocyte capacitance between the two groups of mice. (n=49 sham and 41 GDX cells isolated from N=8 sham and 7 GDX animals; * denotes $P<0.05$).

Table 3.2: Characteristics of cardiomyocytes from sham and GDX male C57BL/6 mice.

Parameter	sham	GDX	P-value
Cell length (μm)	131.2 ± 3.7	123.5 ± 3.8	P=0.16
n	49	41	
Cell width (μm)	28.5 ± 1.1	26.1 ± 1.2	P=0.14
n	49	41	
Cell area (μm^2)	3737.6 ± 185.9	3266.3 ± 206.8	P=0.045 *
n	49	41	
Cell length to width ratio (μm/μm)	5.0 ± 0.2	5.1 ± 0.3	P=0.63
n	49	41	
Cell volume (pL)	32.3 ± 2.1	29.2 ± 2.6	P=0.36
n	24	14	
Cell capacitance (pF)	272.3 ± 17.5	246.3 ± 21.8	P=0.36
n	24	14	

N=8 sham and 7 GDX mice; n=number of sham and GDX cells.
Values represent mean ± SEM.
* denotes significant for P<0.05.

The length to width ratio of sham and GDX myocytes was calculated to determine if cells from one group were longer or wider than cells in the other group, and no difference was found (Figure 3.2D). Cell capacitance, a measure of total membrane area, and the rendered cell volume, were also similar in the two groups (Figure 3.2E,F). These observations suggest that GDX does not lead to marked differences in heart size or cell volume. However, the smaller cell area in the GDX group suggests that there may be small changes in cell size in the GDX ventricle. The mean data for the ventricular myocyte characteristics are summarized in Table 3.2.

3.2 *In vivo* evaluation of ventricular morphology and function in sham and GDX mice

3.2.1 GDX promotes thinning of the ventricular septum

The next series of experiments was designed to determine whether GDX affected ventricular structure as measured by echocardiography. Figure 3.3 shows representative examples of M-mode recordings from a sham (Panel A) and a GDX (Panel B) mouse. These examples show that the structure of the LV from sham and GDX mice looks similar. Mean data are illustrated in Figure 3.4. These data show that the interventricular septum in diastole (IVSd) was thinner in GDX compared to sham (Figure 3.4A). The inner diameter of the LV, and the LV posterior wall in diastole were similar in size in sham and GDX mice (Figure 3.4B,C). Similar results were obtained for these structural parameters in systole (IVSs, LVIDs and LVPWs; Table 3.3). The calculated LV mass (Erkens et al., 2015) was reduced in the hearts of GDX mice

A sham

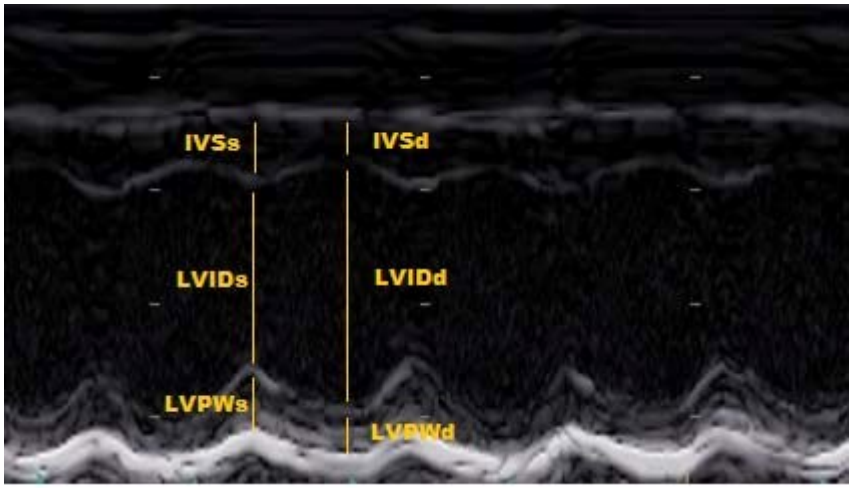

B GDX

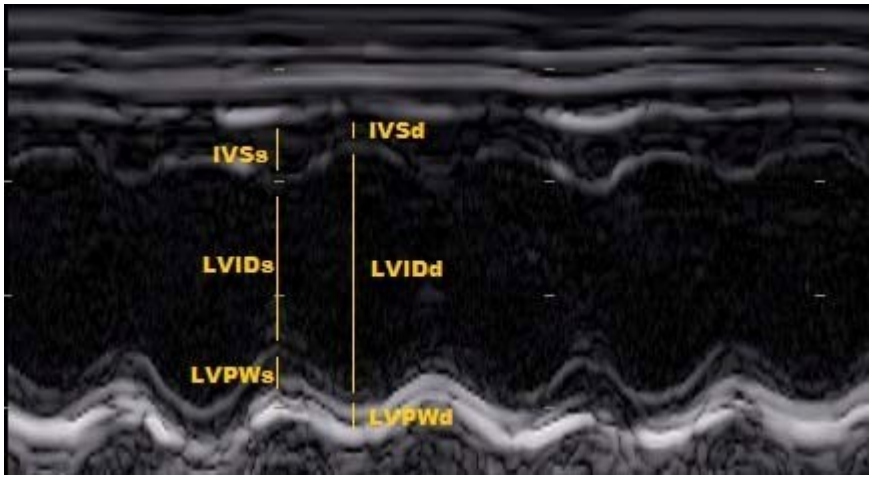

Figure 3.3. Loss of testosterone resulted in a thinning of the interventricular septum. Representative M-mode echocardiograms of the left ventricle from adult male C57Bl/6 mouse after receiving a (A) sham surgery or a (B) gonadectomy (GDX).

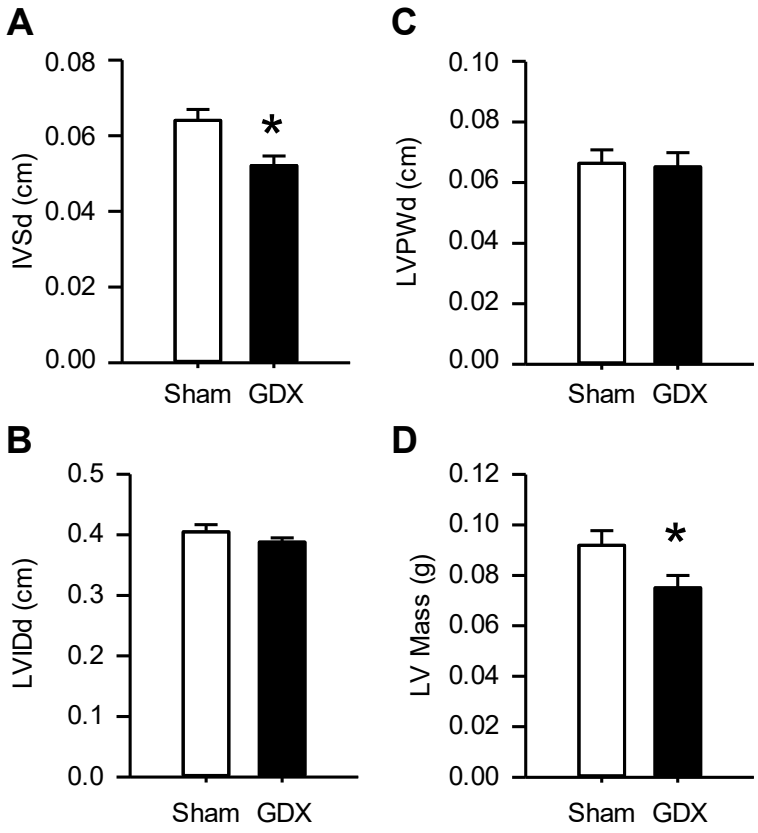

Figure 3.4. Long term testosterone withdrawal thinned the intraventricular septum and reduces left ventricular mass. Left ventricular structural analyses of the C57BL/6 mouse heart with echocardiography. Mice received either a gonadectomy (GDX) or a sham surgery at a approximately 4-5 weeks of age and echocardiography performed at approximately 9 months. A. Intraventricular septum in diastole (IVSd) was thinner in the hearts of GDX mice compared to sham mice. B. The left ventricular (LV) inner diameter in diastole (LVIDd), and (C) the LV posterior wall in diastole (LVPWd) were similar in size in sham and GDX mice. D. The LV mass (LVM), calculated as 1.055 $[(IVSd + LVPWd + LVIDd)^3 - (LVIDd^3)]$, was reduced in the hearts of GDX mice compared to sham. (N=22 sham and 29 GDX animals; * denotes $P<0.05$).

Table 3.3: *In vivo* echocardiographic (M-mode) parameters measured from sham and GDX hearts

Parameter	sham	GDX	P-value
IVSd (mm)	0.64 ± 0.03	0.52 ± 0.03	P=0.003 *
IVSs (mm)	0.97 ± 0.04	0.86 ± 0.04	P=0.04 *
LVIDd (mm)	4.05 ± 0.12	3.88 ± 0.07	P=0.22
LVIDs (mm)	2.99 ± 0.13	2.75 ± 0.09	P=0.12
LVPWd (mm)	0.66 ± 0.05	0.65 ± 0.05	P=0.86
LVPWs (mm)	0.98 ± 0.07	0.91 ± 0.06	P=0.47
Relative Wall thickness	0.33 ± 0.03	0.31 ± 0.02	P=0.48
Calculated LV Mass	0.092 ± 0.006	0.075 ± 0.005	P=0.02 *
Heart rate (BPM)	453.3 ± 15.1	443.4 ± 10.7	P=0.56
Ejection fraction (%)	58.6 ± 2.3	61.8 ± 2.1	P=0.30
Fractional shortening (%)	27.0 ± 1.5	29.2 ± 1.4	P=0.30
End diastolic volume (ml)	0.17 ± 0.02	0.15 ± 0.01	P=0.14
End systolic volume (ml)	0.08 ± 0.01	0.06 ± 0.01	P=0.08
Stroke volume (ml)	0.10 ± 0.01	0.09 ± 0.01	P=0.54

N=22 sham and 29 GDX mice.
LV is left ventricular, IVS is intraventricular septum, LVID is LV inner diameter, LVPWd is LV posterior wall, d is diastole, s is systole.
Data expressed as mean ± SEM.
* denotes significant for $P<0.05$.

compared to sham (Figure 3.4D), although relative wall thickness was not affected (Table 3.3). These observations suggest that the interventricular septum and left ventricular mass decline following GDX. The mean data for the structural parameters of the left ventricle are summarized in Table 3.3.

3.2.2 Effects of GDX on systolic and diastolic function

Function of the ventricles was assessed *in vivo* with M mode echocardiography in sham and GDX hearts as shown in Figure 3.5. The basal heart rates of anesthetized sham and GDX mice were similar (Figure 3.5A). The ejection fraction (Figure 3.5B) and fractional shortening (Figure 3.5C) were not different between groups. The stroke volume of the left ventricle (end-diastolic volume minus end-systolic volume) was also similar in both groups of mice (Figure 3.5D). GDX also had no effect on end-systolic volume or end-diastolic volume (Table 3.3). In summary, there was no difference in ventricular systolic function between sham and GDX mice. The mean data for systolic function are summarized in Table 3.3.

Pulsed waved (PW) Doppler imaging is used to record flow velocities of blood moving through the mitral valve (Quiñones et al., 2002). Diastolic function of the left ventricle was assessed *in vivo* with PW Doppler echocardiography. Figure 3.6 shows representative examples of PW Doppler recordings of the mitral valve from a sham (Panel A) and a GDX (Panel B) mouse. These examples suggest that the filling of the LV in diastole is similar in hearts from sham and GDX mice, as the sizes of the E and A waves were similar. By contrast, the time between aortic valve closure and mitral valve

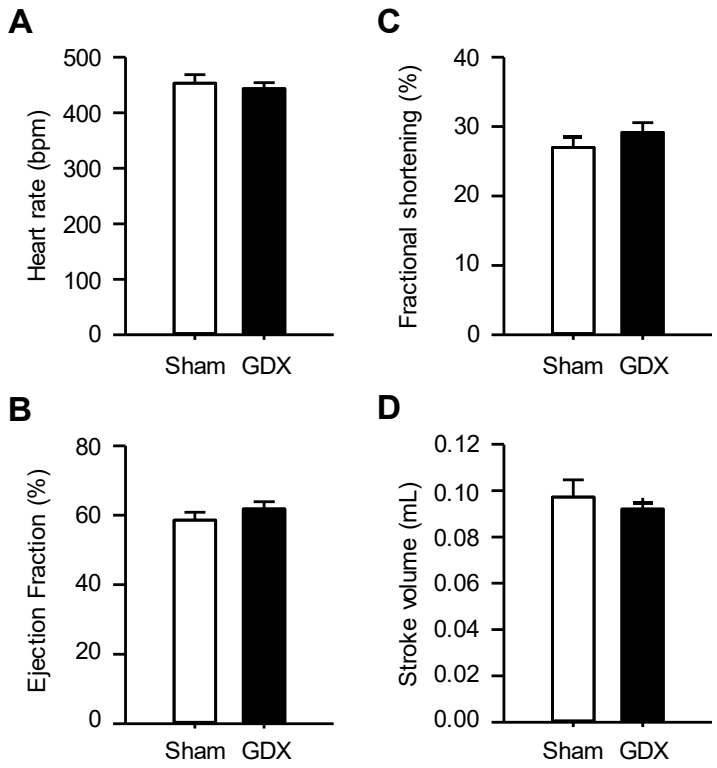

Figure 3.5. Heart rate and left ventricular function in C57BL/6 mice was not affected by chronic testosterone withdrawal. Functional analyses of the hearts of adult C57Bl/6 mice that received either a gonadectomy (GDX) or a sham surgery at approximately 4-5 weeks of age. Echocardiography performed after 9 months. A. The loss of testosterone did not influence basal heart rates. B. The ejection fraction, calculated as [(LVDA - LVSA)/LVDA] x 100, and the (C) fractional shortening, calculated as [(LVIDd - LVIDs)/LVIDd] x 100], were not different between groups of sham and GDX mice. D. The stroke volume of the left ventricle, calculated as [end-diastolic volume (EDV) - end-systolic volume (ESV)] was similar in both groups of mice. (N=22 sham and 29 GDX animals; * denotes $P<0.05$).

A sham

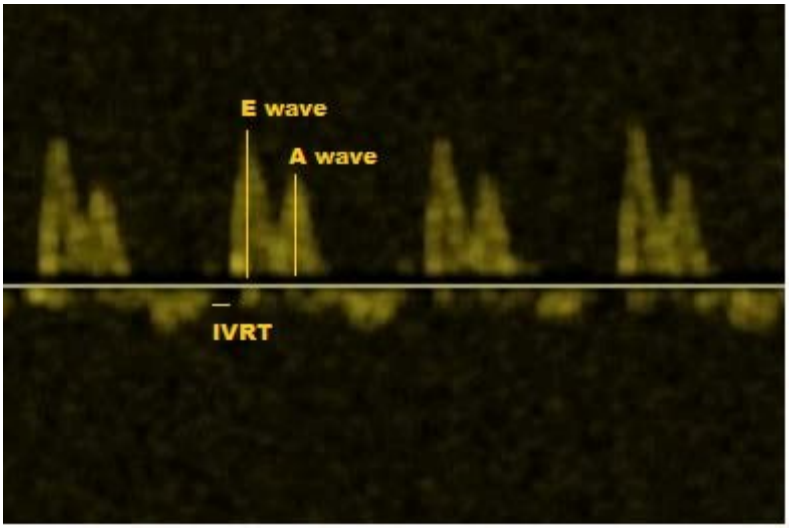

B GDX

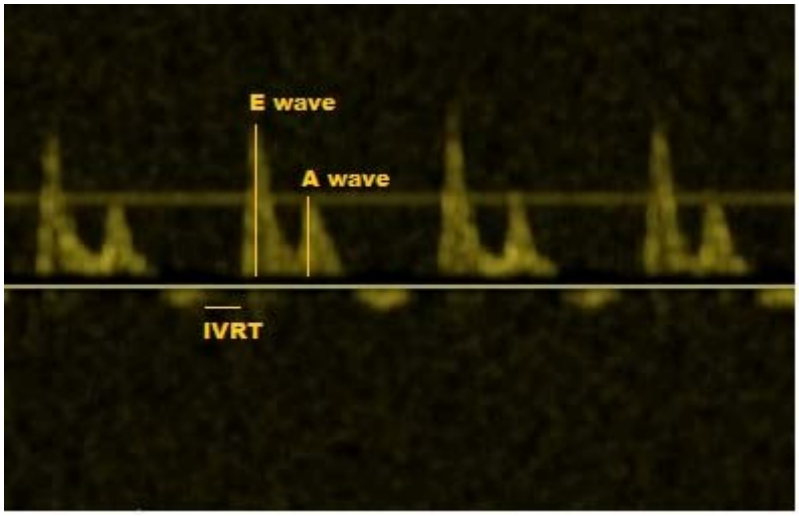

Figure 3.6. The isovolumic relaxation time (IVRT) was increased in GDX hearts compared to sham controls. Representative Doppler echocardiographic images recorded from adult C57Bl/6 mice subjected to either a (A) sham surgery or (B) a gonadectomy (GDX).

opening (IVRT) appeared prolonged in the GDX heart. Mitral valve early velocity values, the deceleration time and the deceleration slope of the E wave were not affected by GDX (Figure 3.7A,B,C). The atrial peak velocity values were also similar in both sham and GDX mice (Figure 3.7D). The ratio of peak E to A waves, a measure of diastolic function, were also not different between sham and GDX mice (Figure 3.7E). However, GDX did increase the time between aortic valve closure and mitral valve opening (IVRT) (Figure 3.7F). These observations suggest that GDX increases the isovolumic relaxation time and attenuates diastolic function. The mean data for diastolic function are summarized in Table 3.4.

3.3 Contractile function and Ca^{2+} homeostasis in field-stimulated ventricular myocytes from sham and GDX mice

3.3.1 Contractions and Ca^{2+} transients were slowed by GDX

The next series of experiments were designed to determine whether GDX affected the contractile capacity of isolated ventricular myocytes when cells were field-stimulated. Figure 3.8 shows representative Ca^{2+} transients (top) and contractions (bottom) from sham (Panel A) and GDX (Panel B) cardiomyocytes stimulated at 2 Hz. These examples suggest that contractions and Ca^{2+} transients were similar in size, but slower in time course in the GDX cell compared to the sham cell. Mean data show that there were no significant differences in peak contractions normalized to resting cell length (cell shortening) and the velocity of shortening when sham and GDX myocytes were stimulated at 2 Hz (Figure 3.9A,B). By contrast, the time course of cell

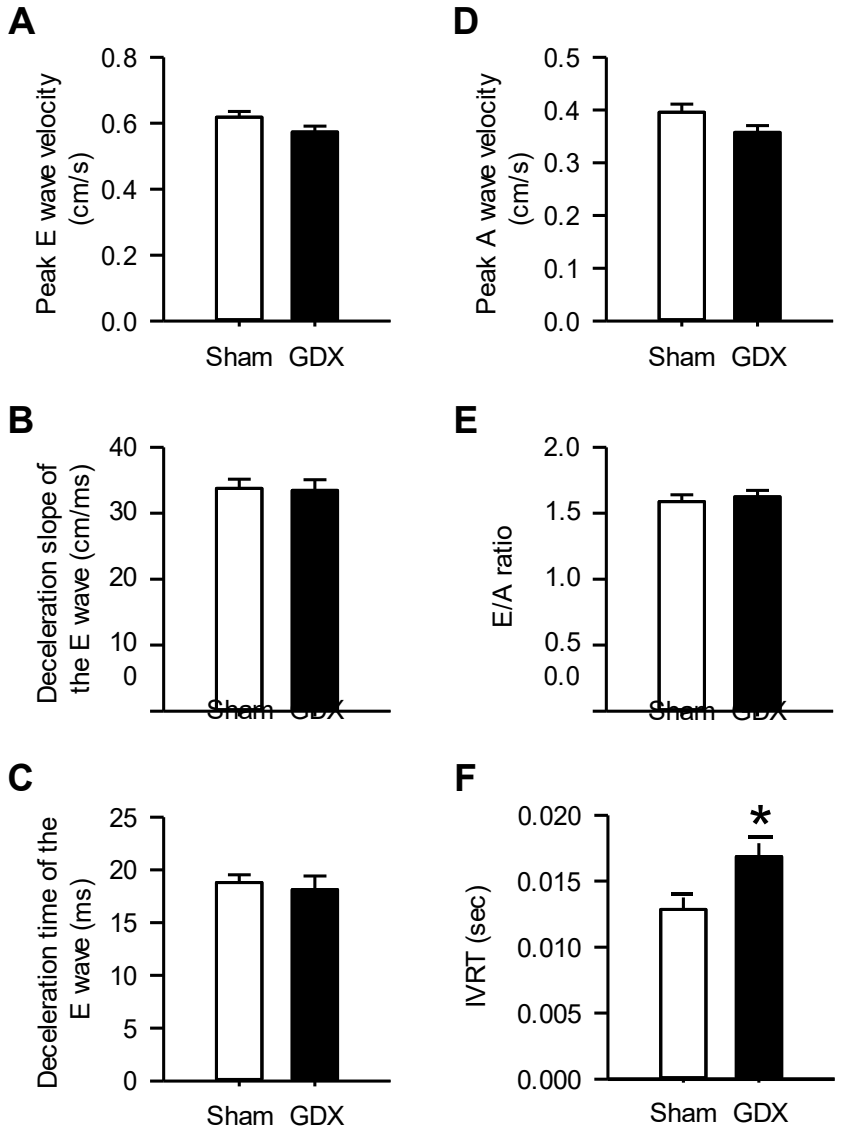

Figure 3.7. The loss of testosterone had no effect on LV diastolic function. The LV of adult male C57Bl/6 mice was assessed by pulse wave Doppler echocardiography at mitral valve inflow. A. Measurements of mitral valve peak early (E) velocity values, (B) the deceleration time, (C) and the deceleration slope of the E wave was not affected by GDX compared to sham controls. D. The atrial (A) peak velocity values were also similar in both sham and GDX mice. E. The E/A ratios, a measure of diastolic function, was not different between sham and GDX mice. F. The isovolumic relaxation time (IVRT) was longer in GDX hearts compared to sham controls. (N=14 sham and 17 GDX animals; * denotes $P<0.05$).

Table 3.4: Pulse wave Doppler echocardiography of mitral valve flow to assess diastolic function in sham and GDX hearts.

Parameter	sham	GDX	P-value
Early mitral inflow velocity (E, m/s)	0.62 ± 0.02	0.57 ± 0.02	P=0.08
N	14	17	
E deceleration time (s)	33.8 ± 1.4	33.5 ± 1.6	P=0.89
N	14	17	
E deceleration slope (m/s^2)	18.8 ± 0.7	18.1 ± 1.3	P=0.67
N	14	17	
A late mitral inflow velocity (A, m/s)	0.40 ± 0.02	0.36 ± 0.01	P=0.07
N	14	17	
E/A Ratio	1.59 ± 0.05	1.63 ± 0.05	P=0.61
N	14	17	
Isovolumic relaxation time (IVRT, s)	0.013 ± 0.001	0.017 ± 0.001	P=0.009 *
N	9	10	
EA velocity time integral (EA VTI)	3.07 ± 0.12	3.13 ± 0.17	P = 0.78
N	9	10	

N=number of sham and GDX mice.
Data expressed as mean ± SEM.
* denotes significant for P<0.05.

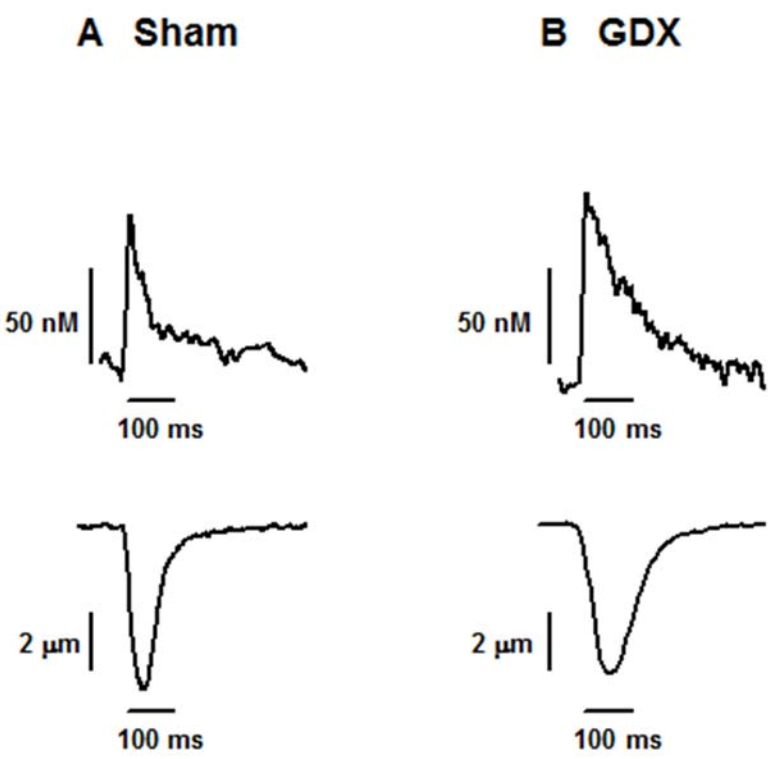

Figure 3.8. Representative Ca^{2+} transients (top) and contractions (bottom) from sham and GDX cardiomyocytes. A,B. This example shows that Ca^{2+} transients and contractions appeared similar in size, but slower in time course in the GDX cell compared to sham control.

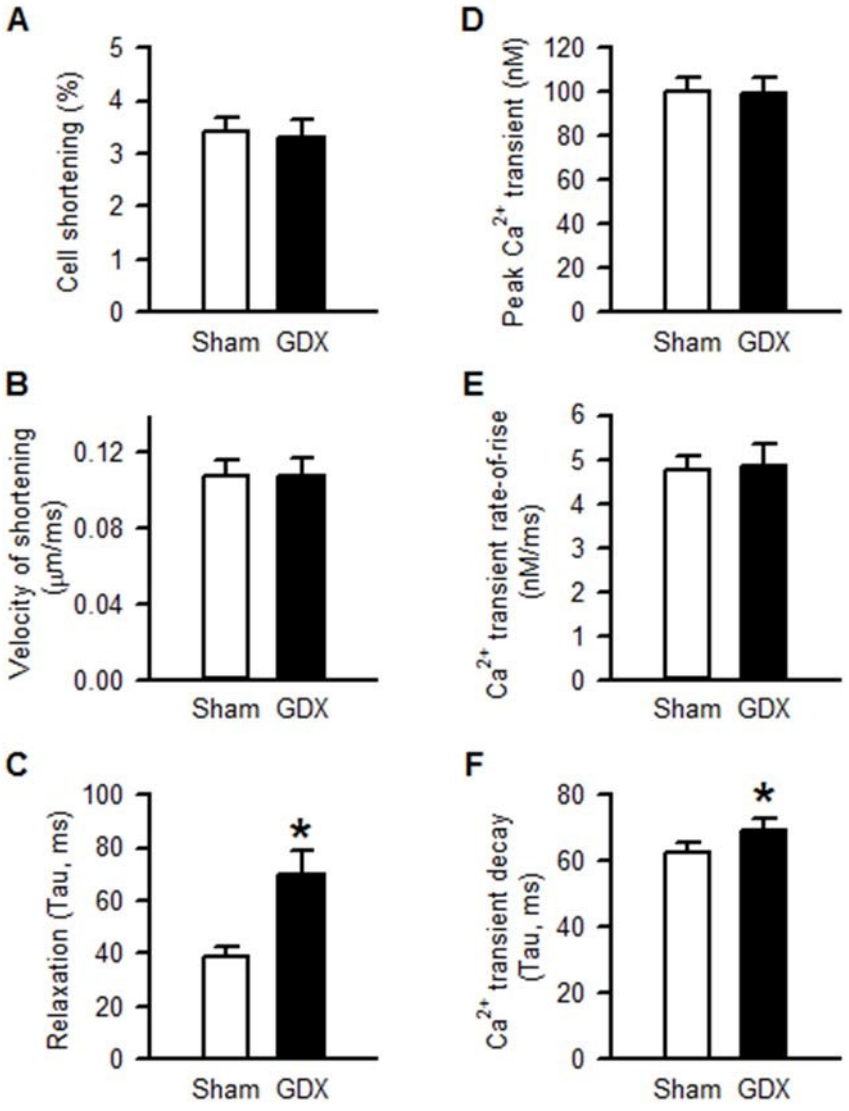

Figure 3.9. Testosterone deficiency prolonged cardiomyocyte contractile relaxation and Ca^{2+} transient decay when cardiomyocytes were field-stimulated at 2 Hz. A. Peak contractions, normalized to resting cell length (cell shortening), and the (B) velocity of shortening were not different between sham and GDX cardiomyocytes. C. GDX prolonged the time course of cell lengthening (Tau) compared to sham controls. D. Peak Ca^{2+} transient amplitudes, and (E) the mean rate-of-rise of Ca^{2+} transients, were not different between sham and GDX myocytes. F. GDX prolonged the time course of Ca^{2+} transient decay (Tau) compared to sham controls. (n=46 sham and 40 GDX cells isolated from N=8 sham and 7 GDX animals; *P<0.05).

lengthening (Tau) was significantly prolonged by GDX compared to sham (Figure 3.9C). There were no differences between groups in peak Ca^{2+} transient amplitudes and the mean rate-of-rise of Ca^{2+} transients (Figure 3.9D,E). However, GDX prolonged the time course of Ca^{2+} transient decay (Tau) (Figure 3.9F). The mean data for contractions and Ca^{2+} transients recorded from myocytes stimulated at a pacing frequency of 2 Hz are summarized in Tables 3.5 and 3.6, respectively. These observations suggest that GDX has no effect on peak contractions and Ca^{2+} transients, but does slow relaxation and Ca^{2+} transient decay in ventricular myocytes paced at a frequency of 2 Hz.

3.3.2 Contractions and Ca^{2+} transients were also slowed by GDX when cells were paced at a higher frequency

To determine if differences between sham and GDX cells would be more obvious at faster pacing rates, in some studies cells were paced at 4 Hz. Cell shortening, and the velocity of shortening, were not different between sham and GDX cardiomyocytes when pacing frequency was increased to 4 Hz (Figure 3.10A,B). By contrast, GDX significantly prolonged the time course of cell lengthening (Tau) compared to sham controls (Figure 3.10C). There was also no difference between the two groups in terms of peak Ca^{2+} transient amplitudes, and the mean rate-of-rise of the Ca^{2+} transients, at the 4 Hz pacing frequency (Figure 3.10D,E). GDX did prolong the time course of Ca^{2+} transient decay (Tau) compared to sham controls at the higher pacing frequency (Figure 3.10F). The mean data for contractions and Ca^{2+} transients from myocytes stimulated at a 4 Hz pacing frequency are summarized in Tables 3.7 and 3.8 respectively. Together, these data indicate that contractions and Ca^{2+} transients in GDX cells decay more slowly

Table 3.5: Characteristics of contractions in sham and GDX cardiomyocytes paced at 2 Hz.

Parameter	sham	GDX	P-value
Cell shortening (%)	3.4 ± 0.3	3.3 ± 0.3	P=0.57
Time to peak (ms)	39.4 ± 1.6	44.9 ± 2.1	P=0.07
Velocity of shortening (μm/ms)	0.11 ± 0.01	0.10 ± 0.01	P=0.20
Half-relaxation time (ms)	29.6 ± 1.7	40.4 ± 3.2	P=0.009 *
Tau of relaxation (ms)	34.2 ± 2.5	46.8 ± 4.8	P=0.03 *

N=8 sham and 7 GDX mice; n=46 sham and 40 GDX cells.
values represent mean ± SEM.
* denotes significant for P<0.05.

Table 3.6: Characteristics of Ca^{2+} transients in sham and GDX cardiomyocytes paced at 2 Hz.

Parameter	sham	GDX	P-value
Peak calcium transient (nM)	101.4 ± 6.8	106.6 ± 9.1	P=0.92
Time to peak (ms)	23.2 ± 1.1	23.5 ± 1.3	P= 0.99
Rate of rise (nM/ms)	4.8 ± 0.4	5.0 ± 0.7	P=0.91
Time to 50% decay (ms)	45.4 ± 2.3	56.6 ± 3.3	P=0.003 *
Ca^{2+} transient decay (Tau, ms)	71.6 ± 3.7	83.3 ± 4.1	P=0.03 *
Diastolic calcium (nM)	242.0 ± 9.7	257.4 ± 12.2	P=0.29
Systolic calcium (nM)	343.4 ± 14.6	364.0 ± 17.9	P=0.26

N=8 sham and 7 GDX mice; n=46 sham and 40 GDX cells.
values represent mean ± SEM.
* denotes significant for P<0.05.

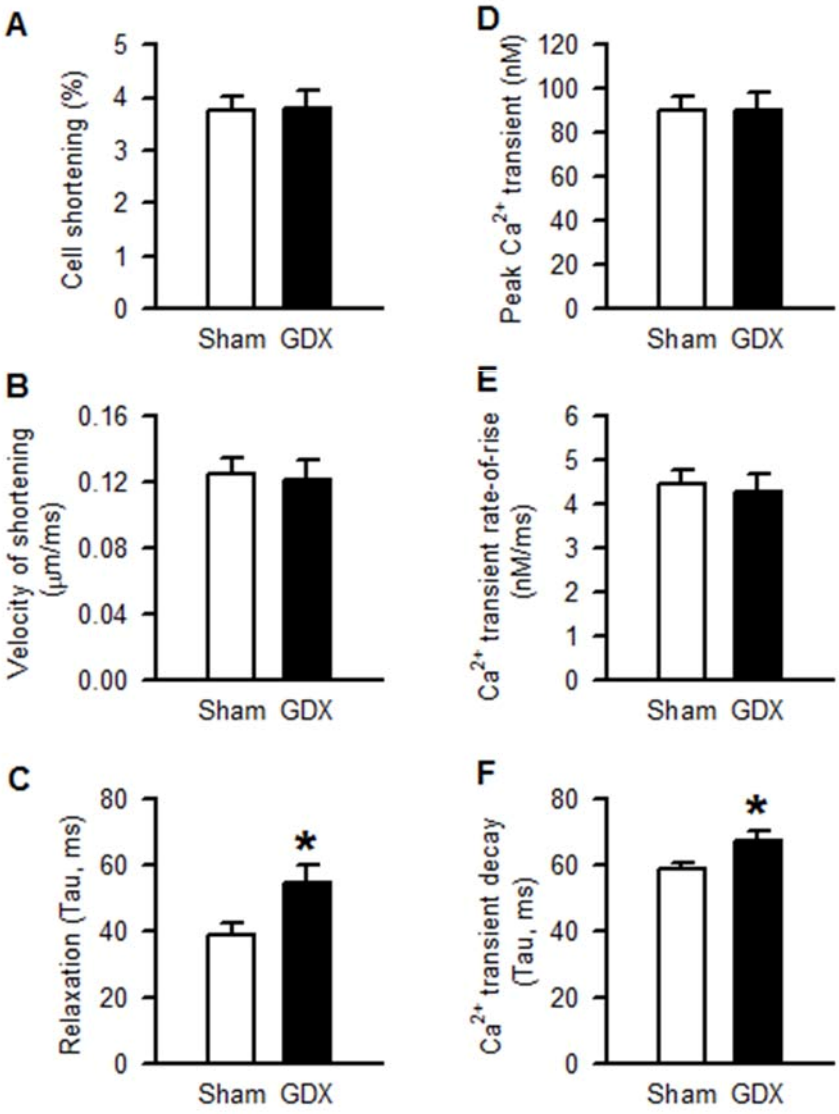

Figure 3.10. GDX prolonged cardiomyocyte contractile relaxation and Ca^{2+} transient decay when the pacing rate was increased to 4 Hz. A. Peak contractions, normalized to resting cell length (cell shortening), and the (B) velocity of shortening were not different between sham and GDX cardiomyocytes. C. GDX prolonged the time course of cell lengthening (Tau) compared to sham controls. D. Peak Ca^{2+} transient amplitudes, and (E) the mean rate-of-rise of Ca^{2+} transients, were not different between sham and GDX myocytes. F. GDX prolonged the time course of Ca^{2+} transient decay (Tau) compared to sham controls. (n=49 sham and 41 GDX cells isolated from N=8 sham and 7 GDX animals; *P<0.05).

Table 3.7: Characteristics of contractions in sham and GDX cardiomyocytes paced at 4 Hz.

Parameter	sham	GDX	P-value
Cell shortening (%)	3.9 ± 0.3	3.8 ± 0.3	P=0.81
Time to peak (ms)	38.8 ± 1.3	41.1 ± 1.6	P=0.22
Velocity of shortening (μm/ms)	0.13 ± 0.01	0.12 ± 0.01	P=0.29
Half-relaxation time (ms)	28.2 ± 1.5	33.7 ± 2.3	P=0.08
Tau of relaxation (ms)	37.4 ± 2.8	54.0 ± 5.6	P=0.04 *

N=8 sham and 7 GDX mice; n=49 sham and 41 GDX cells.
values represent mean ± SEM.
* denotes significant for P<0.05.

Table 3.8: Characteristics of Ca^{2+} transients in sham and GDX cardiomyocytes paced at 4 Hz.

Parameter	sham	GDX	P-value
Peak calcium transient (nM)	91.7 ± 5.5	91.1 ± 7.5	P=0.49
Time to peak (ms)	22.2 ± 0.8	23.2 ± 1.1	P=0.47
Rate of rise (nM/ms)	4.46 ± 0.30	4.38 ± 0.44	P=0.52
Time to 50% decay (ms)	38.9 ± 1.5	44.9 ± 1.7	P=0.01 *
Ca^{2+} transient decay (Tau, ms)	58.3 ± 2.3	68.1 ± 3.5	P=0.04 *
Diastolic calcium (nM)	246.5 ± 7.3	252.4 ± 11.4	P=0.80
Systolic calcium (nM)	338.2 ± 11.4	343.4 ± 16.4	P=0.82

N=8 sham and 7 GDX mice; n=49 sham and 41 GDX cells.
values represent mean ± SEM.
* denotes significant for P<0.05.

than sham controls regardless of pacing frequency, at least when cells were field-stimulated and responses were activated by action potentials.

3.4 Contractile function and Ca^{2+} homeostasis in voltage clamped ventricular myocytes from sham and GDX mice

3.4.1 Peak contractions and Ca^{2+} transients were suppressed by GDX

The next series of experiments investigated whether contractions and Ca^{2+} transients in individual ventricular myocytes were affected by GDX when the duration of depolarization was controlled with a voltage clamp step of fixed duration. Figure 3.11 shows representative Ca^{2+} transients (top) and contractions (bottom) recorded from voltage clamped sham (Panel A) and GDX (Panel B) cardiomyocytes. These examples show that Ca^{2+} transients and contractions were smaller in the GDX cell than in the sham cell. Indeed, mean cell shortening and Ca^{2+} transient amplitudes were significantly smaller in GDX cardiomyocytes compared to sham controls (Figure 3.12A,B). However the rate of relaxation of contraction and Ca^{2+} transient decay rate were similar in sham and GDX cells under voltage clamp conditions (Figure 3.12C,D). In contrast to the effects of GDX in field-stimulated myocytes, these observations suggest that GDX had no effect on contractile relaxation and Ca^{2+} transient decay, but did suppress peak contractions and Ca^{2+} transients when the duration of depolarization was similar in the two groups. This suggests that action potential configuration may be modified by GDX, an idea that will be explored in section 3.7.1. The mean data for contractions and Ca^{2+} transients from voltage clamped myocytes are summarized in Table 3.9.

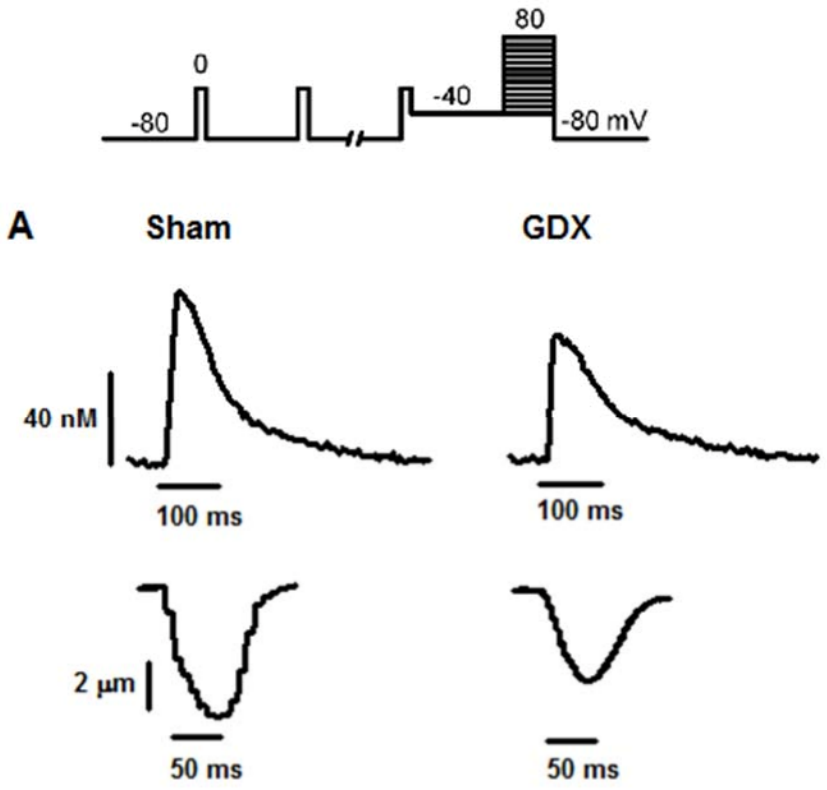

Figure 3.11. (Panel A) Representative Ca^{2+} transients (top) and contractions (bottom) recorded from voltage clamped sham and GDX cardiomyocytes. The voltage clamp protocol is shown at the top. This example shows that Ca^{2+} transients and contractions were smaller in the GDX cell than in the sham cell.

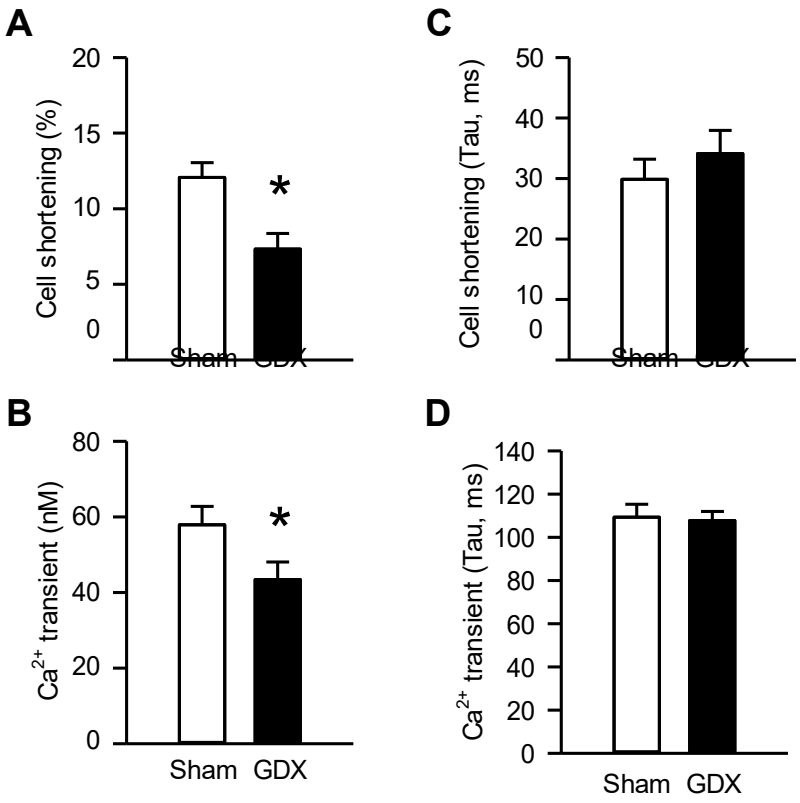

Figure 3.12. Cell shortening and Ca^{2+} transients were smaller in voltage-clamped cardiomyocytes isolated from GDX male C57Bl/6 mice, but contractile relaxation and Ca^{2+} transient decay rates were not affected. A. Peak contractions, when normalized to cell length (cell shortening), and (B) Ca^{2+} transient amplitudes were suppressed in voltage clamped GDX cardiomyocytes compared to sham controls. C. Contractile relaxation and (D) Ca^{2+} transient decay were no longer prolonged compared to sham controls when the cells were voltage clamped. (n=22 sham and 14 GDX myocytes isolated from N=11 sham and 6 GDX animals *P<0.05).

3.4.2 Peak L-type Ca^{2+} currents were smaller in GDX cells than in sham cells

Ca^{2+} currents were recorded during voltage clamp experiments from isolated ventricular cardiomyocytes to determine if smaller peak contractions and Ca^{2+} transients were due changes in the L-type Ca^{2+} current. Figure 3.13A shows representative L-type Ca^{2+} currents recorded from sham (left) and GDX (right) cardiomyocytes. These examples suggest that GDX reduces peak Ca^{2+} currents through the L-type Ca^{2+} channel. The mean data show that peak Ca^{2+} currents were smaller, although Ca^{2+} current decay was prolonged, in GDX ventricular myocytes compared to sham controls (Figure 3.13B,C). Because peak currents were smaller but decay was prolonged, the total Ca^{2+} flux through the L-type Ca^{2+} channel was compared between the two groups. There was no difference in average total Ca^{2+} flux between sham and GDX cells (Figure 3.13D). The gain of EC coupling was also calculated to investigate the amount of Ca^{2+} released per unit Ca^{2+} current. Results showed that the gain of EC coupling was similar in the two groups (Figure 3.13E). Together, these observations suggest that GDX reduces peak Ca^{2+} current, and slows its decay, but does not affect net Ca^{2+} flux across the L-type Ca^{2+} channel. This decrease in peak Ca^{2+} current may help explain the smaller contractions and Ca^{2+} transients observed in GDX cells under voltage clamp conditions. The mean data for these experiments are summarized in Table 3.9.

Table 3.9: Calcium handling properties of sham and GDX myocytes recorded under voltage clamp conditions.

Parameter	sham	GDX	P-value
Cell shortening (%)	12.1 ± 1.0	7.3 ± 1.0	P<0.001 *
n	21	14	
Contraction (tau, ms)	29.9 ± 3.3	34.1 ± 3.8	P=0.42
n	9	9	
Calcium transient (nM)	48.0 ± 3.4	31.0 ± 2.0	P<0.001 *
n	22	14	
Calcium transient (tau, ms)	109.3 ± 5.9	107.7 ± 4.3	P=0.92
n	10	11	
Peak calcium current (pA/pF)	-6.00 ± 0.40	-4.45 ± 0.39	P=0.02 *
n	24	14	
L-type Ca^{2+} current density (pC)	20.6 ± 1.5	20.8 ± 2.2	P=0.97
n	24	14	
Time course of Ca^{2+} current decay (tau, ms)	13.3 ± 0.8	17.3 ± 1.6	P=0.04 *
n	24	14	
Gain of Ca^{2+}release ($nM(pA/pF)^{-1}$)	8.52 ± 0.78	8.33 ± 1.57	P=0.91
n	24	14	

N=11 sham and 6 GDX mice; n=number of sham and GDX cells.
Myocytes were stimulated at 2 Hz.
Data expressed as mean ± SEM.
* denotes significant for P<0.05.

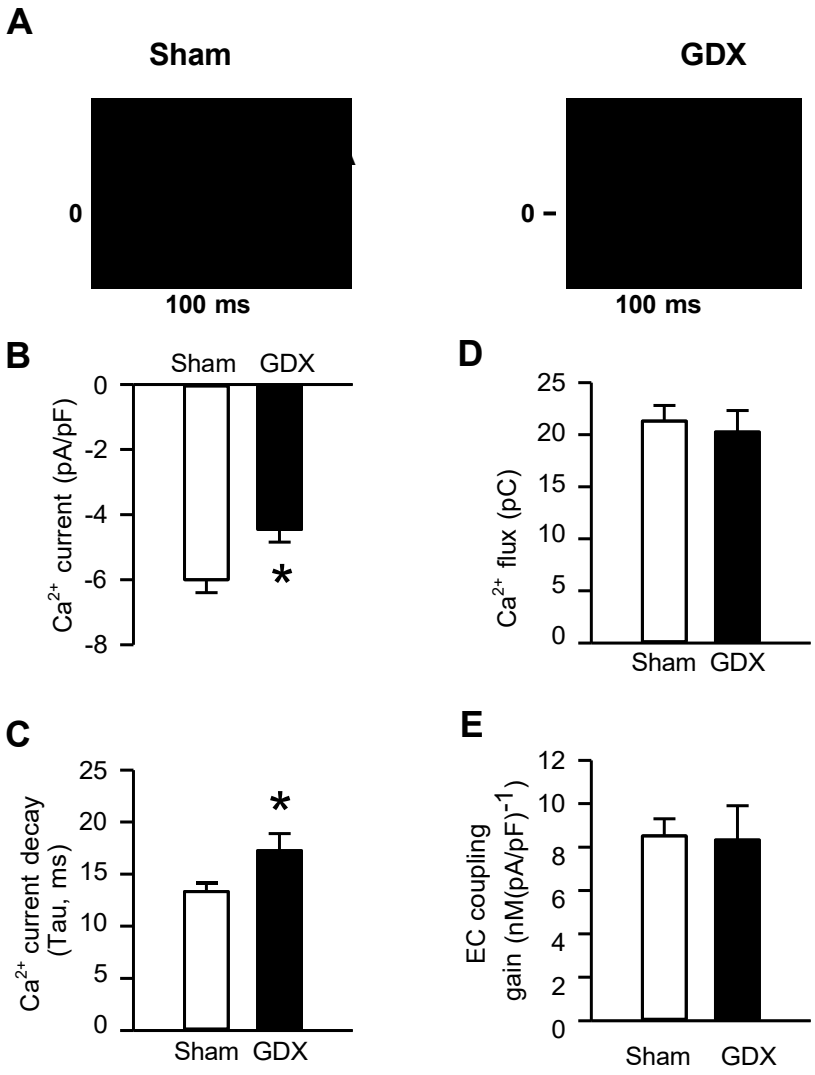

Figure 3.13. Chronic testosterone withdrawal reduced peak Ca^{2+} currents in isolated ventricular cardiomyocytes. A. Representative Ca^{2+} currents through the L-type Ca^{2+} channel recorded from sham (left) and GDX (right) cardiomyocytes. B. Peak Ca^{2+} currents in GDX cells were smaller, however (C) the Ca^{2+} current decay was prolonged in GDX cells compared to sham controls. D. The total Ca^{2+} flux through the L-type Ca^{2+} channel was not different between sham and GDX cells. E. EC coupling gain was not different between sham and GDX cells. (n=24 sham and 14 GDX myocytes isolated from N=11 sham and 6 GDX animals; *P<0.05).

3.5 SR Ca^{2+} content and spontaneous Ca^{2+} release in ventricular myocytes from sham and GDX mice

3.5.1 SR Ca^{2+} content and SR Ca^{2+} release are attenuated by GDX in ventricular myocytes from sham and GDX mice

The next experiment was to quantify SR Ca^{2+} content from caffeine-induced Ca^{2+} transients recorded from ventricular myocytes isolated from sham and GDX C57Bl/6 mice. Figure 3.14A shows the voltage clamp protocol. Figure 3.14B shows representative examples of caffeine-induced Ca^{2+} transients recorded from ventricular myocytes isolated from sham (left) and GDX (right) C57Bl/6 mice. These examples suggest that GDX decreases the amount of Ca^{2+} in the SR. The mean amplitudes of stimulated Ca^{2+} transients were smaller, and the mean amplitudes of caffeine-induced Ca^{2+} release from the SR were reduced in GDX cardiomyocytes compared to sham controls (Figure 3.15A,B). The mean fractional SR Ca^{2+} release, calculated by dividing peak Ca^{2+} transient by peak caffeine-induced SR Ca^{2+} release, was also reduced in GDX myocytes (Figure 3.15C). The diastolic Ca^{2+} levels were also lower in GDX myocytes compared to sham (Figure 3.15D). These observations suggested that SR Ca^{2+} content and fractional release from the SR were reduced by GDX. The mean data for SR Ca^{2+} stores and fractional release in sham and GDX myocytes are summarized in Table 3.10.

3.5.2 Spontaneous Ca^{2+} sparks released from the SR are smaller, less frequent, and decay more slowly by GDX

The next experiments investigated spontaneous Ca^{2+} release from the SR in

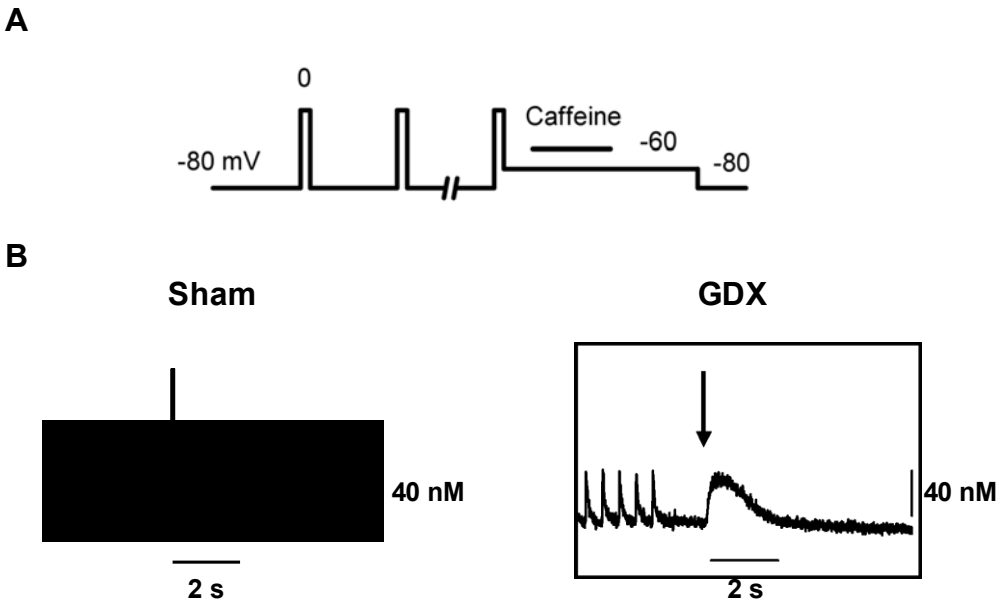

Figure 3.14. (Panel B) Representative examples of caffeine-induced Ca^{2+} transients recorded from ventricular myocytes isolated from sham (left) and GDX (right) C57Bl/6 mice. A. The voltage clamp protocol used in these experiments is shown at the top. B. The arrows denote the application of 10 mM caffeine. Caffeine-induced responses were smaller in the GDX cell than in the sham cell.

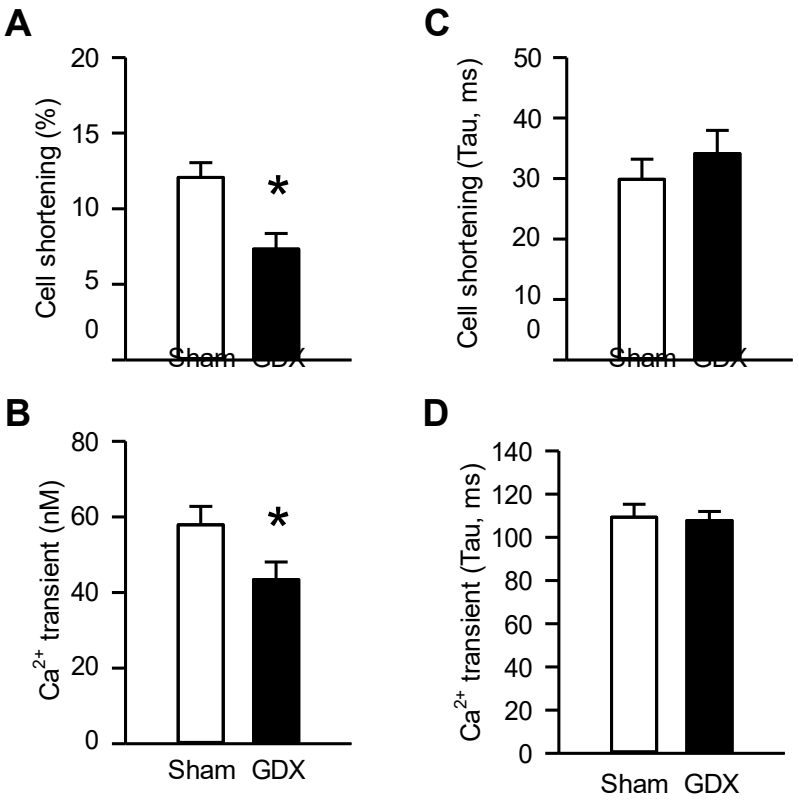

Figure 3.15. SR Ca^{2+} content and fractional sarcoplasmic reticulum (SR) Ca^{2+} release were attenuated by GDX. A. Mean amplitudes of Ca^{2+} transients were smaller in GDX cells compared to sham cells. B. GDX reduced mean amplitudes of caffeine-induced SR Ca^{2+} release compared to sham controls. C. Mean fractional SR Ca^{2+} release, calculated by dividing peak Ca^{2+} transient by peak caffeine-induced SR Ca^{2+} release, was also reduced in GDX myocytes compared to sham controls. D. Diastolic Ca^{2+} levels were lower in GDX cells compared to sham cells. (n=22 sham and 14 GDX myocytes isolated from N=11 sham and 6 GDX animals; *P<0.05).

Table 3.10: SR Ca^{2+} stores in myocytes from sham and GDX mice

Parameter	sham	GDX	P-value
Ca^{2+} transient (nM)	48.0 ± 3.4	31.0 ± 2.0	P=0.002 *
Caffeine transient (nM)	68.0 ± 7.0	48.6 ± 2.1	P=0.03 *
Fractional release (%)	86.4 ± 5.9	64.9 ± 3.5	P=0.009 *
Diastolic Ca^{2+} (nM)	94.3 ± 6.9	67.6 ± 6.8	P =0.01 *

N=11 sham and 6 GDX mice; n=22 sham and 14 GDX cells.
Data expressed as mean ± SEM.
* denotes significant for P<0.05.

ventricular myocytes, by measuring spontaneous Ca^{2+} sparks using confocal microscopy. Figure 3.16 shows representative three dimensional plots of Ca^{2+} sparks recorded from sham (left) and GDX (right) cardiomyocytes. These examples suggest that GDX modifies spontaneous Ca^{2+} spark frequency. The mean frequency of Ca^{2+} sparks was reduced in ventricular myocytes from GDX compared to sham controls (Figure 3.17A). Mean spark amplitudes were smaller in GDX myocytes compared to sham (Figure 3.17B). The mean spark widths, measured as full width at half maximum amplitude (FWHM), were not affected by GDX (Figure 3.17C). The mean spark decay times (Tau) were prolonged by GDX compared to sham controls (Figure 3.17D). These observations suggest that spontaneous Ca^{2+} sparks were smaller, less frequent, and had a prolonged decay in ventricular myocytes from GDX mice compared to sham controls. The mean data for these experiments are summarized in Table 3.11. Taken together, the data from these experiments suggests that modified SR Ca^{2+} release in the GDX heart may be due to changes in the expression of key EC coupling proteins. This will be explored in the next section.

3.6 Protein expression in isolated ventricles from sham and GDX mice

Next, Western blotting experiments were performed to determine if the slower contractions and Ca^{2+} transients, and the decrease in SR Ca^{2+} release in GDX myocytes, were due to changes in the expression of Ca^{2+} handling proteins. Initial experiments examined Ca^{2+} influx mechanisms, specifically the L-type Ca^{2+} channel. Figure 3.18A shows representative blots of the major pore-forming subunit of the L-type Ca^{2+} channel,

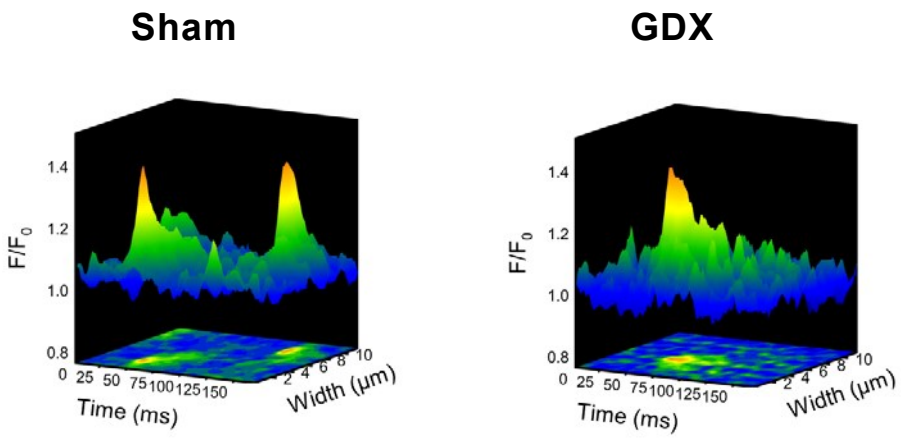

Figure 3.16. (Panel A) Representative three dimensional plots of Ca^{2+} sparks recorded from sham (left) and GDX (right) cardiomyocytes. Spontaneous Ca^{2+} sparks were smaller, less frequent, and decayed more slowly in GDX myocytes compared to sham.

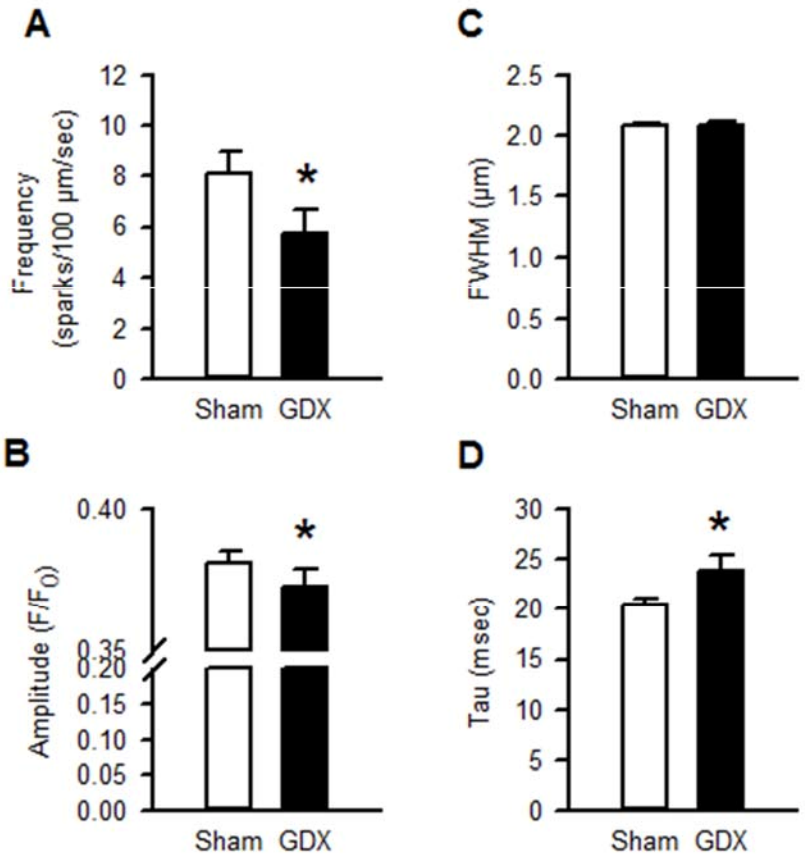

Figure 3.17. Spontaneous Ca^{2+} sparks were smaller, less frequent, and had a prolonged decay in ventricular myocytes from GDX mice compared to sham controls. A. GDX decreased mean spark frequency compared to sham controls. B. Mean spark amplitudes were smaller in GDX myocytes compared to sham controls. C. GDX did not affect mean spark width, measured as full width at half maximum amplitude (FWHM), compared to sham controls. D. GDX prolonged mean spark decay times (Tau) compared to sham controls. (n=118 sham cells (2346 sparks) and 100 GDX cells (1309 sparks) isolated from N=6 sham and 5 GDX mice; *P<0.05).

Table 3.11: Comparison of spontaneous Ca^{2+} sparks recorded from sham and GDX myocytes.

Parameter	sham	GDX	P-value
Ca^{2+} spark amplitude (F/F_0)	0.381 ± 0.004	0.378 ± .006	P=0.01 *
Full width (μm)	3.44 ± 0.03	3.50 ± 0.04	P=0.16
Full width at half-maximum (μm)	2.09 ± 0.02	2.08 ± 0.02	P=0.44
Time to peak (ms)	9.1 ± 0.2	9.4 ± 0.3	P=0.01 *
Full duration (ms)	32.8 ± 0.5	34.2 ± 0.7	P=0.006 *
Full duration at half-maximum (ms)	17.9 ± 0.2	18.6 ± 0.3	P<0.001 *
Time course of spark decay (Tau, ms)	20.5 ± 0.6	22.4 ± 1.3	P=0.002 *
Frequency (sparks/100 μm/sec)	8.07 ± 0.92	5.60 ± 0.81	P=0.02 *

N=6 sham and 5 GDX mice; n=118 sham and 100 GDX cells.
Data expressed as mean ± SEM.
* denotes significant for P<0.05.

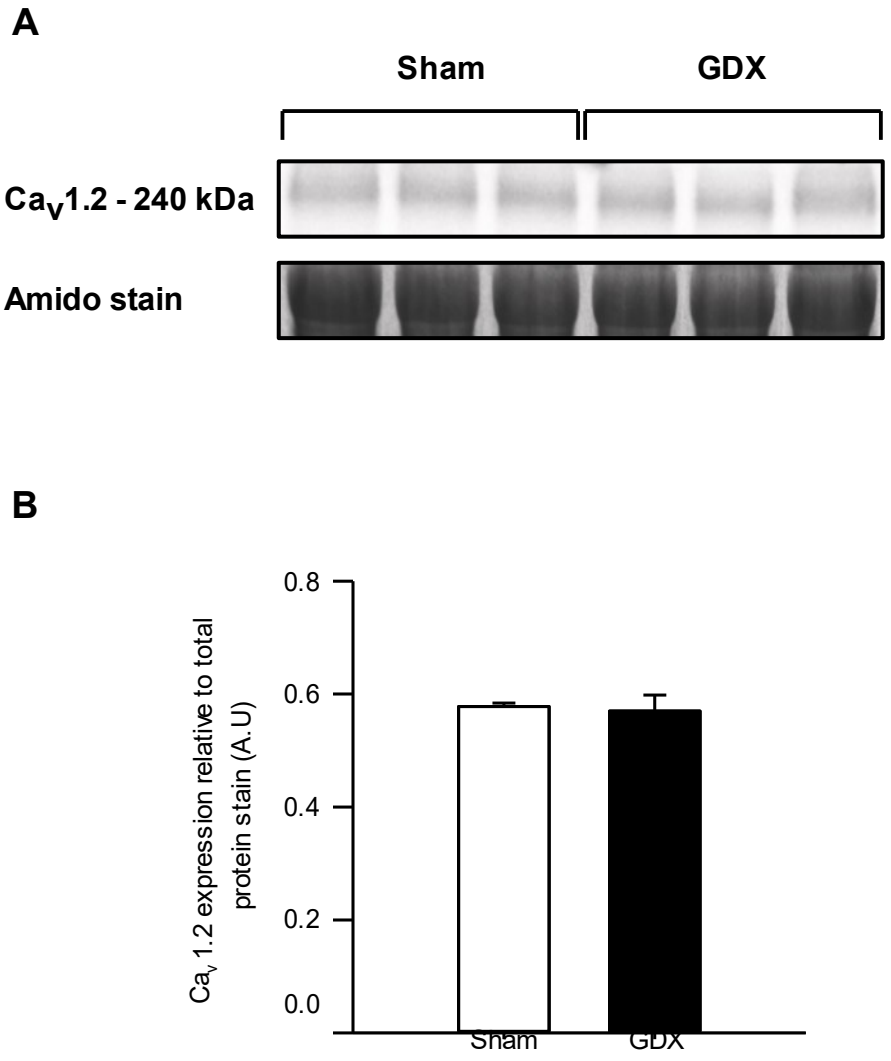

Figure 3.18. GDX had no effect on Cav1.2 expression in the ventricles compared to sham controls. A. Blots of Cav1.2 (top) and total protein (amido black) stain (bottom). B. The ratio of Cav1.2 to total protein levels was not different in ventricles from GDX mice compared to sham controls. n=3 sham, 3 GDX hearts.

Cavl.2 (top), as well as total protein (amido black) stain (bottom). The ratios of Cavl.2 to total protein levels were not different in ventricles from GDX mice compared to sham controls (Figure 3.18B). These data suggest that the density of the L-type Ca^{2+} channel is not affected by GDX. A similar approach was used to investigate NCX, which normally functions to remove Ca^{2+} but can allow Ca^{2+} influx as well. Figure 3.19A shows representative blots for NCX (top) and amido black protein stain (bottom). The ratio of NCX to amido black stain was not different in ventricles from GDX mice compared to sham (Figure 3.19B). These observations indicate that the expression of NCX was not affected by GDX.

The next series of experiments investigated the impact of GDX on expression of specific Ca^{2+} handling proteins in the SR. First, expression of the cardiac isoform of the SR Ca^{2+} release channel/RyR was compared between the two groups. Representative blots for RyR2 (top) and total protein (amido black) stain (bottom) are illustrated in Figure 3.20A. The ratio of RyR2 to total protein stain was similar in ventricles from GDX and sham (Figure 3.20B). The expression of the cardiac-specific isoform of the SERCA pump was also compared in the ventricles of sham and GDX mice. Figure 3.21A shows representative blots of SERCA2 (top) and the loading control (β-actin). The ratio of SERCA to β-actin was similar in ventricles from GDX mice compared to sham controls (Figure 3.21B). Next, expression of the endogenous SERCA inhibitor, PLB, was compared between groups. Figure 3.22A shows a representative blot of PLB (top) and total protein (coomassie) (bottom). The ratio of PLB to total protein was dramatically increased in ventricles from GDX mice compared to sham controls (Figure 3.22B). These observations indicate that, while GDX had no effect on RyR2 and

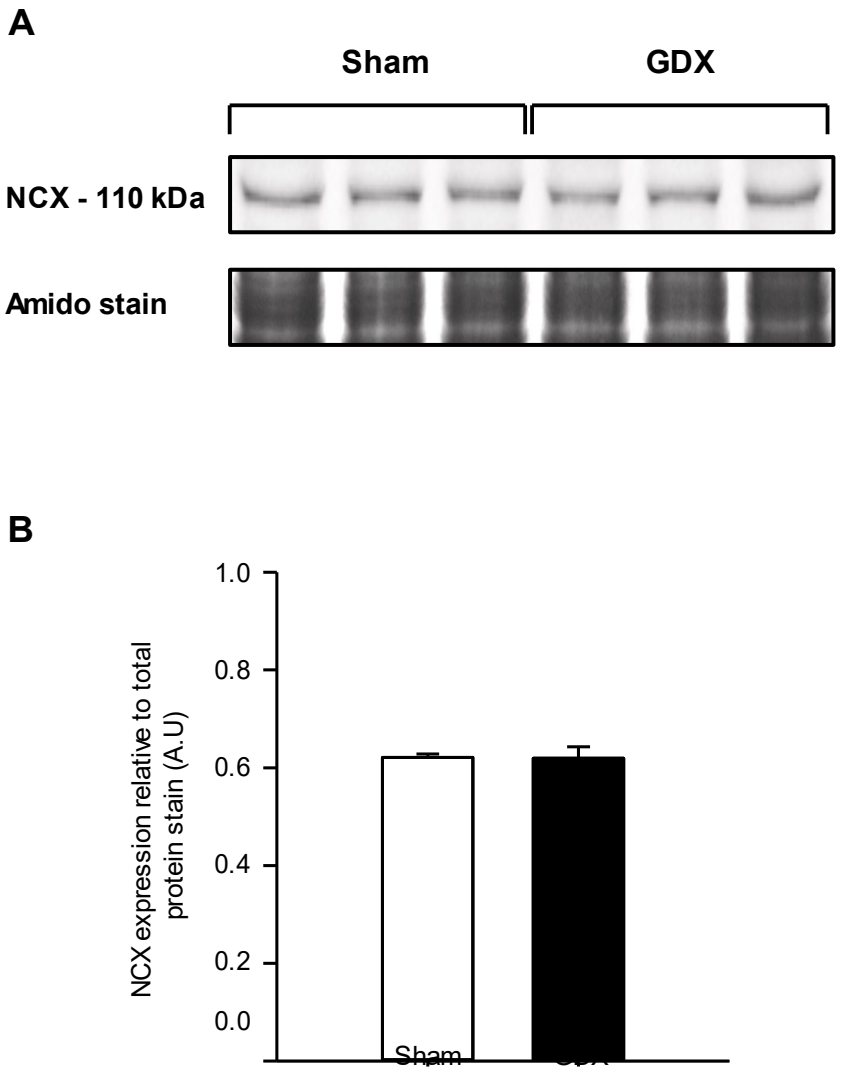

Figure 3.19. GDX had no effect on NCX expression in the ventricles compared to sham controls. A. Blots of NCX (top) and total protein (amido black) stain (bottom). B. The ratio of NCX to total protein levels was not different in ventricles from GDX mice compared to sham controls. n=3 sham, 3 GDX hearts.

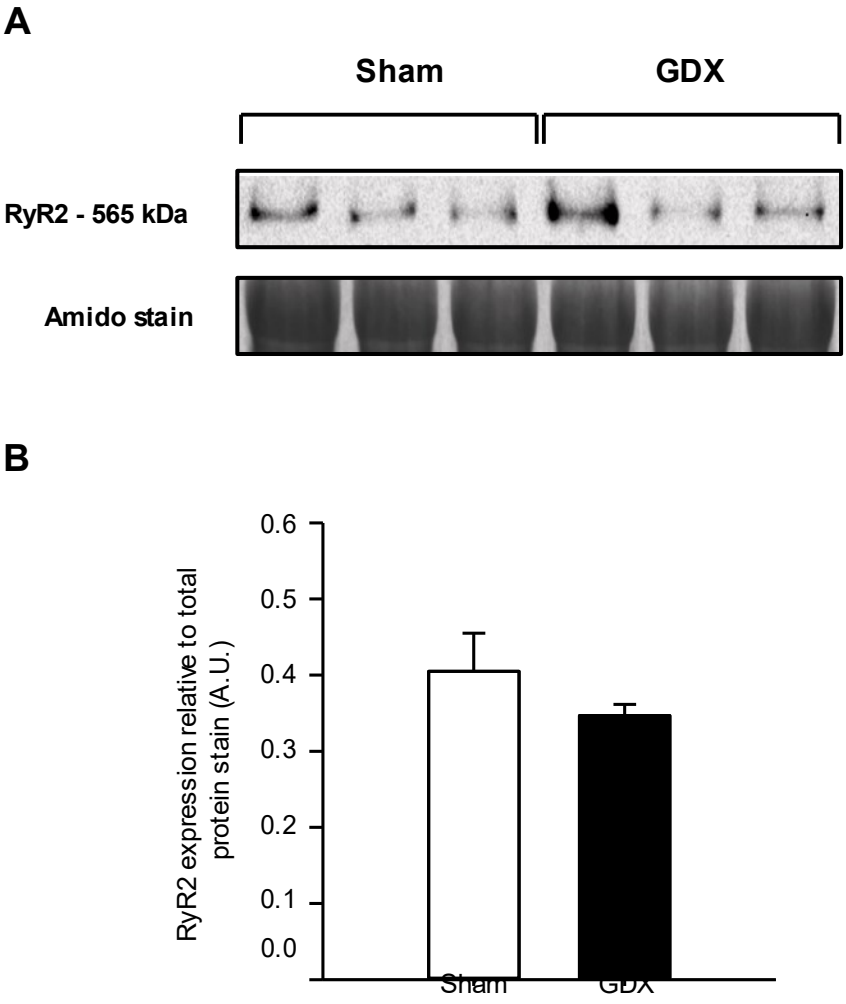

Figure 3.20. RyR2 expression in the ventricles was similar in GDX and sham controls. A. Blots of RyR2 (top) and total protein (Amido black) stain (bottom). B. The ratio of RyR2 to total protein stain was similar in ventricles from GDX mice compared to sham controls. n=3 sham, 3 GDX hearts.

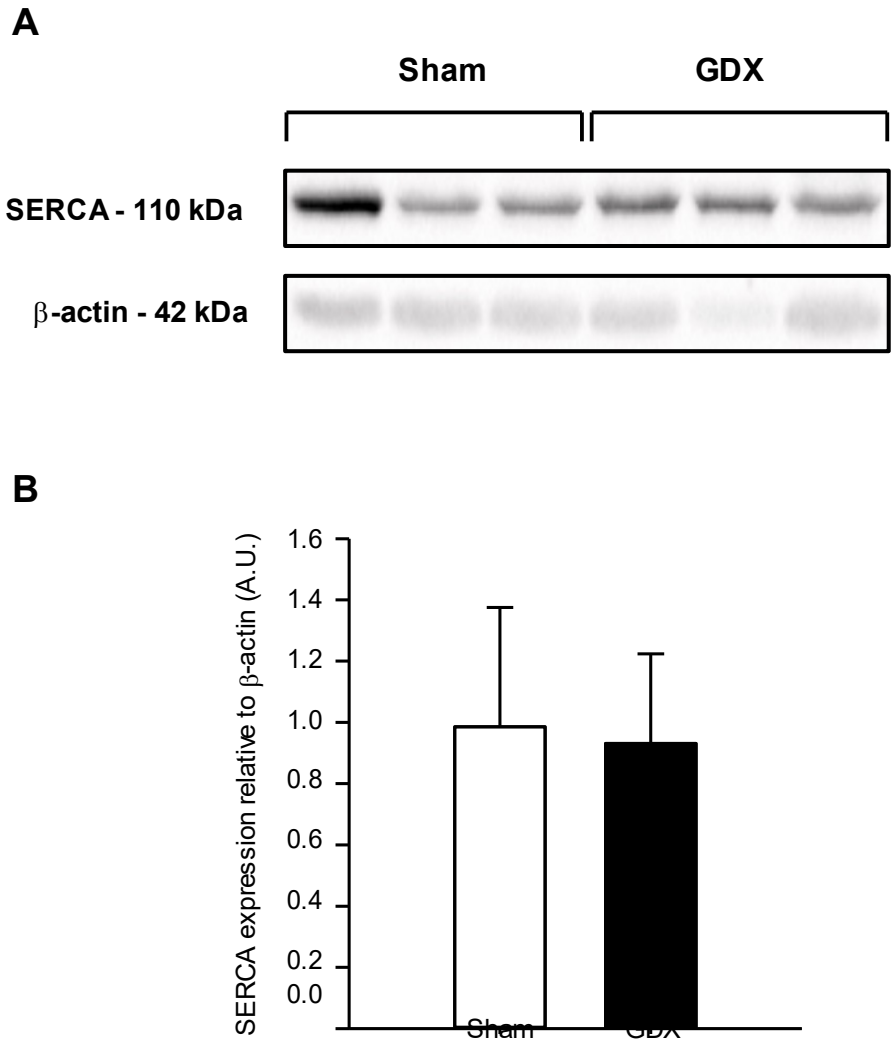

Figure 3.21. SERCA expression in ventricles was similar in GDX and sham controls. A. Blots of SERCA (top) and β-actin (bottom). B. The ratio of SERCA to β-actin was similar in ventricles from GDX mice compared to sham controls. n=3 sham, 3 GDX hearts.

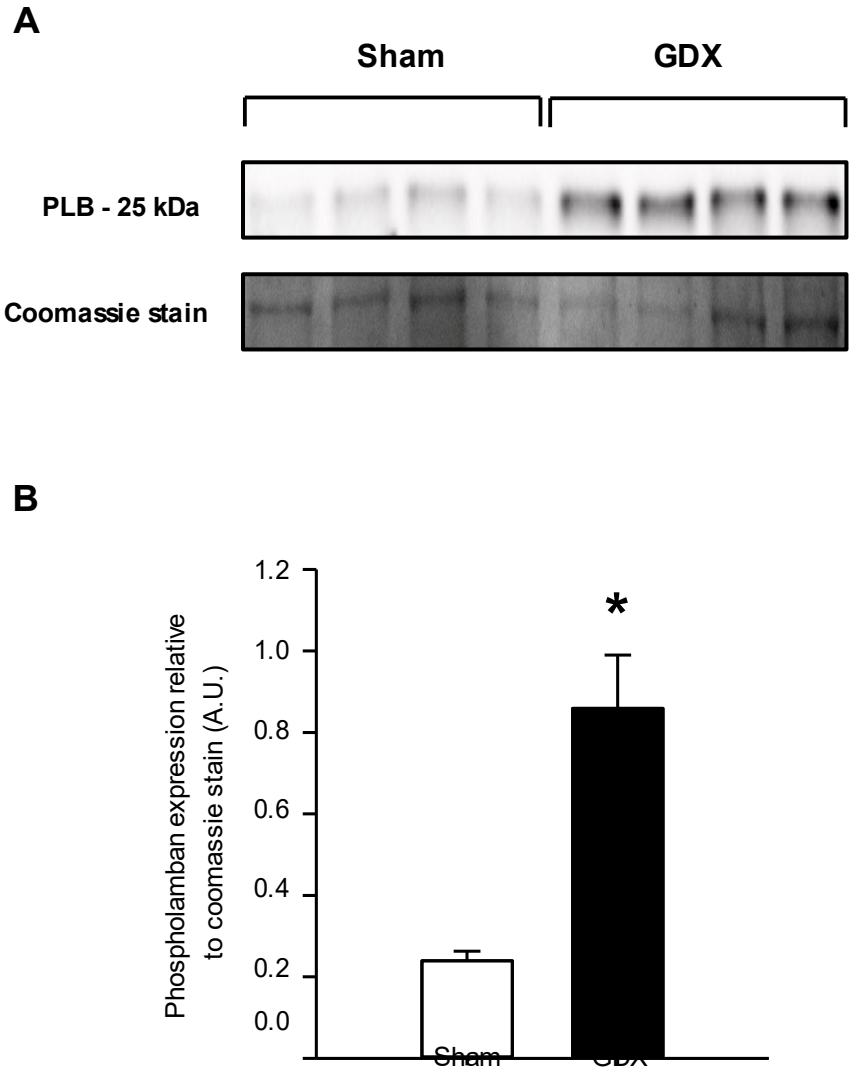

Figure 3.22. GDX increased the expression of PLB relative to total protein stain in ventricles of C57Bl/6 mice compared to sham controls. A. Blots of PLB (top) and total protein (coomassie) stain (bottom) B. The ratio of PLB to total protein (Coomassie stain) was increased in ventricles from GDX mice compared to sham controls. n=4 sham, 4 GDX hearts (* denotes $P<0.05$ compared to sham control).

SERCA2 protein expression, GDX increased the expression of PLB in ventricles. Higher levels of PLB with no change in SERCA expression would be expected to reduce the rate of SR Ca^{2+} uptake in the GDX heart.

3.7 Action potentials in isolated ventricular myocytes from sham and GDX mice

3.7.1 Action potentials are prolonged by GDX in ventricular myocytes

Next, ventricular myocytes from sham and GDX mice were current clamped to record action potentials. Figure 3.23A shows representative action potentials recorded from sham (solid line) and GDX (dashed line) myocytes. These examples suggest that action potential repolarization is prolonged by GDX. Mean data show that there was no difference in average values for resting membrane potentials in sham and GDX ventricular myocytes (Figure 3.23B). Mean action potential durations at 50% repolarization (APD_{50}) were similar in sham and GDX cells (Figure 3.23C). By contrast, GDX prolonged the duration to 90% repolarization (APD_{90}) compared to sham controls (Figure 3.23D). These observations suggest that GDX prolongs action potential repolarization in Phase 3 of the action potential. These prolonged action potentials in the GDX heart may contribute to the slower contractions and Ca^{2+} transients seen in GDX hearts. The mean data for action potentials is summarized in Table 3.12.

3.7.2 Kv1.5 expression is not different in sham and GDX ventricles

The increase in APD in GDX cells suggests that GDX may either enhance

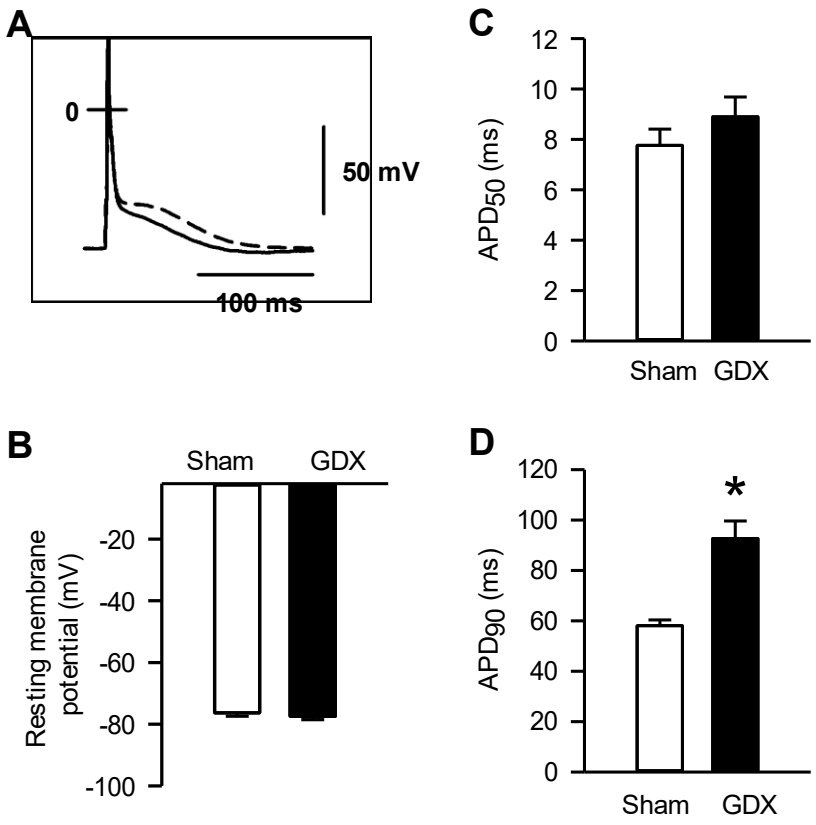

Figure 3.23. Chronic testosterone withdrawal prolonged the time for action potential repolarization in isolated cardiomyocytes from adult C57Bl/6 mice. A. Representative action potentials recorded from voltage clamped sham (solid) and GDX (dashed) ventricular myocytes stimulated at 2 Hz. B. Average values for resting membrane potentials (RMP) were similar in sham and GDX myocytes. C. Mean action potential durations at 50% repolarization (APD_{50}) were similar in sham and GDX cells. D. GDX prolonged the duration to 90% repolarization (APD_{90}) compared to sham controls. (n=9 sham and 12 GDX myocytes isolated from N=3 sham and 3 GDX mice; *P<0.05).

Table 3.12: Mean characteristics of resting and action potentials recorded from sham and GDX myocytes.

Parameter	sham	GDX	P-value
RMP (mV)	76.3 ± 1.1	77.4 ± 1.1	P=0.41
APD_{50} (ms)	7.8 ± 0.7	8.9 ± 0.8	P=0.30
APD_{70} (ms)	15.5 ± 1.6	38.3 ± 4.3	P<0.001 *
APD_{90} (ms)	58.1 ± 2.3	92.6 ± 7.0	P<0.001 *

N=3 sham and 3 GDX mice; n=9 sham and 12 GDX cells.
Myocytes were stimulated at 2 Hz.
Data expressed as mean ± SEM.
* denotes significant for P<0.05.

inward, depolarizing currents such as Ca^{2+} currents or inhibit outward, repolarizing currents such as K^+ current. Our previous data shows that peak L-type Ca^{2+} currents are smaller in GDX cells and channel expression is similar in sham and GDX hearts, so an increase in inward Ca^{2+} currents is unlikely to account for longer APD in GDX cells. Additional Western blotting experiments were performed to determine whether a decrease in the expression of K^+ channels involved in action potential repolarization in the mouse ventricle could account for this difference. Kv1.5 channels conduct the ultrarapid delayed rectifier current (I_{Kur}) that contribute to action potential repolarization in the mouse ventricle (Herring et al., 2013). Figure 3.24A shows representative blots of Kvl.5 (top) and β-actin (bottom). The ratios of Kvl.5 expression to β-actin expression were similar in ventricles from sham and GDX hearts (Figure 3.24B). These observations suggests that I_{Kur} was not affected by GDX.

3.8 Pro-arrhythmic mechanisms in isolated ventricular myocytes from sham and GDX mice

3.8.1 Early after-depolarizations (EADs) in isolated ventricular myocytes

Longer action potentials are known to trigger abnormal activity in the heart, including EADs (Weiss et al., 2010). Therefore, experiments were performed in current clamped ventricular myocytes to determine whether EADs were more frequent in GDX cells. Figure 3.25 shows representative examples of EADs in (A) sham and (B) GDX ventricular myocytes. These examples suggest that there are a greater number of EADs in GDX ventricular myocytes compared to sham. Mean data show that there was a

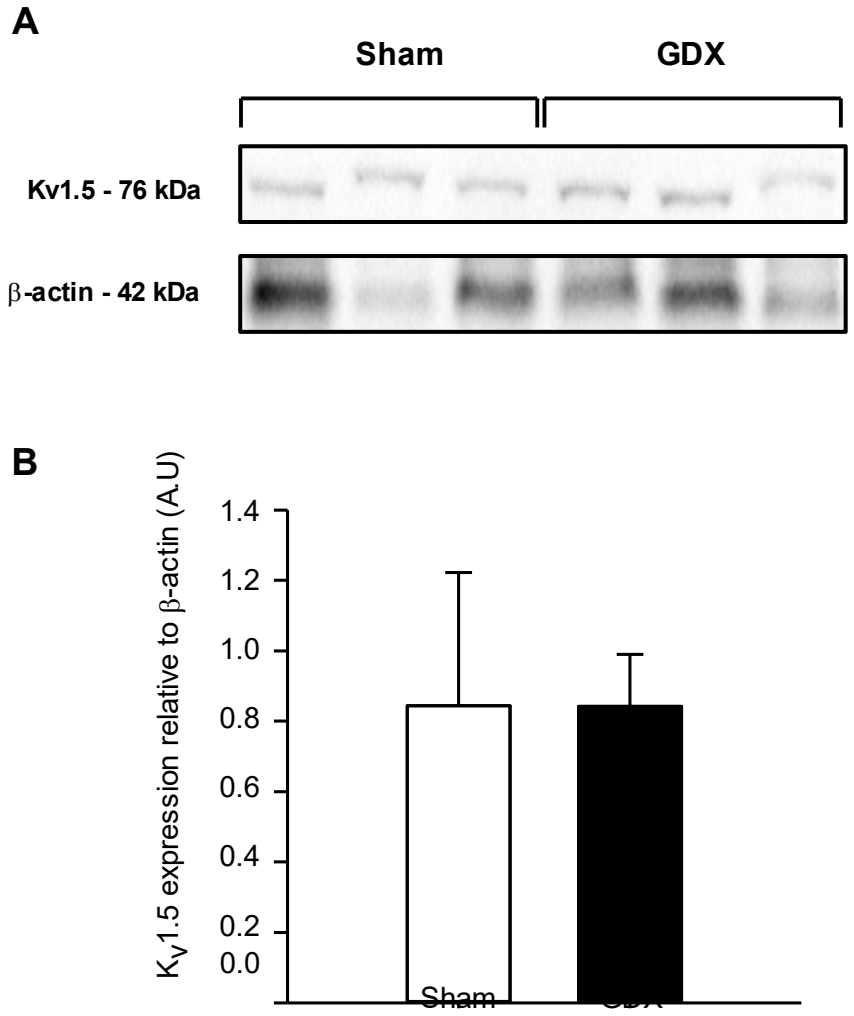

Figure 3.24. GDX had no effect on Kv1.5 expression in ventricles compared to sham controls. A. Blots of Kv1.5 (top) and β-actin (bottom). B. The ratio of Kv1.5 to β-actin was similar in ventricles from GDX mice compared to sham controls. n=3 sham, 3 GDX hearts.

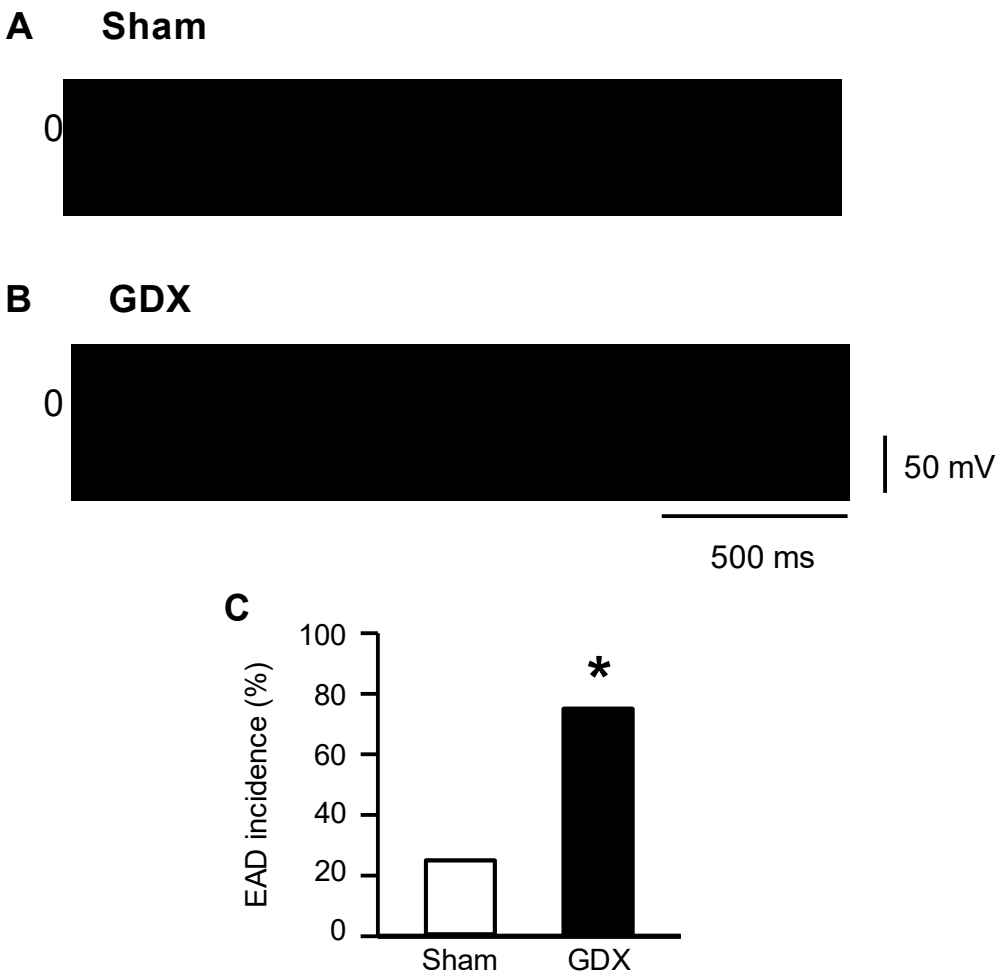

Figure 3.25. Chronic testosterone withdrawal increased early after-depolarizations (EADs) in isolated ventricular myocytes. Representative examples of EADs in (A) sham and (B) GDX cardiomyocytes stimulated at 2 Hz. C. GDX cardiomyocytes had a larger incidence of EADs compared to sham controls. (n=12 sham and 16 GDX myocytes isolated from N=3 sham and 4 GDX mice; *P<0.05).

higher incidence of EADs in GDX ventricular myocytes compared to sham controls (Figure 3.25C). These observations suggest that GDX may increase electrical disturbances in the action potential and could promote arrhythmias in the GDX heart. These data are summarized in Table 3.13.

3.8.2 Spontaneous contractions in ventricular myocytes

The next series of experiments determined whether GDX increased the number of spontaneous contractions in ventricular myocytes. Myocytes were field stimulated at 2 Hz and then the stimulation was stopped to record spontaneous contractions. There was a small increase in the incidence of spontaneous contractions in GDX ventricular myocytes compared to sham controls, although this was not statistically significant (Figure 3.26A). However, there were more spontaneous contractions in GDX ventricular myocytes in a 10 s period compared to sham controls (Figure 3.26B). These observations suggest that GDX increases spontaneous contractile activity in ventricular myocytes. Taken together, these data suggest that spontaneous contractions may be generated by the disturbances in action potentials seen in GDX cells. The data are summarized in Table 3.13.

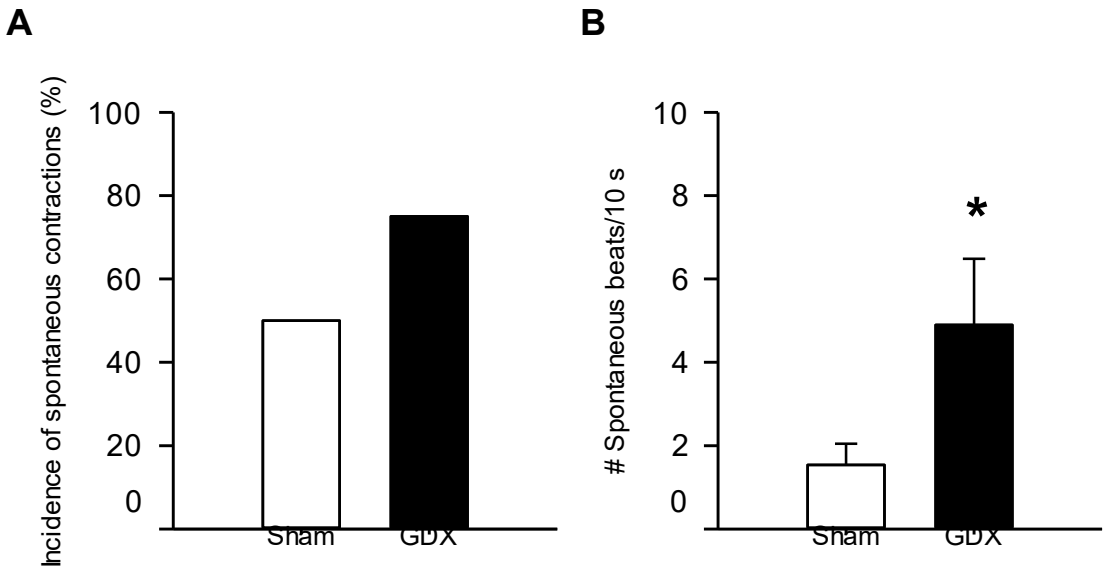

Figure 3.26. Loss of testosterone increased the number of spontaneous contractions in ventricular myocytes. Myocytes were field stimulated at 2 Hz for a 10 s period and then stimulation was stopped to record spontaneous activity for 10 s. A. Testosterone withdrawal caused a small increase in the incidence of spontaneous contractions compared to sham controls, although this was not statistically significant. B. Testosterone withdrawal caused more spontaneous contractions in GDX cardiomyocytes in a 10 s period compared to sham controls. (n=24 sham and 20 GDX myocytes isolated from N=4 sham and 3 GDX mice; *P<0.05).

Table 3.13: Spontaneous contractile activity in field stimulated cardiomyocytes (2 Hz)

Parameter	sham	GDX	P-value
Incidence of spontaneous contractions (2 Hz)	13/24	15/20	P=0.10
Incidence of spontaneous contractions (4 Hz)	15/24	17/20	P=0.25
# spontaneous contractions in 10s after pacing (2 Hz)	1.5 ± 0.5	4.9 ± 1.6	P=0.02 *
# spontaneous contractions in 10s after pacing (4 Hz)	3.3 ± 0.7	3.8 ± 0.7	P=0.45
Diastolic Ca^{2+} levels of spontaneously contracting cells (2 Hz)	250.1 ± 25.8	285.4 ± 31.2	P=0.20
Diastolic Ca^{2+} levels of spontaneously contracting cells (4 Hz)	242.9 ± 9.8	232.0 ± 9.3	P=0.42
Incidence of EADs (4 Hz)	3	12	P=0.03 *

N=4 sham and 3 GDX mice; n=24 sham and 20 GDX cells.
Data expressed as mean ± SEM.
* denotes significant for P<0.05.

Chapter 4 Discussion

4.1 Overall summary of Key findings

The overall objective of this thesis was to determine whether chronic testosterone withdrawal adversely affected the function of the heart and whether this occurred due to changes in the expression and/or function of key components of the EC coupling pathway. This work has highlighted a number of key findings regarding the impact of GDX that shed light on the role of testosterone on the heart.

This study first investigated the effect of GDX on myocardial structure and function *in vivo*. In terms of heart structure, results showed that the hearts of GDX mice had a thinner IVSd compared to sham controls and the mass of the left ventricle was smaller in the hearts of GDX mice compared to sham mice. These observations suggest that low testosterone levels cause dilation of the ventricles. There were also effects of GDX on *in vivo* function. While most functional parameters were similar in the two groups, the isovolumic relaxation time was prolonged in GDX mice compared to sham. These observations suggest testosterone modulates myocardial structure and diastolic function in the intact animal.

This study further investigated the effects of GDX on the structure and function of the heart at the level of the myocyte. Results showed that isolated ventricular myocytes from GDX hearts were slightly smaller than myocytes from sham hearts. There were no differences between groups in peak cell shortening and Ca^{2+} transients in field-stimulated ventricular myocytes however, the time course of relaxation and Ca^{2+} transient decay was significantly prolonged in GDX myocytes compared to sham. Interestingly, when the duration of depolarization was controlled by voltage clamp, GDX suppressed peak cell shortening and Ca^{2+} transients compared to sham controls, but

abolished the effects on the time course of cell relaxation and Ca^{2+} transient decay seen when cells were field-stimulated and responses were activated by action potentials. In voltage clamp experiments, the duration of depolarization is controlled while field stimulating cells allows them to contract based on their own action potential. Therefore, these observations show that GDX affects Ca^{2+} handling and contractile function at the level of the myocytes and suggest that GDX may influence action potential configuration.

Further experiments explored the mechanisms involved in the differences in results between field stimulation and voltage clamp experiments. These experiments evaluated the effect of GDX on the action potential, and on key components of the EC coupling pathway. The first component of the pathway is Ca^{2+} induced Ca^{2+} release where the influx of Ca^{2+} from the L-type Ca^{2+} channel opens RyRs in the SR. As shown in the results, peak Ca^{2+} current was smaller in GDX myocytes compared to sham controls, although expression of the major pore-forming subunit (Cav1.2) was unaffected by GDX. This observation suggests that GDX may result in smaller amount of Ca^{2+} release from the SR, and thus reduced cell shortening. There was no change in the net Ca^{2+} flux across the sarcolemma, however, as the Ca^{2+} current decay was prolonged in GDX myocytes compared to sham. Nonetheless, these observations suggest that the smaller peak Ca^{2+} current may contribute to the smaller contractions observed in voltage clamp experiments. The prolonged Ca^{2+} current decay may help prolong the action potential, and thus contribute to the slowed contractile relaxation and Ca^{2+} transient decay in field-stimulated cells.

The next part of the EC coupling process that was explored was the release and reuptake of Ca^{2+} from the SR. Interestingly, GDX reduced SR Ca^{2+} load and thus

reduced the fractional release of Ca^{2+} from the SR compared to sham controls. GDX also decreased Ca^{2+} spark amplitude, and prolonged the Ca^{2+} spark decay compared to sham controls but it had no effect on RyR expression. The frequency of spontaneous Ca^{2+} sparks released from the SR was also decreased by GDX, as expected with a lower SR content. These observations suggest that GDX affects components of the EC coupling pathway that influence SR Ca^{2+} loading, such as the SERCA pump and/or PLB. There were no changes in the expression of SERCA, however, the expression of SERCA's endogenous inhibitor, PLB, was increased by GDX. Higher levels of PLB may inhibit SERCA, and contribute to the slower Ca^{2+} reuptake into the SR.

Key sarcolemma channels involved in EC coupling influence action potential configuration, so action potentials were recorded and compared in cells from sham and GDX mice. The duration of the action potential was prolonged in GDX myocytes compared to sham controls. This can help explain the different observations in field stimulation experiments, where myocytes contracted under their own action potential, and voltage clamped myocytes, where the duration of depolarization was controlled. The increased time of action potential repolarization suggested decreased K^+ channel expression, such as Ikur, although Western blotting experiments showed no change in its expression. However, prolongation of the Ca^{2+} current may contribute to the longer action potentials seen in GDX cells.

Prolonged action potential repolarization is known to disrupt electrical activity in the myocyte and can trigger arrhythmias in the intact heart. Results of current clamp experiments showed that GDX increased the number of EADs. As EADs can trigger extra beats, the occurrence of spontaneous contractions was also compared in sham and GDX cells. GDX increased the number of spontaneous contractions recorded in a 10 s

period. This suggests that GDX may promote the development of arrhythmias in the heart.

Taken together, the results in this thesis demonstrate that testosterone withdrawal adversely affects the function of the heart by affecting key components of the EC coupling pathway, which results in abnormal Ca^{2+} handling and disturbances in electrical activity at the cellular level.

4.2 GDX changes myocardial structure and function in vivo

Testosterone, as well as other hormones, work to influence the size of the myocardium (Cavasin et al., 2003). Previous studies have used echocardiography to demonstrate that athletes abusing anabolic steroids have enlarged hearts (Payne et al., 2004). Less is known about the effects of low testosterone levels on heart structure *in vivo*. Results of this thesis showed that GDX affected myocardial structure. The heart weights of sham and GDX mice were not significantly different, although GDX hearts tended to be smaller. Heart weights were normalized to body weight and tibia bone length to measure if GDX affected the size of the heart. Heart weights were not different between both groups of mice when normalized to their own body weight, which indicated that there was no change in gross heart size with GDX. It is common to use the length of the tibia bone to normalize heart weight, and test for changes in heart size (Yin et al., 1982). This is generally a reliable physical parameter for normalization due to the adult tibia bone being resistant to changes in size after puberty. There was no difference in heart size when heart weights were normalized to tibia bone length.

However, this thesis suggests that using the tibia bone to normalize heart weight in GDX studies may not produce accurate results. This is because this study showed that

the length of the tibia bones from adult GDX mice were significantly longer compared to sham. The finding that GDX increases the length of tibia bones has been reported in some studies (Sandstedt et al., 1994), however, this has not been reported in all studies. Densitometry of the tibia bones of sham and GDX mice showed that there was no difference in bone mineral content, suggesting the GDX tibias are both longer and thinner than sham controls. Heart weights were normalized to tibia bone mineral content and there was still no indication of changes in heart size due to GDX. Taken together, these results suggest that low testosterone levels due to GDX does not affect the gross morphological size of the heart.

This is one of very few studies that has examined how GDX affected cardiac structure with echocardiography. Results showed that there was no difference in the size of the LVID in either systole or diastole. In addition, the LVPW in both systole and diastole was not affected by GDX. Interestingly, GDX mice had a thinner interventricular septum compared to sham controls. This suggests that the inner chamber of the left ventricle may be dilated. A key finding of this study is that the mass of the left ventricle was smaller in GDX mice compared to sham. Interestingly, previous work in an animal model has shown that testosterone supplementation increases the mass of the left ventricle (Papamitsou et al., 2011). One previous study has observed a reduced left ventricular mass following GDX, however, this was in the context of pathological hypertrophy induced by myocardial infarction (Montalvo et al., 2012). Together with the work presented in this thesis, these observations suggest that GDX causes dilation of the ventricles and reduces the mass of the left ventricle.

This study also provided evidence that GDX promoted contractile dysfunction. Echocardiography studies indicated that there were no changes in heart rate, ejection

fraction, and fractional shortening, which suggests that systolic function is not affected by GDX. While measurements of diastolic function showed that the early and late filling in diastole were not affected by GDX, the isovolumic relaxation time of the ventricles was significantly prolonged by GDX compared to sham. These observations suggest that, although systolic function was not affected by GDX, the loss of testosterone did promote diastolic dysfunction in the heart. Based on these findings, it is possible that low testosterone levels may contribute to the pathogenesis of diastolic heart failure, which is characterized by abnormal LV relaxation, reduced LV diastolic distensibility, and abnormal LV filling (Mottram, 2005). One previous study supports these observations, noting that low testosterone levels are associated with diastolic dysfunction in both men and women (Čulić and Bušić, 2015). This suggests that testosterone supplementation may be help prevent diastolic dysfunction.

The mechanisms by which low testosterone may promote diastolic dysfunction are not yet known. It is possible that low testosterone levels may promote diastolic dysfunction by increasing ventricular stiffness in the heart. This may arise because low testosterone causes arterial stiffening, which increases the load on the left ventricle and induces myocardial fibrosis (Smith et al., 2001; Ikeda et al., 2012). Slower Ca^{2+} uptake into the SR, as reported in this thesis, may also help delay relaxation in the GDX heart.

Animal studies have suggested that testosterone produces effects on the heart at the level of the myocyte and that these effects are androgen receptor-mediated (Marsh et al., 1998). Low testosterone levels may cause changes in cardiomyocyte structure as results showed cells from GDX were smaller than control and LV mass was reduced by GDX. In support of this, subphysiological testosterone levels are known to cause myocyte hypertrophy (Bušić and Čulić, 2015). Testosterone has been shown to induce

protein synthesis and promote hypertrophy in cardiomyocytes by increasing amino acid incorporation into proteins (Kloner et al., 2016). Low testosterone may have the opposite effect and reduce the rate of protein synthesis in the hearts of GDX mice.

The results of this study suggest that GDX causes changes in myocardial structure and function *in vivo*. This includes dilation of the ventricles, reduced LV mass, and smaller myocytes, as well as diastolic dysfunction due to low testosterone levels. These changes may arise from deficits at the cellular level. This may also result in abnormal contractile Ca^{2+} handling and function, as discussed in the next section.

4.3 GDX modifies myocyte Ca^{2+} handling and contraction in field stimulated and voltage-clamped myocytes differently

Our results showed that myocardial function also was affected by GDX in studies done *in vitro* in isolated ventricular myocytes. The results of this study showed that contractions and Ca^{2+} transients were prolonged by GDX, with no effect on peak responses when myocytes were field-stimulated. This study was unique in simultaneously measuring contractions and Ca^{2+} transients at two higher pacing rates (e.g. 2 and 4 Hz), and it explored effects of chronic testosterone withdrawal. Only a few previous studies in the literature have investigated contractile function and Ca^{2+} handling in field stimulated myocytes after GDX and none have explored both responses simultaneously. However, these earlier studies also showed contractions and Ca^{2+} transients were prolonged by GDX, with no effect on peak responses (Curl et al., 2009; Tsang et al., 2009). Interestingly, there are several differences between the present study and the ones previously conducted. Previous investigators explored isolated myocytes from rats and used slow pacing rates (0.2-0.5 Hz) (Tsang et al., 2009; Golden et al.,

2003; Curl et al., 2009). By contrast, this study investigated ventricular myocytes from mice at higher pacing rates (e.g. 2 and 4 Hz), which are closer to physiological rates for rodents (Roth et al., 2014). In addition, previous studies investigated shorter times after GDX (2-16 weeks) (Tsang et al., 2009; Golden et al., 2003; Curl et al., 2009), while the current study investigated longer term GDX (~9 month). Together with the results of the present study, this suggests that contractions and Ca^{2+} transients are prolonged by GDX over a wide range of pacing frequencies and time frames after GDX.

The present study is the first study to investigate the effect of GDX on contractions and Ca^{2+} transients with voltage clamp techniques. Interestingly, a novel finding of this study is that when depolarization was controlled in isolated ventricular myocytes by voltage clamp, GDX suppressed peak cell shortening and peak Ca^{2+} transients however, the prolonged responses were abolished. In voltage clamp experiments the duration of depolarization of the myocyte is controlled and set to a fixed duration, while field-stimulated myocytes contract in response to their own action potential. This suggests that differences in the duration of depolarization may contribute to the differences in responses between sham and GDX cells. Together these observations show that GDX affects Ca^{2+} handling and contractile function at the level of the myocyte and suggest that GDX may influence action potential configuration – this will be explored later in the discussion. The effects of GDX on contraction and Ca^{2+} transients may also be due, at least in part, to effects on components of the EC coupling process, as discussed in the next section.

4.4 GDX affects mechanisms involved in EC coupling

Several components of the EC coupling process affect the action potential, thus key mechanisms involved in EC coupling were investigated in this thesis. The first component of Ca^{2+} induced Ca^{2+} release is the trigger, which is the influx of Ca^{2+} from the L-type Ca^{2+} channels that opens RyRs in the SR. The results of this study show that peak Ca^{2+} current was decreased by GDX. This would be expected to trigger a smaller amount of Ca^{2+} release from the SR through RyR, and this may help explain the smaller contractions and Ca^{2+} transients observed in voltage clamp experiments. The mechanisms responsible for the smaller peak Ca^{2+} current were then explored. This study showed that the expression of the major pore-forming subunit (Cav1.2) for the L channel was unaffected by GDX. Only a few prior studies have examined the expression of the L type Ca^{2+} channel in ventricles of GDX rodents. These studies only noted that the mRNA expression is decreased by GDX, but they did not assess protein expression (Golden et al., 2002; Golden et al., 2003; Bowles et al., 2004). They found that GDX caused a reduction in mRNA for the Ca^{2+} channel, which agrees with the results of this study (Golden et al., 2002; Golden et al., 2003; Bowles et al., 2004). However, the present study is the only work that has measured L-channel protein expression and found that expression of Cav1.2 is not affected by chronic exposure to low testosterone. The present study is the first to quantify Ca^{2+} currents in isolated ventricular myocytes from sham and GDX hearts, as well as the only study conducted in rodents. A previous study in isolated smooth muscle cells from the coronary artery of swine found that GDX reduced peak Ca^{2+} current (Bowles et al., 2004), similar to the observations reported in this thesis. By contrast, another study in epicardial and endocardial myocytes isolated from the left ventricle of rabbits reported no change in peak Ca^{2+} current with GDX

(Pham et al., 2002). Differences in experimental models or conditions could account for the differences in results between these two studies. Nonetheless, the smaller peak Ca^{2+} current can account for the smaller contractions and Ca^{2+} transients observed in GDX cells under voltage clamp experiments.

Interestingly, this study also found that GDX prolonged Ca^{2+} current decay, while there was no change in the net Ca^{2+} flux across the sarcolemma. GDX may regulate the L-type Ca^{2+} channel via phosphorylation, to cause the smaller peak Ca^{2+} current and the prolonged inactivation of the channel. The L-type Ca^{2+} channel is regulated by phosphorylation through various protein kinases. Mechanisms that increase cAMP levels, such as β-adrenergic stimulation, increase phosphorylation of the L-type Ca^{2+} channel by PKA, and this has been demonstrated to increase Ca^{2+} flux through the channel (Brodde and Michel, 1999). Several phosphorylation sites on the L-type Ca^{2+} channel have been described in the literature (Ganesan et al., 2006; Lemke et al., 2008; Bunemann et al., 1999), but the exact mechanism of how phosphorylation affects the Ca^{2+} current has not been fully determined. GDX may reduce cAMP levels in the myocyte, or may decrease the phosphorylation of the L-type Ca^{2+} channel by other mechanisms, and thus cause the smaller Ca^{2+} current observed. GDX may also slow down mechanisms that inactivate the L-type Ca^{2+} channel. GDX may increase CaMKII phosphorylation of the L-type Ca^{2+} channel to promote mode 2 gating, which is associated with a reduced peak Ca^{2+} current, and a prolonged channel inactivation (Dzhura et al., 2000). Mode 2 gating of the L-type Ca^{2+} channel is also associated with an increased incidence of early after-depolarizations, which may lead to arrhythmias (Wu et al., 1999; Koval et al.,2010; Anderson et al., 1998). This may be the mechanism which contributes to a reduced peak Ca^{2+} current, and a prolonged decay of the Ca^{2+}

current. The prolonged Ca^{2+} current decay may help prolong the action potential, and thus contribute to the slowed contractile relaxation and Ca^{2+} transient decay in field stimulated cells.

The next step in the Ca^{2+} induced Ca^{2+} release process was then investigated. The L-type Ca^{2+} current opens RyR channels in the SR, releasing Ca^{2+} into the cytosol. Ca^{2+} is released from the SR in small, fundamental units called Ca^{2+} sparks, which sum to form the Ca^{2+} transient. The results of this study report the novel observation that GDX had no effect on the spark width, but it reduced the size and frequency of spontaneous Ca^{2+} sparks. Interestingly, this study also showed that GDX prolonged the decay of Ca^{2+} sparks. These changes in spark duration would be expected to affect EC coupling in hearts chronically exposed to low levels of testosterone. In this case, the increase in spark duration may contribute to the slower contractions and Ca^{2+} transients observed in GDX cells.

GDX may modulate the expression or activity of RyRs to affect the release of Ca^{2+} from the SR. The results of this study showed that GDX did not affect the expression of the major cardiac isoform, RyR2. The only other study which has investigated the effects of GDX on the expression of RyR found that RyR expression was unaffected by GDX, which supports the findings of the present study (Callies et al., 2003). On the other hand, evidence that GDX may modify RyRs as a mechanism to decrease Ca^{2+} release from the SR is supported by a study which found that 9 weeks of GDX decreased Ca^{2+} flux through the RyR (Tsang et al., 2009). Phosphorylation of RyR by PKA at Ser2808 and Ser2030 and/or at Ser2814 by CaMKII, increases the channels open probability (Niggli et al., 2013). GDX may decrease the phosphorylation of RyR by PKA or by CaMKII, and thus reduce the channel's open probability. This may be the

mechanism underlying the smaller Ca^{2+} sparks observed in this study, although additional experiments would be required to test this idea.

A novel finding reported in this thesis is the observation that GDX reduced SR Ca^{2+} content and reduced the fractional release of Ca^{2+} from the SR. A decrease in SR Ca^{2+} content could be due to a decrease in the rate at which Ca^{2+} is sequestered into the SR by SERCA. The results of this thesis showed that GDX did not affect the expression of SERCA2, the major cardiac isoform of SERCA. This finding is supported by previous studies that reported that 2-11 weeks of GDX in rodents had no effect on SERCA2 expression in the heart (Callies et al., 2003; Witayavanitkul et al., 2012; Sebag et al., 2011). This suggests that a decrease in the expression of the SERCA pump is not responsible for the decrease in SR Ca^{2+} content following GDX.

The rate of Ca^{2+} uptake into the SR by SERCA is regulated by its endogenous inhibitor PLB. PLB binds directly to SERCA and effectively lowers its affinity for Ca^{2+}, thus reducing Ca^{2+} transport into the SR. Interestingly, a novel finding of this study is that GDX increased the expression of PLB in the ventricles. This has not been reported in the literature before. Several previous studies on the effect of GDX on PLB expression have reported no change in expression (Callies et al., 2003; Witayavanitkul et al., 2012; Tsang et al., 2008; Sebag et al., 2011). However, these studies investigated PLB expression after a much shorter period of GDX (2-11 weeks) compared to the current study (~9 months). The increased expression of PLB reported in this study can account for the decrease in SR Ca^{2+} load in GDX hearts. It also may help explain the prolonged decay of the Ca^{2+} transient and contractions observed in GDX myocytes. This is likely as there was no change in the expression of NCX in the GDX heart; NCX is the

other major protein responsible for removing Ca^{2+} from the cytosol following its release from the SR.

Phosphorylation of PLB at Ser16 by PKA and/or phosphorylation at Thr17 by CaMKII results in release of PLB from SERCA, relief of this inhibition, and increased Ca^{2+} uptake by the SR (Vangheluwe et al., 2005). Phosphorylation at both sites has been thought to occur sequentially, however, evidence suggests that Thr17 may be differentially regulated when compared to Ser16 (Traaseth et al., 2008; Bhupathy et al., 2007). Two previous studies did report that 10-11 weeks of GDX reduced the expression of phosphorylated PLB at either at one (Thr17; Witayavanitkul et al., 2012) or both phosphorylation sites (Sebag et al., 2011). Thus, GDX may decrease phosphorylation of PLB, and thus increase its affinity to SERCA, and further reduce the rate of Ca^{2+} uptake into the SR. This may be a mechanism which contributes to the lower SR Ca^{2+} stores and prolonged Ca^{2+} transient decay seen in GDX myocytes. Reduced SR Ca^{2+} content in GDX cells is also consistent with the decrease in the frequency of spontaneous Ca^{2+} sparks observed in GDX myocytes. Spontaneous Ca^{2+} sparks are believed to be a protective mechanism that limits SR Ca^{2+} overload in the heart (Satoh et al., 1997). Therefore, if the SR contains less Ca^{2+}, a decrease in Ca^{2+} sparks would be expected.

4.5 GDX affects action potential repolarization

The results of this study showed that GDX did not affect the duration of the action potential at 50% repolarization (APD_{50}), however, the action potential was prolonged at 90% repolarization (APD_{90}). There are only two other studies that have investigated the effects of GDX on action potential duration. In one study, APD_{50} was

significantly prolonged after 4 weeks of GDX in ventricular cells isolated from rats (D'Antona et al., 2001). In another study, both APD_{50} and APD_{90} in increased in epicardial ventricular myocytes isolated from mice 37 days after GDX (Brouillette et al., 2003). Together with the results of this thesis these findings suggest that GDX prolongs repolarization of the action potential across several species and over a wide range of durations after GDX surgery.

The mechanism by which action potentials are prolonged by GDX has not been fully established in the literature. Some previous studies report that GDX affects the expression and function of various K^+ channels, to help explain the prolonged repolarization of the action potential. In phase 2 of the action potential, there is an influx of Ca^{2+} through L-type Ca^{2+} channels, which is electrically balanced by K^+ efflux through several delayed rectifier K^+ channels including IKr, IKs, and IKur. In phase 3 of the action potential, the L-type Ca^{2+} channels close, and some K^+ channels remain open until repolarization is complete. GDX may affect action potential repolarization by affecting the expression or function of various repolarizing K^+ currents. The results of this study demonstrated that GDX did not affect the expression of Kv1.5 in the ventricles, which is a major component of IKur. In contrast to this, another previous study found that 13 weeks of GDX caused a decrease in Kv1.5 expression, associated with a reduction in IKur current (Brouillette et al., 2005). This study also reported no change in the function or expression of other K^+ currents including Ito, Iss, and 1K1 (Brouillette et al., 2003). The effects of GDX on K^+ currents however, are clearly controversial as one previous study found that 8 weeks of GDX decreased the IKs current in ventricular myocytes isolated from rabbits (Zhu et al., 2013). Our results indicate that the prolonged action potential repolarization in the present study was not

caused by effects of GDX on the expression of Kv1.5. Differences in results between studies may be due to different technical approaches and/or the use of different mouse strains or species.

GDX may prolong action potential repolarization by effects on currents other than K^+ currents. For example, GDX may increase the magnitude of the late Na^+ current. Depolarization of the cell membrane causes fast Na^+ channels open for a short period producing the early peak sodium current. However, there is also a sustained Na^+ current component called the late Na^+ current (INa,late). INa,late allows the influx of Na^+ throughout the plateau phase of the action potential. The dominant isoform of voltage-dependent sodium channels in cardiac tissues is Nav1.5. The INa,late current density generally occurs on a small proportion of Na^+ channels (Horvath and Bers, 2014). However, GDX may change the gating mode of the Na^+ channels which would result in increased INa,late current, and potentially prolong action potential repolarization. Clinical evidence has indicated that an increased INa,late current causes longer action potentials in the ventricles, which is presented as a longer QT interval on the ECG (Horvath et al., 2013; Studenik et al., 2001). An increased INa,late impairs repolarization and increases intracellular sodium concentration in cardiomyocytes. This would promote cardiac arrhythmias and contractile dysfunction (Horvath and Bers, 2014). A previous study did not support this hypothesis, and found that 16 weeks of GDX had no effect on the expression of voltage gated sodium channels (Nav1.5), however, expression was measured by immunoreactivity and not Western blotting (Eleawa et al., 2013). Additional studies of the effect of GDX on the protein expression of Nav1.5 in the ventricles would be of interest.

The results of previous studies suggest that GDX may prolong action potential repolarization by affecting the function or expression of some K^+ channels although this was not observed in the present study. In theory, GDX may prolong the action potential by promoting the INa,late current, however, this is not supported in the literature. Interestingly, the present thesis shows, for the first time, that GDX prolongs the Ca^{2+} current, which would be expected to increase the influx of Ca^{2+} during the action potential and prolong repolarization. This could account for the longer action potentials observed in GDX cells in this study. Increasing the duration of the action potential is associated with electrical disturbances in cardiomyocytes such as EADs (Wang et al., 1996; Cardona et al., 2010). Therefore, longer action potentials secondary to prolonged Ca^{2+} influx could be a mechanism for how GDX may promote electrical disturbances in the whole heart, as discussed below.

4.6 GDX increases the incidence of EADS and spontaneous contractions

The prolonged action repolarization observed in this study may lead disturbances in the electrical activity of the cardiomyocyte such as EADs. This may be clinically important as prolongation of the action potential can increase the probability of early after depolarizations, which can trigger arrhythmias such as “torsade de pointes” (January et al., 1989; Guo et al., 2007). An EAD is defined as a slowing or reversal of normal repolarization during phase 2 or phase 3 of the action potential. EADs occur when the net outward current required to repolarize the myocyte is compromised or the net inward current is increased. The results of this study showed that GDX increased the incidence of early EADs. Interesting, this study also showed that GDX increased the incidence of spontaneous contractions.

Several mechanisms may cause a prolonged action potential repolarization and promote EADs, which can lead to arrhythmias. The results of the current study show that GDX may prolong action potential repolarization by prolonging the Ca^{2+} current. The prolonged Ca^{2+} current observed in this study may result from GDX promoting CaMKII phosphorylation of Gate 2 mode of L-type Ca^{2+} channel, which increases the time for channel inactivation (Swaminathan et al., 2012). Some studies have suggested that a prolonged action potential may be caused by GDX changing the function or expression of K^+ channels, which would prolong the action potential. GDX may also promote the INa,late current by affecting the gating mechanism of the Na^+ channel and prolong action potential repolarization. Clinical studies have reported that an increased INa,late current leads to a longer ventricular action potential, which presents as a longer QT interval on the ECG (Horvath et al., 2013; Studenik et al., 2001). GDX may promote several of these mechanisms to prolong action potential repolarization, as discussed above. The longer action potential promotes EADs and this may lead to the spontaneous contractions in cardiomyocytes observed in this study.

4.7 Summary

Chronic testosterone withdrawal adversely affected the structure and function of the heart. GDX had effects on myocardial structure *in vivo*. Results showed that the hearts of GDX mice had a thinner IVSd and the mass of the left ventricle was smaller, which indicated that there was dilation of the ventricles. There were also effects of GDX on *in vivo* function. The isovolumic relaxation time was prolonged by GDX, suggesting that testosterone modulates diastolic function. GDX also affected structure and function at the cellular level. Results showed that GDX caused isolated ventricular myocytes to

be slightly smaller than normal. Peak responses of cell shortening and Ca^{2+} transients were not different in field-stimulated ventricular myocytes, however, the time course of relaxation and Ca^{2+} transient decay was significantly prolonged by GDX. Interestingly, when the duration of depolarization was controlled by voltage clamp, GDX suppressed peak cell shortening and Ca^{2+} transients, but abolished the effects on the time course of cell relaxation and Ca^{2+} transient decay. These observations suggest that GDX may influence action potential configuration, and may affect key components of the EC coupling pathway.

GDX did affect Ca^{2+} handling in the heart. It caused a smaller peak Ca^{2+} current, although expression of Cav1.2 was unaffected. There was no effect on net Ca^{2+} flux across the sarcolemma by GDX, however, the Ca^{2+} current decay was prolonged. The prolonged Ca^{2+} current decay likely prolonged the action potential, and this might contribute to the slowed contractile relaxation and Ca^{2+} transient decay. The release and reuptake of Ca^{2+} from the SR also was affected by GDX. GDX reduced SR Ca^{2+} load and the fractional release of Ca^{2+} from the SR. The smaller peak Ca^{2+} current contributes to the smaller contractions observed in voltage clamp experiments. The Ca^{2+} spark amplitude was decreased by GDX, and the Ca^{2+} spark decay was prolonged. There was no effect of GDX on the expression of RyR2 to explain these results. GDX decreased the frequency of spontaneous Ca^{2+} sparks released from the SR. GDX had effects components of the EC coupling pathway that influence SR Ca^{2+} loading. The expression of the SERCA pump was not affected, however, the expression of SERCA's endogenous inhibitor, PLB, was increased by GDX. The slower Ca^{2+} reuptake into the SR was due to GDX increasing PLB expression.

GDX prolonged the duration of the action potential, which helps explain the different observations in field stimulation and voltage clamped experiments. Voltage clamp experiments control the duration of depolarization in myocytes, while in field stimulation they contract in response to the action potential. The prolonged action potential repolarization was not due to changes in the expression of Kv1.5 (Ikur). The duration of action potential repolarization may be increased by GDX by prolonging the Ca^{2+} current. The prolonged action potential repolarization can disrupt electrical activity in the myocyte and result in EADs. GDX increased the number of EADs, which is an important mechanisms for generation of life-threatening arrhythmias that can also trigger spontaneous contractions in the heart.

This thesis demonstrates that chronic testosterone withdrawal adversely affects the structure and function of the heart. Key components of the EC coupling pathway are affected by GDX, which results in abnormal Ca^{2+} handling and disturbances in the electrical activity at the cellular level. These observations suggest that chronic testosterone withdrawal promotes changes the heart which may promote diastolic dysfunction and fatal arrhythmias such as "torsade de pointes" in older men with low testosterone (Jin et al., 2014; Tisdale, 2016).

4.8 Future work

This thesis provides evidence that chronic testosterone withdrawal promotes disturbed electrical activity in the heart. Future examination of the effect of GDX on electrocardiogram would be of interest, to confirm the presence of arrhythmic activity *in vivo*. This study demonstrated that chronic testosterone withdrawal affects cellular Ca2+ handling and contraction. Future investigations should determine how gonadectomy

affects the activity of PKA and CaMKII in the cell. It would also be interesting to investigate if testosterone treatment can reverse effects of GDX seen at the organ and cellular levels. The impact of GDX performed later in life with varying levels of testosterone replacement would also be of interest to more closely model older men who are receiving testosterone supplementation. It would also of interest to conduct studies of the effects of variable doses of testosterone in older female animals to see how the effects of aging and testosterone on the heart interact in females.

REFERENCES

Ahtiainen, J.P., Hulmi, J.J., Kraemer, W.J., Lehti, M., Nyman, K., Selänne, H., Alen, M., Pakarinenf, A., Komulainen, J., Kovanen, V., Mero, A.A., Häkkinen, K., 2011. Heavy resistance exercise training and skeletal muscle androgen receptor expression in younger and older men. Steroids 76, 183–192.

Alagiakrishnan, K., Banach, M., Jones, L.G., Datta, S., Ahmed, A., Aronow, W.S., 2013. Update on diastolic heart failure or heart failure with preserved ejection fraction in the older adults. Ann Med 45, 37–50.

Alkamel, A., Shafiee, A., Jalali, A., Boroumand, M., Nozari, Y., 2014. The association between premature coronary artery disease and level of testosterone in young adult males. Arch Iran Med 17(8), 545–550.

Altamirano, F., Oyarce, C., Silva, P., Toyos, M., Wilson, C., Lavandero, S., Uhlén, P., Estrada, M., 2009. Testosterone induces cardiomyocyte hypertrophy through mammalian target of rapamycin complex 1 pathway. J Endocrinol 202, 299–307.

Amery, A., Fagard, R., Guo, C., Staessen, J., Thijs, L., 1991. Isolated systolic hypertension in the elderly: an epidemiologic review. Am J Med 90, 64S–70S.

Anderson, M.E., Braun, A.P., Wu, Y., Lu, T., Wu, Y., Schulman, H., Sung, R.J., 1998. KN-93, an inhibitor of multifunctional Ca2+/calmodulin-dependent protein kinase, decreases early afterdepolarizations in rabbit heart. J Pharmacol Exp Ther 287, 996–1006.

Angell, P.J., Chester, N., Green, D.J., Shah, R., Somauroo, J., Whyte, G., George, K., 2012. Anabolic steroid use and longitudinal, radial, and circumferential cardiac motion. Med Sci Sports Exerc 44(4), 583–590.

Angell, P.J., Ismail, T.F., Jabbour, A., Smith, G., Dahl, A., Wage, R., Whyte, G., Green, D.J., Prasad, S., George, K., 2014. Ventricular structure, function, and focal fibrosis in anabolic steroid users: a CMR study. Eur J Appl Physiol 114, 921–928.

Araujo, A.B., Dixon, J.M., Suarez, E.A., Murad, M.H., Guey, L.T., Wittert, G.A., 2011. Clinical review: Endogenous testosterone and mortality in men: a systematic review and meta-analysis. J Clin Endocrinol Metab 96(10), 3007-3019.

Araujo, A.B., O'Donnell, A.B., Brambilla, D.J., Simpson, W.B., Longcope, C., Matsumoto, A.M. McKinlay, J.B., 2004. Prevalence and incidence of androgen deficiency in middle-aged and older men: estimates from the Massachusetts Male Aging Study. J Clin Endocrinol Metab 89(12), 5920–5926.

Ashley, E.A., Niebauer, J., 2004. Cardiology Explained. London: Remedica; Chapter 5, Coronary artery disease. Available from: https://www.ncbi.nlm.nih.gov/books/NBK2216/

Barp, J., Araújo, A.S., Fernandes, T.R., Rigatto, K.V., Llesuy, S., Belló-Klein, A., Singal, P., 2002. Myocardial antioxidant and oxidative stress changes due to sex hormones. Braz J Med Biol Res 35, 1075–1081.

Barrett-Connor, E.L., 1995. Testosterone and risk factors for cardiovascular disease in men. Diabete Metab 21(3), 156-161.

Bassil, N., Alkaade, S., Morley, J.E., 2009. The benefits and risks of testosterone replacement therapy: A review. Therapeutics and Clinical Risk Management 5(1), 427–448.

Bauersachs, J., Widder, J.D., 2008. Endothelial dysfunction in heart failure. Pharmacol Rep 60, 119–126.

Bers, D.M., 2014. Cardiac sarcoplasmic reticulum calcium leak: basis and roles in cardiac dysfunction. Annu Rev Physiol 76, 107–127.

Bell, J.R., Bernasochi, G.B., Varma, U., Boon, W.C., Ellem, S.J., Risbridger, G.P., Delbridge, L.M., 2014. Aromatase transgenic upregulation modulates basal cardiac performance and the response to ischemic stress in male mice. Am J Physiol Heart Circ Physiol 306, H1265–H1274.

Ben Driss, A., Devaux, C., Henrion, D., Duriez, M., Thuillez, C., Levy, B.I., Michel, J.B., 2000. Hemodynamic stresses induce endothelial dysfunction and remodeling of pulmonary artery in experimental compensated heart failure. Circulation 101, 2764–2770.

Bhasin, S., Cunningham, G.R., Hayes, F.J., Matsumoto, A.M., Snyder, P.J., Swerdloff, R.S., Montori, V.M., 2010. Testosterone therapy in men with androgen deficiency syndromes: an endocrine society clinical practice guideline. J Clin Endocrinol Metab 95, 2536–2559.

Bhupathy, P., Babu, G.J., Periasamy, M., 2007. Sarcolipin and phospholamban as regulators of cardiac sarcoplasmic reticulum Ca2+ ATPase. J Mol Cell Cardiol 42(5), 903-911.

Bocalini, D.S., Beutel, A., Bergamaschi, C.T., Tucci, P.J., Campos, R.R., 2014. Treadmill exercise training prevents myocardial mechanical dysfunction induced by androgenic-anabolic steroid treatment in rats. PLoS One 9, e87106.

Borlaug, B.A., Redfield, M.M., 2011. Diastolic and systolic heart failure are distinct phenotypes within the heart failure spectrum, Circulation 123, 2006–2014.

Borst, S.E., Mulligan, T., 2007. Testosterone replacement therapy for older men. Clin Interv Aging 2(4), 561–566.

Bowles, D.K., Maddali, K.K., Ganjam, V.K., Rubin, L.J., Tharp, D.L., Turk, J.R., Heaps, C.L., 2004. Endogenous testosterone increases L-type Ca^{2+} channel expression in porcine coronary smooth muscle. 65211, 2091–2098.

Braunwald, E., 2013. Heart failure. JACC Heart Fail 1(1), 1–20.

Brodde, O.E., Michel, M.C., 1999. Adrenergic and Muscarinic Receptors in the Human Heart. 51(4), 651-690.

Brouillette, J., Rivard, K., Lizotte, E., Fiset, C., 2005. Sex and strain differences in adult mouse cardiac repolarization: importance of androgens. Cardiovasc Res 65, 148–157.

Brouillette, J., Trépanier-Boulay, V., Fiset, C., 2003. Effect of androgen deficiency on mouse ventricular repolarization. J Physiol 546, 403–413.

Bünemann, M., Gerhardstein, B.L., Gao, T., Hosey, M.M., 1999. Functional regulation of L-type calcium channels via protein kinase A-mediated phosphorylation of the β2 subunit. J Biol Chem 274(48), 33851-33854.

Buonanno, C., Arbustini, E., Rossi, L., Dander, B., Vassanelli, C., Paris, B., Poppi, A., 1982. Left ventricular function in men and women. Another difference between sexes. Eur Heart J 3(6), 525–528.

Buus, N.H., Bottcher, M., Hermansen, F., Sander, M., Nielsen, T.T., Mulvany, M.J., 2001. Influence of nitric oxide synthase and adrenergic inhibition on adenosine-induced myocardial hyperemia. Circulation 104, 2305–2310.

Callies, F., Strömer, H., Schwinger, R.H., Bölck, B., Hu, K., Frantz, S., Leupold, A., Beer, S., Allolio, B., Bonz, A.W., 2003. Administration of testosterone is associated with a reduced susceptibility to myocardial ischemia. Endocrinology. 144, 4478–4483.

Caminiti, G., Iellamo, F., Manzi, V., Fossati, C., Cioffi, V., Punzo, N., Murugesan, J., Volterrani, M., Rosano, G., 2014. Anabolic hormonal response to different exercise training intensities in men with chronic heart failure. Int J Cardiol 176, 1433–1434.

Caminiti, G., Volterrani, M., Iellamo, F., Marazzi, G., Massaro, R., Miceli, M., Mammi, C., Piepoli, M., Fini, M., Rosano, G.M., 2009. Effect of long-acting testosterone treatment on functional exercise capacity, skeletal muscle performance, insulin resistance, and baroreflex sensitivity in elderly patients with chronic heart failure a double-blind, placebo-controlled, randomized study. J Am Coll Cardiol 54, 919–927.

Canadian Council on Animal Care, Ottawa, ON: Vol. 1, 2nd ed., 1993; Vol. 2, 1984. "Guide to the Care and Use of Experimental Animals"

Canty, J.M., Jr, Suzuki, G., 2012. Myocardial perfusion and contraction in acute ischemia and chronic ischemic heart disease. J Mol Cell Cardiol 52, 822–31.

Cardona, K., Trenor, B., Rajamani, S., Romero, L., Ferrero, J.M., Saiz, J., 2010. Effects of late sodium current enhancement during LQT-related arrhythmias. A simulation study. Conf Proc IEEE Eng Med Biol Soc 2010:3237-3240.

Cassimatis, D.C., Crim, M.T., Wenger, N. K., 2016. Low Testosterone in Men with Cardiovascular Disease or Risk Factors: To Treat or Not To Treat? Curr Treat Options Cardio Med 18(12), 75.

Cavasin, M.A., Sankey, S.S., Yu, A.L., Menon, S., Yang, X.P., 2003. Estrogen and testosterone have opposing effects on chronic cardiac remodeling and function in mice with myocardial infarction. Am J Physiol Heart Circ Physiol 284, H1560–H1569.

Cavasin, M.A., Tao, Z.Y., Yu, A.L., Yang, X.P., 2006. Testosterone enhances early cardiac remodeling after myocardial infarction, causing rupture and degrading cardiac function. Am J Physiol Heart Circ Physiol 290, H2043–H2050.

Cheatham, S.A., Hosey, R.G., Johnson, D.L., 2008. Performance-enhancing drugs and today's athlete: a growing concern. Orthopedics 31, 10.

Chen, H., Midzak, A., Luo, L., Zirkin, B.R., 2007. Aging and the decline of androgen production, In: Payne AH, Hardy MP (ed.), The Leydig cell in health and disease. Humana Press, New Jersey.

Cheng, H., Lederer, W.J., 2008. Calcium Sparks. Physiol Rev 88(4), 1491–1545.

Chung, C.C., Hsu, R.C., Kao, Y.H., Liou, J.P., Chen, Y.J., 2014. Androgen attenuates cardiac fibroblasts activations through modulations of transforming growth factor-β and angiotensin II signaling. Int J Cardiol 176, 386–393.

Chung, T., Kelleher, S., Liu, P.Y., Conway, A.J., Kritharides, L., Handelsman, D.J., 2007. Effects of testosterone and nandrolone on cardiac function: a randomized, placebo-controlled study. Clin Endocrinol (Oxf) 66(2), 235–245.

Corona, G., Rastrelli, G., Monami, M., Guay, A., Buvat, J., Sforza, A., Forti, G., Mannucci, E., Maggi, M., 2011. Hypogonadism as a risk factor for cardiovascular mortality in men: a meta-analytic study. Eur J Endocrinol 165, 687–701.

Credit, S.L., Benghuzzi, H.A., Tucci, M., Farah, I., Cameron, J.A., 2002. Localization of cytokines in heart ventricular and apex tissues exposed to sustained delivery of AED, T, and DHT using a rat model. Biomed Sci Instrum 38, 95–100.

Crossman, D.C., 2004. The pathophysiology of myocardial ischaemia. Heart 90, 576-580.

Čulić, V., 2015. Androgens in cardiac fibrosis and other cardiovascular mechanisms. Int J Cardiol 179, 190–192.

Čulić, V., Bušić, Ž., 2013. Severity of acute heart failure in men according to diabetes mellitus: the role of testosterone and renal dysfunction. Int J Cardiol 168, 5039–5041.

Čulić, V., Bušić, Ž., 2015. Testosterone may influence left ventricular diastolic function depending on previous myocardial infarction and smoking. Int J Cardiol 186, 67–71.

Čulić, V., Bušić, Z., Bušić, M., 2016. Circulating sex hormones, alcohol consumption and echocardiographic parameters of cardiac function in men with heart failure. Int J Cardiol 224, 245–251.

Curl, C.L., Delbridge, L.M., Canny, B.J., Wendt, I.R., 2009. Testosterone modulates cardiomyocyte Ca^{2+} handling and contractile function. Physiol Res 58(2), 293–297.

Currie, S., Smith, G.L., 1999. Enhanced phosphorylation of phospholamban and downregulation of sarco/endoplasmic reticulum Ca^{2+} ATPase type 2 (SERCA 2) in cardiac sarcoplasmic reticulum from rabbits with heart failure. Cardiovasc Res 41(1), 135–146.

Czesla, M., Mehlhorn, G., Fritzsche, D., Asmussen, G., 1997. Cardiomyoplasty—improvement of muscle fiber type transformation by an anabolic steroid (metenolone). J Mol Cell Cardiol 29, 2989–2996.

Dart, D.A., Waxman, J., Aboagye, E.O., Bevan, C.L., 2013. Visualising androgen receptor activity in male and female mice. PLoS One 8, e71694.

D'Antona, G., Gualea, M.R., Ceriani, T., 2001. Effects of gonadectomy, testosterone replacement and supplementation on cardiac action potentials in the rat. Basic Appl Myol 11, 23–29.

Davignon, J., Ganz, P., 2004. Role of endothelial dysfunction in atherosclerosis. Circulation 109, III 27–32.

Davison, S.L., Davis, S.R., 2003. Androgens in women. J Steroid Biochem Mol Biol 85(2-5), 363–366.

Dent, J.R., Fletcher, D.K., McGuigan, M.R., 2012. Evidence for a non-genomic action of testosterone in skeletal muscle which may improve athletic performance: Implications for the female athlete. J Sports Sci Med 11(3), 363–370.

De Piccoli, B., Giada, F., Benettin, A., Sartori, F., Piccolo, E., 1991. Anabolic steroid use in body builders: an echocardiographic study of left ventricle morphology and function. Int J Sports Med 12(4), 408–412.

De Tombe, P.P., 2003. Cardiac myofilaments: Mechanics and regulation. J Biomech 36(5), 721–730.

Dockery, F., Bulpitt, C.J., Agarwal, S., Donaldson, M., Rajkumar, C., 2003. Testosterone suppression in men with prostate cancer leads to an increase in arterial stiffness and hyperinsulinaemia. Clinical Science 104, 195–201.

Dubey, R.K., Oparil, S., Imthurn, B., Jackson, E.K., 2002. Sex hormones and hypertension. Cardiovasc Res 53(3), 688–708.

Dzhura, I., Wu, Y., Colbran, R.J., Balser, J.R., Anderson, M.E., 2000. Calmodulin kinase determines calcium-dependent facilitation of L-type calcium channels. Nat Cell Biol 2, 173-177.

Edelman, S., Butler, J., Hershatter, B.W., Khan M.K., 2014. The effects of androgen deprivation therapy on cardiac function and heart failure: implications for management of prostate cancer. Clin Genitourin Cancer 12(6), 399–407.

Eleawa, S.M., Sakr, H.F., Hussein, A.M., Assiri, A.S., Bayoumy, N.M., Alkhateeb, M., 2013. Effect of testosterone replacement therapy on cardiac performance and oxidative stress in orchidectomized rats. Acta Physiol (Oxf) 209, 136–147.

Elsherbiny, A., Tricomi, M., Bhatt, D., Dandapantula, H.K., 2017. State-of-the-Art: a Review of Cardiovascular Effects of Testosterone Replacement Therapy in Adult Males. Curr Cardiol Rep 19(4), 35.

Ely, D., Caplea, A., Dunphy, G., Daneshvar, H., Turner, M., Milsted, A., Takiyyudin, M., 1997. Spontaneously hypertensive rat Y chromosome increases indexes of sympathetic nervous systemactivity. Hypertension 29, 613–618.

English, K.M., Mandour, O., Steeds, R.P., Diver, M.J., Jones, T.H., Channer, K.S., 2000. Men with coronary artery disease have lower levels of androgens than men with normal coronary angiograms. Eur Heart J 21(11), 890-894.

English, K.M., Steeds, R.P., Jones, T.H., Diver, M.J., Channer, K.S., 2000. Low-dose transdermal testosterone therapy improves angina threshold in men with chronic stable angina: a randomized, double-blind, placebo-controlled study. Circulation 102(16), 1906–1911.

Er, F., Gassanov, N., Brandt, M.C., Madershahian, N., Hoppe, U.C., 2009. Impact of dihydrotestosterone on L-type calcium channels in human ventricular cardiomyocytes. Endocr Res 34, 59–67.

Er, F., Michels, G., Brandt, M.C., Khan, I., Haase, H., Eicks, M., Lindner, M., Hoppe, U.C., 2007. Impact of testosterone on cardiac L-type calcium channels and Ca^{2+} sparks: acute actions antagonize chronic effects. Cell Calcium 41, 467–477.

Er, F., Michels, G., Gassanov, N., Rivero, F., Hoppe, U.C., 2004. Testosterone induces cytoprotection by activating ATP-sensitive K^{+} channels in the cardiac mitochondrial inner membrane. Circulation 110(19), 3100–3107.

Erkens, R., Kramer, C.M., Lückstädt, W., Panknin, C., Krause, L., Weidenbach, M., Dirzka, J., Krenz, T., Mergia, E., Suvorava, T., Kelm, M., Cortese-Krott, M.M., 2015. Left ventricular diastolic dysfunction in Nrf2 knock out mice is associated with cardiac hypertrophy, decreased expression of SERCA2a, and preserved endothelial function. Free Radic Biol Med 89, 906-917.

Esposito, F., Mathieu-Costello, O., Shabetai, R., Wagner, P.D., Richardson, R.S., 2010. Limited maximal exercise capacity in patients with chronic heart failure: partitioning the contributors. J Am Coll Cardiol 55, 1945–1954.

Fares, E., Howlett, S.E., 2010. Effect of age on cardiac excitation-contraction coupling. Clin Exp Pharmacol Physiol 37(1), 1-7.

Fares, E., Parks, R.J., MacDonald, J.K., Egar, J.M., Howlett, S.E., 2012. Ovariectomy enhances SR Ca^{2+} release and increases Ca^{2+} spark amplitudes in isolated ventricular myocytes. J Mol Cell Cardiol 52 (1), 32-42.

Farias, J.M., Tinetti, M., Khoury, M., Umpierrez, G.E., 2014. Low testosterone concentration and atherosclerosis disease markers in male patients with type 2 diabetes. J Clin Endocrinol Metab 99, 4698-4703.

Fearnley, C.J., Roderick, H.L., Bootman, M.D., 2011. Calcium signaling in cardiac myocytes. Cold Spring Harb Perspect Biol 3(11), 1–20.

Feldman, H.A., Longcope, C., Derby, C.A., Johannes, C.B., Araujo, A.B., Coviello, A.D., Bremner, W.J., McKinlay, J.B., 2002. Age trends in the level of serum testosterone

and other hormones in middle-aged men: longitudinal results from the Massachusetts male aging study. J Clin Endocrinol Metab 87(2), 589–598.

Fink, M., Noble, D., 2010. Pharmacodynamic effects in the cardiovascular system: the modeller's view. Basic Clin Pharmacol Toxicol 106, 243–249.

Fogari, R., Preti, P., Zoppi, A., Fogari, E., Rinaldi, A., Corradi, L., Mugellini, A., 2005. Serum testosterone levels and arterial blood pressure in the elderly. Hypertens Res 28, 625–630.

Fogari, R., Zoppi, A., Preti, P., Rinaldi, A., Marasi, G., Vanasia, A., Mugellini, A., 2002. Sexual activity and plasma testosterone levels in hypertensive males. Am J Hypertens 15(3), 217–221.

Fonarow, G.C., Stough, W.G., Abraham, W.T., Albert, N.M., Gheorghiade, M., Greenberg, B.H., O'Connor, C.M., Sun, J.L., Yancy, C.W., Young, J.B., 2007; OPTIMIZE-HF Investigators and Hospitals. Characteristics, treatments, and outcomes of patients with preserved systolic function hospitalized for heart failure: a report from the OPTIMIZE-HF Registry. J Am Coll Cardiol 50(8), 768-777.

Fontes-Carvalho, R., Leite-Moreira, A., 2011. Heart Failure with Preserved Ejection Fraction: Fighting Misconceptions for a New Approach. Arq Bras Cardiol 96(6), 504-514.

Franklin, S.S., Jacobs, M.J., Wong, N.D., L'Italien, G.J., Lapuerta, P., 2001. Predominance of isolated systolic hypertension among middle-aged and elderly US hypertensives: analysis based on National Health and Nutrition Examination Survey (NHANES) III. Hypertension 37, 869–874.

Freshour, J.R., Chase, S.E., Vikstrom, K.L., 2003. Gender differences in cardiac ACE expression are normalized in androgen-deprived male mice. Am J Physiol Heart Circ Physiol 283(5), H1997–2003.

Fukuta, H., Little, W.C., 2008. The cardiac cycle and the physiologic basis of left ventricular contraction, ejection, relaxation, and filling. Heart Fail Clin 4(1), 1–11.

Ganesan, A.N., Maack, C., Johns, D.C., Sidor, A., O'Rourke, B., 2006. Beta-adrenergic stimulation of L-type Ca^{2+} channels in cardiac myocytes requires the distal carboxyl terminus of alpha1C but not serine 1928. Circ Res 98, e11–e18.

Gencer, B., Mach, F., 2015. Testosterone: a hormone preventing cardiovascular disease or a therapy increasing cardiovascular events? Eur Heart J 37, 3569–3575.

Giusti, G., Gonnelli, P., Borrelli, D., Fiorelli, G., Forti, G., Pazzagli, M., Serio, M., 1975. Age-related secretion of androstenedione, testosterone and dihydrotestosterone by the human testis. Exp Gerontol 10, 241–245.

Glaser, R., Dimitrakakis, C., 2013. Testosterone therapy in women: Myths and misconceptions. Maturitas 74(3), 230–234.

Go, A.S., Mozaffarian, D., Roger, V.L., Benjamin, E.J., Berry, J.D., Borden, W.B., Bravata, D.M, Dai, S., Ford, E.S., Fox, C.S., Franco, S., Fullerton, H.J., Gillespie, C.,

Hailpern, S.M., Heit, J.A., Howard, V.J., Huffman, M.D., Kissela, B.M., Kittner, S.J., Lackland, D.T., Lichtman, J.H., Lisabeth, L.D., Magid, D., Marcus, G.M., Marelli, A., Matchar, D.B., McGuire, D.K., Mohler, E.R., Moy, C.S., Mussolino, M.E., Nichol, G., Paynter, N.P., Schreiner, P.J., Sorlie, P.D., Stein, J., Turan, T.N., Virani, S.S., Wong, N.D., Woo, D., Turner, M.B.; American Heart Association Statistics Committee and Stroke Statistics Subcommittee, 2013. Heart disease and stroke statistics–2013 update: a report from the American Heart Association. Circulation 127, e6–245.

Golden, K.L., Marsh, J.D., Jiang, Y., 2002. Castration reduces mRNA levels for calcium regulatory proteins in rat heart. Endocrine 19, 339–344.

Golden, K.L., Marsh, J.D., Jiang, Y., Brown, T., Moulden J., 2003. Gonadectomy of adult male rats reduces contractility of isolated cardiac myocytes. Am J Physiol Endocrinol Metab 285, E449–E453.

Golden, K.L., Marsh, J.D., Jiang, Y., Moulden, J., 2004. Gonadectomy alters myosin heavy chain composition in isolated cardiac myocytes. Endocrine 24, 137–140.

Gordan, R., Gwathmey, J.K., Xie, L.H., 2015. Autonomic and endocrine control of cardiovascular function. World J Cardiol 7(4), 204-214.

Gray, A., Feldman, H.A., McKinlay, J.B., Longcope, C., 1991. Age, disease, and changing sex hormone levels in middle-aged men: results of the Massachusetts Male Aging Study. J Clin Endocrinol Metab 73(5), 1016–1025.

Grynkiewicz, G., Poenie, M., Tsien, R.Y., 1985. A new generation of Ca^{2+} indicators with greatly improved fluorescence properties. J Biol Chem 260(6), 3440-3450.

Gunning, P.W., Hardeman, E.C., Lappalainen, P., Mulvihill, D.P., 2015. Tropomyosin - master regulator of actin filament function in the cytoskeleton. J Cell Sci 128, 2965-2974.

Hackney, A.C., Hosick, K.P., Myer, A., Rubin, D.A., Battaglini, C.L., 2012. Testosterone responses to intensive interval versus steady-state endurance exercise. J. Endocrinol Invest 35, 947–950.

Hadi, H.A.R., Carr, C.S., Suwaidi, J.A., 2005. Endothelial dysfunction: cardiovascular risk factors, therapy, and outcome. Vasc Health Risk Manag 1(3), 183–198.

Hajimoradi, B., Kazerani, H., 2013. Echocardiographic findings in power athletes abusing anabolic androgenic steroids. Asian J Sports Med 4, 10–14.

Hak, A.E., Witteman, J.C., de Jong F.H., Geerlings, M.I., Hofman, A., Pols, H.A., 2002. Low levels of endogenous androgens increase the risk of atherosclerosis in elderly men: the Rotterdam study. J Clin Endocrinol Metab 87(8), 3632–3639

Hanley, P.C., Zinsmeister, A.R., Clements, I.P., Bove, A.A., Brown, M.L., Gibbons, R.J., 1989. Gender-related differences in cardiac response to supine exercise assessed by radionuclide angiography. J Am Coll Cardiol 13(3), 624–629.

Haring, R., Völzke, H.V., Steveling, A., Krebs, A., Felix, S.B., Schöfl, C., Dörr, M., Nauck, M., Wallaschofski, H., 2010. Low serum testosterone levels are associated with

increased risk of mortality in a population-based cohort of men aged 20-79. Eur Heart J 31, 1494–1501.

Harman, S.M., Metter, E.J., Tobin, J.D., Pearson, J., Blackman, M.R., 2001. Longitudinal effects of aging on serum total and free testosterone levels in healthy men. Baltimore Longitudinal Study of Aging. J Clin Endocrinol Metab 86, 724–731.

Hanukoglu, I., 1992. Steroidogenic enzymes: structure, function, and role in regulation of steroid hormone biosynthesis. J Steroid Biochem Mol Biol 43, 779–804.

Hawkins, V.N., Foster-Schubert, K., Chubak, J., Sorensen, B., Ulrich, C.M., Stancyzk, F.Z., Plymate, S., Stanford, J., White, E., Potter, J.D., McTiernan, A., 2008. Effect of exercise on serum sex hormones in men: a 12-month randomized clinical trial. Med Sci Sports Exerc 40, 223–233.

Heinlein, C.A., Chang, C., 2002. The roles of androgen receptors and androgen-binding proteins in nongenomic androgen actions. Mol Endocrinol 16(10), 2181-2187.

Herbison, A.E., Porteous, R., Pape, J.R., Mora, J.M., Hurst, P.R., 2008. Gonadotropin-releasing hormone neuron requirements for puberty, ovulation, and fertility. Endocrinology 149, 597–604.

Herring, M.J., Oskui, P.M., Hale, S.L., Kloner, R.A., 2013. Testosterone and the cardiovascular system: a comprehensive review of the basic science literature. J Am Heart Assoc 2(4), e000271.

Horvath, B., Banyasz, T., Jian, Z., Hegyi, B., Kistamas, K., Nanasi, P.P., Izu, L.T., Ye, C.I., 2013. Dynamics of the late Na+ current during cardiac action potential and its contribution to afterdepolarizations. J Mol Cell Cardiol 64, 59-68.

Horvath, B., Bers, D.M., 2014. The late sodium current in heart failure: pathophysiology and clinical relevance. ESC Heart Failure 1, 26–40.

Hu, X., Rui, L., Zhu, T., Xia, H., Yang, X., Wang, X., Liu, H., Lu, Z., Jiang, H., 2011. Low testosterone level in middle-aged male patients with coronary artery disease. Eur J Intern Med 22(6), e133–136.

Hyde, Z., Norman, P.E., Flicker, L., Hankey, G.J., Almeida, O.P., McCaul, K.A., Chubb, S.A., Yeap, B.B., 2012. Low free testosterone predicts mortality from cardiovascular disease but not other causes: the Health in Men Study. J Clin Endocrinol Metab 97, 179–189.

Iellamo, F., Volterrani, M., Caminiti, G., Karam, R., Massaro, R., Fini, M., Collins, P., Rosano, G.M., 2010. Testosterone therapy in women with chronic heart failure: a pilot double-blind, randomized, placebo-controlled study. J Am Coll Cardiol 56, 1310–1316.

Ikeda, Y., Aihara, K., Yoshida, Y., Akaike, M., Matsumoto, T., 2012. Effects of androgens on cardiovascular remodeling. J Endocrinol 214, 1–10.

James, A.F., Arberry, L.A., Hancox, J.C., 2004. Gender-related differences in ventricular myocyte repolarization in the guinea pig. Basic Res Cardiol 99, 183–192.

James, A.F., Hancox, J.C., 2003. Sex, drugs and arrhythmia: are gender differences in risk of torsades de pointes simply a matter of testosterone? Cardiovasc Res 57, 1–4.

Jankowska, E.A., Filippatos, G., Ponikowska, B., Borodulin-Nadzieja, L., Anker, S.D., Banasiak, W., Poole-Wilson, P.A., Ponikowski, P., 2009. Reduction in circulating testosterone relates to exercise capacity in men with chronic heart failure. J Card Fail 15, 442–450.

Jiang, M., Ma, Y., Chen, C., Fu, X., Yang, S., Li, X., Yu, G., Mao, Y., Xie, Y., Li, Y., 2009. Androgen-responsive gene database: integrated knowledge on androgen-responsive genes. Mol Endocrinol 23, 1927–1933.

Jin, H.J., Kim, J., Yu, J., 2013. Androgen receptor genomic regulation. Transl Androl Urol 2(3), 158–177.

Jin, Q., Lou, Y., Chen, H., Li, T., Bao, X., Liu, Q., He, X., 2014. Lower free testosterone level is correlated with left ventricular diastolic dysfunction in asymptomatic middle-aged men with type 2 diabetes mellitus. Int J Clin Pract 68, 1454–1461.

Jones, R.D., Pugh, P.J., Jones, T.H., Channer, K.S., 2003. The vasodilatory action of testosterone: a potassium-channel opening or a calcium antagonistic action? Br J Pharmacol 138, 733–744.

Kanayama, G., Hudson, J.I., Pope, H.G., Jr, 2010. Illicit anabolic-androgenic steroid use. Horm Behav 58, 111–121.

Kang, N.N., Fu, L., Xu, J., Han, Y., Cao, J.X., Sun, J.F., Zheng, M., 2012. Testosterone improves cardiac function and alters angiotensin II receptors in isoproterenol-induced heart failure. Arch Cardiovasc Dis 105, 68–76.

Kaushik, M., Sontineni, S.P., Hunter, C., 2010. Cardiovascular disease and androgens: A review. Int J Cardiol 142(1), 8–14.

Kelly, D.M., Jones, T.H., 2013. Testosterone: A vascular hormone in health and disease. J Endocrinol 217(3), R47–R71.

Khaw, K.T., Barrett-Connor, E., 1988. Blood pressure and endogenous testosterone in men: an inverse relationship. J Hypertens 6, 329–332.

Khaw, K.T., Dowsett, M., Folkerd, E., Bingham, S., Wareham, N., Luben, R., Welch, A., Day, N., 2007. Endogenous testosterone and mortality due to all causes, cardiovascular disease, and cancer in men: European prospective investigation into cancer in Norfolk (EPIC-Norfolk) prospective population study. Circulation 116(23), 2694–2701.

Kloner, R.A., Carson, C., Dobs, A., Kopecky, S., Mohler, E.R., 2016. Testosterone and Cardiovascular Disease. J Am Coll Cardiol 67(5), 545–557.

Komamura, K., 2013. Similarities and Differences between the Pathogenesis and Pathophysiology of Diastolic and Systolic Heart Failure. Cardiol Res Pract 824135.

Kontoleon, P.E., Anastasiou-Nana, M.I., Papapetrou, P.D., Alexopoulos, G., Ktenas, V., Rapti, A.C., Tsagalou, E.P., Nanas, J.N., 2006. Hormonal profile in patients with congestive heart failure. Int J Cardiol 87(2-3), 179-183.

Koval, O.M., Guan, X., Wu, Y., Joiner, M.L., Gao, Z., Chen, B., Grumbach, I.M., Luczak, E.D., Colbran, R.J., Song, L.S., Hund, T.J., Mohler, P.J., Anderson, M.E., 2010. CaV1.2 β-subunit coordinates CaMKII-triggered cardiomyocyte death and afterdepolarizations. Proc Natl Acad Sci USA 107, 4996.

Krause, W., 2006. Androgens in the demography of male life course–a review. Soc Biol 53, 4–12.

Kuhar, P., Lunder, M., Drevensek, G., 2007. The role of gender and sex hormones in ischemic-reperfusion injury in isolated rat hearts. Eur J Pharmacol 561, 151–159.

Kushnir, M.M., Rockwood, A.L., Roberts, W.L., Pattison, E.G., Bunker, A.M., Fitzgerald, R.L., Meikle, A.W., 2006. Performance characteristics of a novel tandem mass spectrometry assay for serum testosterone. Clin Chem 52, 120–128.

Labrie, F., Belanger, A., Cusan, L., Gomez, J.L., Candas, B., 1997. Marked decline in serum concentrations of adrenal C19 sex steroid precursors and conjugated androgen metabolites during aging. J Clin Endocrinol Metab 82, 2396–2402.

Launikonis, B.S., Zhou, J., Santiago, D., Brum, G., Ríos, E., 2006. The Changes in Ca^{2+} Sparks Associated with Measured Modifications of Intra-store Ca^{2+} Concentration in Skeletal Muscle. J Gen Physiol 128(1), 45-54.

LeGros, T., McConnell, D., Murry, T., Edavettal, M., Racey-Burns, L.A., Shepherd, R.E., Burns, A.H., 2000. The effects of 17 alpha-methyltestosterone on myocardial function in vitro. Med Sci Sports Exerc 32, 897–903.

Lemke, T., Welling, A., Christel, C.J., Blaich, A., Bernhard, D., Lenhardt, P., Hofmann, F., Moosmang, S., 2008. Unchanged beta-adrenergic stimulation of cardiac L-type calcium channels in Cav1.2 phosphorylation site S1928A mutant mice. J Biol Chem 283, 34738–34744.

Levine, J.E., 1997. New concepts of the neuroendocrine regulation of gonadotropin surges in rats. Biol Reprod 56, 293–302.

Li, L., Guo, C.Y., Jia, E.Z., Zhu, T.B., Wang, L.S., Cao, K.J., Ma, W.Z., Yang, Z.J., 2012. Testosterone is negatively associated with the severity of coronary atherosclerosis in men. Asian J Androl 14, 875–878.

Liang, M.T., Paulson, D.J., Kopp, S.J., Glonek, T., Meneses, P., Gierke, L.W., Schwartz, F.N., 1993. Effects of anabolic steroids and endurance exercise on cardiac performance. Int J Sports Med 14(6), 324–329.

Lim, Y.K., Retnam, L., Bhagavath, B., Sethi, S.K., bin Ali, A., Lim, S.K., 2002. Gonadal effects on plasma ACE activity in mice. Atherosclerosis 160(2), 311–316.

Lin, A.L., McGill, H.C., Jr, Shain, S.A., 1981. Hormone receptors of the baboon cardiovascular system. Biochemical characterization of myocardial cytoplasmic androgen receptors. Circ Res 49, 1010–1016.

Liu, J., Tsang, S., Wong, T.M., 2006. Testosterone is required for delayed cardioprotection and enhanced heat shock protein 70 expression induced by preconditioning. Endocrinology 147(10), 4569–4577.

Liu, P.Y., Death, A.K., Handelsman, D.J., 2003. Androgens and cardiovascular disease. Endocr Rev 24(3), 313-340.

Lizotte, E., Grandy, S.A., Tremblay, A., Allen, B.G., Fiset, C., 2009. Expression, distribution and regulation of sex steroid hormone receptors in mouse heart. Cell Physiol Biochem 23(1-3), 75–86.

Longcope, C., Jaffee, W., Griffing, G., 1981. Production rates of androgens and estrogens in post-menopausal women. Maturitas 3(3-4), 215–223.

Lopes, R.A.M., Neves, K.B., Carneiro, F.S., Tostes, R.C., 2012. Testosterone and vascular function in aging. Front Physiol 3, 1–9.

MacDonald, J.K., Pyle, W.G., Reitz, C.J., Howlett, S.E., 2014. Cardiac contraction, calcium transients, and myofilament calcium sensitivity fluctuate with the estrous cycle in young adult female mice. Am J Physiol Heart Circ Physiol 306, H938–H953.

Mäkinen, J., Järvisalo, M.J., Pöllänen, P., Perheentupa, A., Irjala, K., Koskenvuo, M., Mäkinen, J., Huhtaniemi, I., Raitakari, O.T., 2005. Increased carotid atherosclerosis in andropausal middle-aged men. J Am Coll Cardiol 45, 1603–1608.

Malkin, C.J., Pugh, P.J., West, J.N., van Beek, E.J., Jones, T.H., Channer, K.S., 2006. Testosterone therapy in men with moderate severity heart failure: a double-blind randomized placebo controlled trial. Eur Heart J 27(1), 57-64.

Malkin, C.J., Pugh, P.J., Morris, P.D., Asif, S., Jones, T.H. Channer, K.S., 2010. Low serum testosterone and increased mortality in men with coronary heart disease. Heart 96(22), 1821–1825.

Manni, A., Pardridge, W.M., Cefalu, W., Nisula, B.C., Bardin, C.W., Santner, S.J., Santen, R.J., 1985. Bioavailability of albumin bound testosterone. J Clin Endocrinol Metab 61, 705–710.

Marsh, J.D., Lehmann, M.H., Ritchie, R.H., Gwathmey, J.K., Green, G.E., Schiebinger, R.J., 1998. Androgen receptors mediate hypertrophy in cardiac myocytes. Circulation 98, 256–261.

Marti, C.N., Gheorghiade, M., Kalogeropoulos, A.P., Kalogeropoulos, A.P., Georgiopoulou, V.V., Quyyumi, A.A., Butler, J., 2012. Endothelial dysfunction, arterial stiffness, and heart failure. J Am Coll Cardiol 60, 1455–1469.

Massion, P.B., Feron, O., Dessy, C., Balligand, J.L., 2003. Nitric oxide and cardiac function: ten years after, and continuing. Circ Res 93, 388–98.

Mathur, A., Malkin, C., Saleem, B., Muthusammy, R., Jones, C.H., Channer, K., 2009. The long term benefits of testosterone on angina threshold and atheroma in men. Eur J Endocrinol 161(3), 443–449.

Matsumoto, T., Sakari, M., Okada, M., Yokoyama, A., Takahashi, S., Kouzmenko, A., 2013. The androgen receptor in health and disease. Annu Rev Physiol 75, 201–224.

Merz, C.N., Moriel, M., Rozanski, A., Klein, J., Berman, D.S., 1996. Gender-related differences in exercise ventricular function among healthy subjects and patients. Am Heart J 131(4), 704–709.

Mellström, B., Naranjo, J.R., 2001. Mechanisms of Ca^{2+}-dependent transcription. Curr Opin Neurobiol 11(3), 312-319.

McCubrey, J.A., Steelman, L.S., Chappell, W.H., Abrams, S.L., Wong, E.W., Chang, F., Lehmann, B., Terrian, D.M., Milella, M., Tafuri, A., Stivala, F., Libra, M., Basecke, J., Evangelisti, C., Martelli, A.M., Franklin, R.A., 2007. Roles of the Raf/MEK/ERK pathway in cell growth, malignant transformation and drug resistance. Biochim Biophys Acta 1773(8), 1263-1284.

McGill, H.C., Jr, Anselmo, V.C., Buchanan, J.M., Sheridan, P.J., 1980. The heart is a target organ for androgen. Science 207(4432), 775–777.

Michels, G., Er, F., Eicks, M., Herzig, S., Hoppe, U.C., 2006. Long-term and immediate effect of testosterone on single T-type calcium channel in neonatal rat cardiomyocytes. Endocrinology 147, 5160–5169.

Midzak, A.S., Chen, H., Papadopoulos, V., Zirkin, B.R., 2009. Leydig cell aging and the mechanisms of reduced testosterone synthesis. Mol Cell Endocrinol 299(1), 23–31.

Miller, V.M., Mulvagh, S.L., 2007. Sex steroids and endothelial function: translating basic science to clinical practice. Trends Pharmacol Sci 28, 263–270.

Miller, W.L., 2013. Steroid hormone synthesis in mitochondria. Mol Cell Endocrinol 379, 62–73.

Miller, W.L., Auchus, R.J., 2011. The molecular biology, biochemistry, and physiology of human steroidogenesis and its disorders. Endocr Rev 32, 81–151.

Miller-Davis, C., Marden, S., Leidy, N.K., 2006. The New York Heart Association Classes and functional status: What are we really measuring? Heart Lung 35(4), 217-224.

Mirdamadi, A., Garakyaraghi, M., Pourmoghaddas, A., Bahmani, A., Mahmoudi, H., Gharipour, M., 2014. Beneficial effects of testosterone therapy on functional capacity, cardiovascular parameters, and quality of life in patients with congestive heart failure. Biomed Res Int 2014, 392432.

Miyata, S., Minobe, W., Bristow, M.R., Leinwand, L.A., 2000. Myosin Heavy Chain Isoform Expression in the Failing and Nonfailing Human Heart. Circ Res 86, 386-390.

Montalvo, C., Villar, A.V., Merino, D., García, R., Ares, M., Llano, M., Cobo, M., Hurlé, M.A., Nistal, J.F., 2012. Androgens contribute to sex differences in myocardial remodeling under pressure overload by a mechanism involving TGF-β. PLoS One 7(4), e35635.

Moraes, D.L., Colucci, W.S., Givertz, M.M., 2000. Secondary pulmonary hypertension in chronic heart failure: the role of the endothelium in pathophysiology and management. Circulation 102, 1718–1723.

Morris, P.D., Channer, K.S., 2012. Testosterone and cardiovascular disease in men. Asian Journal of Andrology 14(3), 428–435.

Morgentaler, A., Khera, M., Maggi, M., Zitzmann, M., 2014. Commentary: who is a candidate for testosterone therapy? A synthesis of international expert opinions. J Sex Med 11(7), 1636–1645.

Mottram, P.M., Marwick, T.H., 2005. Assessment of diastolic function: what the general cardiologist needs to know. Heart 91(5), 681–695.

Moutinho, M.A., Colucci, F.A., Alcoforado, V., Tavares, L.R., Rachid, M.B., Rosa, M.L., Ribeiro, M.L., Abdalah, R., Garcia, J.L., Mesquita, E.T., 2008. Heart failure with preserved ejection fraction and systolic dysfunction in the community. Arq Bras Cardiol 90(2), 132-137.

Muller, M., van den Beld, A.W., Bots, M.L., Grobbee, D.E., Lamberts, S.W., van der Schouw, Y.T., 2004. Endogenous sex hormones and progression of carotid atherosclerosis in elderly men. Circulation 109(17), 2074–2079.

Nahrendorf, M., Frantz, S., Hu, K., von zur Mühlen, C., Tomaszewski, M., Scheuermann, H., Kaiser, R., Jazbutyte, V., Beer, S., Bauer, W., Neubauer, S., Ertl, G., Allolio, B., Callies, F., 2003. Effect of testosterone on post-myocardial infarction remodeling and function. Cardiovasc Res 57, 370–378.

Negro-Vilar, A., 1999. Selective andro- gen receptor modulators (SARMs): a novel approach to androgen therapy for the new millennium. J Clin Endocrinol Metab 84, 3459–3462.

Nerbonne, J.M., Kass, R.S., 2005. Molecular physiology of cardiac repolarization. Physiol Rev 85, 1205–1253.

Niggli, E., Ullrich, N.D., Gutierrez, D., Kyrychenko, S., Poláková, E., Shirokova, N., 2013. Posttranslational modifications of cardiac ryanodine receptors: Ca^{2+} signaling and EC-coupling. Biochimica et Biophysica Acta 1833(4), 866–875.

Nottin, S., Nguyen, L.D., Terbah, M., Obert, P., 2006. Cardiovascular effects of androgenic anabolic steroids in male bodybuilders determined by tissue Doppler imaging. Am J Cardiol 97, 912–915.

Oskui, P.M., French, W.J., Herring, M.J., Mayeda, G.S., Burstein, S., Kloner, R.A., 2013. Testosterone and the cardiovascular system: a comprehensive review of the clinical literature. J Am Heart Assoc 2, e000272.

Palatini, P., Giada, F., Garavelli, G., Sinisi, F., Mario, L., Michieletto, M., Baldo-Enzi, G., 1996. Cardiovascular effects of anabolic steroids in weight-trained subjects. J Clin Pharmacol 36, 1132–1140.

Pardridge, W.M., Landaw, E.M., 1985. Testosterone transport in brain: Primary role of plasma protein-bound hormone. Am J Physiol 249, E534–E542.

Parks, R.J., Howlett, S.E., 2013. Sex differences in mechanisms of cardiac excitation-contraction coupling. Pflugers Arch 465, 747–763.

Parks, R.J., Ray, G., Bienvenu, L.A., Rose, R.A., Howlett, S.E., 2014. Sex differences in SR Ca^{2+} release in murine ventricular myocytes are regulated by the cAMP/PKA pathway. J Mol Cell Cardiol 75, 162-173.

Papamitsou, T., Barlagiannis, D., Papaliagkas, V., Kotanidou, E., Dermentzopoulou-Theodoridou, M., 2011. Testosterone-induced hypertrophy, fibrosis and apoptosis of cardiac cells - an ultrastructural and immunohistochemical study. Med Sci Monit 17(9), BR266-BR273.

Payne, J.R., Kotwinski, P.J., Montgomery, H.E., 2004. Cardiac effects of anabolic steroids. Heart 90(5), 473–475.

Perusquía, M., Stallone, J.N., 2010. Do androgens play a beneficial role in the regulation of vascular tone? Nongenomic vascular effects of testosterone metabolites. Am J Physiol Heart Circ Physiol 298(5), H1301–H1307.

Pham, T.V., Robinson, R.B., Danilo, P., Jr, Rosen, M.R., 2002. Effects of gonadal steroids on gender-related differences in transmural dispersion of L-type calcium current. Cardiovasc Res 53, 752–762.

Picht, E., Zima, A.V., Blatter, L.A., Bers, D.M., 2007. SparkMaster: automated calcium spark analysis with ImageJ. Am J Physiol Cell Physiol 293, C1073-C1081.

Pluchino, N., Carmignani, A., Cubeddu, A., Santoro, A., Cela, V., Errasti, T., 2013. Androgen therapy in women: for whom and when. Arch Gynecol Obstet 288(4), 731–737.

Pluciennik, F., Verrecchia, F., Bastide, B., Hervé, J.C., Joffre, M., Délèze, J., 1996. Reversible interruption of gap junctional communication by testosterone propionate in cultured Sertoli cells and cardiac myocytes. J Membr Biol 149(3), 169–177.

Pugh, P.J., Jones, T.H., Channer, K.S., 2003. Acute haemodynamic effects of testosterone in men with chronic heart failure. Eur Heart J 24, 909-915.

Pugh, P.J., Jones, R.D., West, J.N., Jones, T.H., Channer, K.S., 2004. Testosterone treatment for men with chronic heart failure. Heart 90(4), 446–447.

Quinn, U., Tomlinson, L.A., Cockcroft, J.R., 2012. Arterial stiffness. JRSM Cardiovasc Dis 1, 18.

Quiñones, M.A., Otto, C.M., Stoddard, M., Waggoner, A., Zoghbi, W.A., 2002. Recommendations for quantification of Doppler echocardiography: a report from the

Doppler Quantification Task Force of the Nomenclature and Standards Committee of the American Society of Echocardiography. J Am Soc Echocardiogr 15(2), 167–184.

Rahman, F., Christian, H.C., 2007. Non-classical actions of testosterone: an update. Trends Endocrinol Metab 18(10), 371–378.

Raymond, I., Pedersen, F., Steensgaard-Hansen, F., Green, A., Busch-Sorensen, M., Tuxen, C., Appel, J., Jacobsen, J., Atar, D., Hildebrandt, P., 2003. Prevalence of impaired left ventricular systolic function and heart failure in a middle aged and elderly urban population segment of Copenhagen. Heart 89(12), 1422-1429.

Reckelhoff, J.F., Zhang, H., Srivastava, K., Granger, J.P., 1999. Gender differences in hypertension in spontaneously hypertensive rats: role of androgens and androgen receptor. Hypertension 34(4 Pt 2), 920–923.

Roberts, P.J., Der, C.J., 2007. Targeting the Raf-MEK-ERK mitogen-activated protein kinase cascade for the treatment of cancer. Oncogene 26(22), 3291-3310.

Rocha, F.L., Carmo, E.C., Roque, F.R., Hashimoto, N.Y., Rossoni, L.V., Frimm, C., Anéas, I., Negrão, C.E., Krieger, J.E., Oliveira, E.M., 2007. Anabolic steroids induce cardiac renin-angiotensin system and impair the beneficial effects of aerobic training in rats. Am J Physiol Heart Circ Physiol 293(6), H3575–H3583.

Roger, V.L., Go, A.S., Lloyd-Jones, D.M., Benjamin, E.J., Berry, J.D., Borden, W.B., Bravata, D.M., Dai, S., Ford, E.S., Fox, C.S., Fullerton, H.J., Gillespie, C., Hailpern, S.M., Heit, J.A., Howard, V.J., Kissela, B.M., Kittner, S.J., Lackland, D.T., Lichtman, J.H., Lisabeth, L.D., Makuc, D.M., Marcus, G.M., Marelli, A., Matchar, D.B., Moy, C.S., Mozaffarian, D., Mussolino, M.E., Nichol, G., Paynter, N.P., Soliman, E.Z., Sorlie, P.D., Sotoodehnia, N., Turan, T.N., Virani, S.S., Wong, N.D., Woo, D., Turner, M.B.; American Heart Association Statistics Committee and Stroke Statistics Subcommittee, 2012. Heart disease and stroke statistics–2012 update: a report from the American Heart Association. Circulation 125, e2–220.

Rosano, G.M., Sheiban, I., Massaro, R., Pagnotta, P., Marazzi, G., Vitale, C., Mercuro, G., Volterrani, M., Aversa, A., Fini, M., 2007. Low testosterone levels are associated with coronary artery disease in male patients with angina. Int J Impot Res 19(2), 176–182.

Roth, G.M., Bader, D.M., Pfaltzgraff, E.R., 2014. Isolation and Physiological Analysis of Mouse Cardiomyocytes. J Vis Exp 91, e51109.

Ruige, J.B., Mahmoud, A.M., De Bacquer, D., Kaufman, J.M., 2011. Endogenous testosterone and cardiovascular disease in healthy men: a meta-analysis. Heart 97, 870–875.

Saccà, L., 2009. Heart failure as a multiple hormonal deficiency syndrome. Circulation: Heart Failure 2(2), 151–156.

Saito, T., Ciobotaru, A., Bopassa, J.C., Toro, L., Stefani, E., Eghbali, M., 2009. Estrogen contributes to gender differences in mouse ventricular repolarization. Circ Res 105, 343–352.

Salameh, W.A., Redor-Goldman, M.M., Clarke, N.J., Reitz, R.E., Caufield, M.P., 2010. Validation of a total testosterone assay using high-turbulence liquid chromatography tandem mass spectrometry: Total and free testosterone reference ranges. Steroids 75(2), 169–175.

Salke, R.C., Rowland, T.W., Burke, E.J., 1985. Left ventricular size and function in body builders using anabolic steroids. Med Sci Sports Exerc 17(6), 701–704.

Sandstedt, J., Ohlsson, C., Norjavaara, E., Nilsson, J., Törnell, J., 1994. Bone Growth and Reduced Weight Male Bovine Growth Hormone. Endocrinol 135(6), 2574–2580.

Satoh, H., Blatter, L.A., Bers, D.M., 1997. Effects of $[Ca^{2+}]i$, SR Ca^{2+} load, and rest on Ca^{2+} spark frequency in ventricular myocytes. Am J Physiol 272, H657-H668.

Schaible, T.F., Malhotra, A., Ciambrone, G., Scheuer, J., 1984. The effects of gonadectomy on left ventricular function and cardiac contractile proteins in male and female rats. Circ Res. 54, 38–49.

Scherrer-Crosbie, M., Ullrich, R., Bloch, K.D., Nakajima, H., Nasseri, B., Aretz, H.T., Lindsey, M.L., Vançon, A.C., Huang, P.L., Lee, R.T., Zapol, W.M., Picard, M.H., 2001. Endothelial nitric oxide synthase limits left ventricular remodeling after myocardial infarction in mice. Circulation 104, 1286–1291.

Scheuer, J., Malhotra, A., Schaible, T.F., Capasso, J., 1987. Effects of gonadectomy and hormonal replacement on rat hearts. Circ Res 61, 12–19.

Schwarz, E.R., Phan, A., Willix, R.D., Jr, 2011. Andropause and the development of cardiovascular disease presentation-more than an epi-phenomenon. J Geriatr Cardiol 8, 35–43.

Sebag, I.A., Gillis, M.A., Calderone, A., Kasneci, A., Meilleur, M., Haddad, R., Noiles, W., Patel, B., Chalifour, L.E., 2011. Sex hormone control of left ventricular structure/function: mechanistic insights using echocardiography, expression, and DNA methylation analyses in adult mice. Am J Physiol Heart Circ Physiol 301, H1706–H1715.

Sen-Chowdhry, S., Jacoby, D., Moon, J.C., McKenna, W.J., 2016. Update on hypertrophic cardiomyopathy and a guide to the guidelines. Nat Rev Cardiol 13(11), 651–675.

Siwik, D.A., Pagano, P.J., Colucci, W.S., 2001. Oxidative stress regulates collagen synthesis and matrix metalloproteinase activity in cardiac fibroblasts. Am J Physiol Cell Physiol 280, C53–C60.

Smith, J.C., Bennett, S., Evans, L.M., Kynaston, H.G., Parmar, M., Mason, M.D., Cockcroft, J.R., Scanlon, M.F., Davies, J.S., 2001. The effects of induced hypogonadism on arterial stiffness, body composition, and metabolic parameters in males with prostate cancer. J Clin Endocrinol Metab 86, 4261–4267.

Spencer, J.B., Klein, M., Kumar, A., Azziz, R., 2007. The age-associated decline of androgens in reproductive age and menopausal black and white women. J Clin Endocrinol Metab 92(12), 4730–4733.

Sternfeld, B., Liu, K., Quesenberry, C.P., Jr, Wang, H., Jiang, S.F., Daviglus, M., Fornage, M., Lewis, C.E., Mahan, J., Schreiner, P.J., Schwartz, S.M., Sidney, S., Williams, O.D., Siscovick, D.S., 2008. Changes over 14 years in androgenicity and body mass index in a biracial cohort of reproductive-age women. J Clin Endocrinol Metab 93(6), 2158–2165.

Stocco, C., 2012. Tissue physiology and pathology of aromatase. Steroids 77, 27–35.

Studenik, C.R., Zhou, Z., January, C.T., 2001. Differences in action potential and early afterdepolarization properties in LQT2 and LQT3 models of long QT syndrome. Br J Pharmacol 132(1), 85-92.

Svartberg, J., von Mühlen, D., Mathiesen, E., Joakimsen, O., Bønaa, K.H., Stensland-Bugge, E., 2006. Low testosterone levels are associated with carotid atherosclerosis in men. J Intern Med 259, 576–582.

Swaminathan, P.D., Purohit, A., Hund, T.J., Anderson, M.E., 2012. Calmodulin-dependent protein kinase II: linking heart failure and arrhythmias. Circ Res 110(12), 1661–1677.

Thompson, P.D., Sadaniantz, A., Cullinane, E.M., Bodziony, K.S., Catlin, D.H., Torek-Both, G., Douglas, P.S., 1992. Left ventricular function is not impaired in weight-lifters who use anabolic steroids. J Am Coll Cardiol 19, 278–282.

Tisdale, J.E., 2016. Drug-induced QT interval prolongation and torsades de pointes: Role of the pharmacist in risk assessment, prevention and management. Can Pharm J 149(3), 139–152.

Toma, M., McAlister, F.A., Coglianese, E.E., Vidi, V., Vasaiwala, S., Bakal, J.A., Armstrong, P.W., Ezekowitz, J.A., 2012. Testosterone supplementation in heart failure: a meta-analysis. Circ Heart Fail 5, 315–321.

Traaseth, N.J., Ha, K.N., Verardi, R., Shi, L., Buffy, J.J., Masterson, L.R., Veglia, G., 2008. Structural and dynamic basis of phospholamban and sarcolipin inhibition of Ca(2+)-ATPase. Biochem 47(1), 3-13.

Treasure, C.B., Vita, J.A., Cox, D.A., Fish, R.D., Gordon, J.B., Mudge, G.H., Colucci, W.S., Sutton, M.G., Selwyn, A.P., Alexander, R.W., Ganz, P., 1990. Endothelium-dependent dilation of the coronary microvasculature is impaired in dilated cardiomyopathy. Circulation 81, 772–779.

Tribouilloy, C., Rusinaru, D., Mahjoub, H., Soulière, V., Lévy, F., Peltier, M., Slama, M., Massy, Z., 2008. Prognosis of heart failure with preserved ejection fraction: a 5 year prospective population-based study. Eur Heart J 29(3), 339-347.

Tsang, S., Wong, S.S., Wu, S., Kravtsov, G.M., Wong, T.M., 2009. Testosterone-augmented contractile responses to alpha1-and beta1-adrenoceptor stimulation are associated with increased activities of RyR, SERCA, and NCX in the heart. Am J Physiol Cell Physiol 296, C766–C782.

Tsien, R.Y., 1981. A non-disruptive technique for loading calcium buffers and indicators into cells. Nature 290, 527-528.

Tsujimura, A., 2013. The relationship between testosterone deficiency and men's health. World J Mens Health 31(2), 126–135.

Upadhya, B., Haykowsky, M.J., Eggebeen, J., Kitzman, D.W., 2015. Exercise intolerance in heart failure with preserved ejection fraction: more than a heart problem. J Geriatr Cardiol 12(3), 294–304.

Urhausen, A., Hölpes, R., Kindermann, W., 1989. One- and two- dimensional echocardiography in bodybuilders using anabolic steroids. Eur J Appl Physiol Occup Physiol 58, 633–640.

Vangheluwe, P., Raeymaekers, L., Dode, L., Wuytack, F., 2005. Modulating sarco(endo)plasmic reticulum Ca^{2+} ATPase 2 (SERCA2) activity: cell biological implications. Cell Calcium 38(3-4), 291-302.

Varin, R., Mulder, P., Tamion, F., Richard, V., Henry, J.P., Lallemand, F., Lerebours, G., Thuillez, C., 2000. Improvement of endothelial function by chronic angiotensin-converting enzyme inhibition in heart failure: role of nitric oxide, prostanoids, oxidant stress, and bradykinin. Circulation 102, 351–356.

Vermeulen, A., Kaufman, J.M., 1995. Ageing of the hypothalamo-pituitary-testicular axis in men. Horm Res 43, 25–28.

Vicencio, J.M., Estrada, M., Galvis, D., Bravo, R., Contreras, A.E., Rotter, D., Szabadkai, G., Hill, J.A., Rothermel, B.A., Jaimovich, E., Lavandero, S., 2011. Anabolic androgenic steroids and intracellular calcium signaling: a mini review on mechanisms and physiological implications. Mini Rev Med Chem 11(5), 390–398.

Vicencio, J.M., Ibarra, C., Estrada, M., Chiong, M., Soto, D., Parra, V., Diaz-Araya, G., Jaimovich, E., Lavandero, S., 2006. Testosterone induces an intracellular calcium increase by a nongenomic mechanism in cultured rat cardiac myocytes. Endocrinology 147, 1386–1395.

Vingren, J.L., Kraemer, W.J., Ratamess, N.A., Anderson, J.M., Volek, J.S., Maresh, C.M., 2010. Testosterone physiology in resistance exercise and training: the up-stream regulatory elements. Sports Med 40, 1037–1053.

Vitale, C., Mendelsohn, M.E., Rosano, G.M., 2009. Gender differences in the cardiovascular effect of sex hormones. Nat Rev Cardiol 6(8), 532–542.

Walker, W.H., 2011. Testosterone signaling and the regulation of spermatogenesis. Spermatogenesis 1(2), 116–120.

Wang, D.W., Yazawa, K., George, A.L., Bennett, P.B., 1996. Characterization of human cardiac Na^{+} channel mutations in the congenital long QT syndrome. Proc Natl Acad Sci USA 93(23), 13200-13205.

Wang, S.Q., Song, L.S., Lakatta, E.G., Cheng, H., 2001. Ca^{2+} signalling between single L-type Ca^{2+} channels and ryanodine receptors in heart cells. Nature 410(6828), 592–596.

Wang, M., Tsai, B.M., Kher, A., Baker, L.B., Wairiuko, G.M., Meldrum, D.R., 2005. Role of endogenous testosterone in myocardial proinflammatory and proapoptotic

signaling after acute ischemia-reperfusion. Am J Physiol Heart Circ Physiol 288, H221–H226.

Webb, C., McNeill, J., Hayward, C., de Zeigler, D., Collins, P., 1999. Effects of testosterone on coronary vasomotor regulation in men with coronary heart disease. Circulation 100, 1690–1696.

Wehrens, X.H.T., Lehnart, S.E., Marks, A.R., 2005. Intracellular Calcium Release and Cardiac Disease. Annu Rev Physiol 67, 69–98.

Weiss, J.N., Garfinkel, A., Karagueuzian, H.S., Chen, P., Qu, Z., 2010. Early Afterdepolarizations and Cardiac Arrhythmias. Heart Rhythm 7(12), 1891–1899.

Wierman, M.E., Arlt, W., Basson, R., Davis, S.R., Miller, K.K., Murad, M.H., Rosner, W., Santoro, N., 2014. Androgen therapy in women: an Endocrine Society Clinical Practice guideline. J Clin Endocrinol Metab 91, 3489–3510.

Williams, G.S.B., Smith, G.D., Sobie, E.A., Jafri, M.S., 2010. Models of cardiac excitation-contraction coupling in ventricular myocytes. Mathematical Biosciences 226(1), 1–15.

Wilson, C., Maass, R., Estrada, M., 2011. Cardiovascular Effects of Androgens, Basic and Clinical Endocrinology Up-to-Date, Dr. Fulya Akin (Ed.), ISBN: 978-953-307-340-8, InTech, Available from: http://www.intechopen.com/books/basic-and-clinical-endocrinology-up-to-date/cardiovascular-effects-of- androgens.

Wilson, J.R., Mancini, D.M., Dunkman, W.B., 1993. Exertional fatigue due to skeletal muscle dysfunction in patients with heart failure. Circulation 87, 470–475.

Winslow, R.L., Hinch, R., Greenstein, J.L., 2005. Mechanisms and Models of Cardiac Excitation-Contraction Coupling. Biomed Eng 131, 97–131.

Winslow, R.L., Greenstein, J.L., Hinch, R., 2006. Mechanisms of Excitation-Contraction Coupling in an Integrative Model of the Cardiac Ventricular Myocyte. Biophys J 90(1), 77–91.

Witayavanitkul, N., Woranush, W., Bupha-Intr, T., Wattanapermpool, J., 2013. Testosterone regulates cardiac contractile activation by modulating SERCA but not NCX activity. Am J Physiol Heart Circ Physiol 304, H465–H472.

Woerdeman, J., de Ronde, W., 2011. Therapeutic effects of anabolic androgenic steroids on chronic diseases associated with muscle wasting. Expert Opin Investig Drugs 20, 87–97.

Wu, Y., MacMillan, L.B., McNeill, R.B., Colbran, R.J., Anderson, M.E., 1999. CaM kinase augments cardiac L-type Ca2+ current: a cellular mechanism for long Q-T arrhythmias. Am J Physiol 276(6 Pt 2), H2168–H2178.

Yaron, M., Greenman, Y., Rosenfeld, J.B., Izkhakov, E., Limor, R., Osher, E., Shenkerman, G., Tordjman, K., Stern, N., 2009. Effect of testosterone replacement therapy on arterial stiffness in older hypogonadal men. Eur J Endocrinol 160, 839–846.

Ye, L., Su, Z.J., Ge, R.S., 2011. Inhibitors of testosterone biosynthetic and metabolic activation enzymes. Molecules 16, 9983–10001.

Yin, F., Spurgeon, H., Rakusan, K., Weisfeldt, M., Lakatta, E., 1982. Use of tibial length to quantify cardiac hypertrophy: Application in the aging rat. Am J Physiol 243(6), H941-H947.

Zhang, Y.Z., Xing, X.W., He, B., Wang, L.X., 2007. Effects of testosterone on cytokines and left ventricular remodeling following heart failure. Cell Physiol Biochem 20(6), 847–852.

Zhu, Y., Ai, X., Oster, R.A., Bers, D.M., Pogwizd, S.M., 2013. Sex differences in repolarization and slow delayed rectifier potassium current and their regulation by sympathetic stimulation in rabbits. Pflugers Arch 465, 805–818.

Zirkin, B.R., Tenover, J.L., 2012. Aging and declining testosterone: past, present, and hopes for the future. J Androl 33(6), 1111–1118.

Zitzmann, M., Faber, S., Nieschlag, E., 2006. Association of specific symptoms and metabolic risks with serum testosterone in older men. J Clin Endocrinol Metab 91(11), 4335–4343.